

Helsinki University of Technology Department of Signal Processing and Acoustics
Teknillinen korkeakoulu Signaalinkäsittelyn ja akustiikan laitos
Espoo 2009

Report 10

CONTRIBUTIONS TO MEASUREMENT-BASED DYNAMIC MIMO CHANNEL MODELING AND PROPAGATION PARAMETER ESTIMATION

Jussi Salmi

Dissertation for the degree of Doctor of Science in Technology to be presented with due permission of the Department of Signal Processing and Acoustics for public examination and debate in Auditorium S1 at Helsinki University of Technology (Espoo, Finland) on the 14th of August, 2009, at 12 o'clock noon.

Helsinki University of Technology
Faculty of Electronics, Communications and Automation
Department of Signal Processing and Acoustics

Teknillinen korkeakoulu
Elektroniikan, tietoliikenteen ja automaation tiedekunta
Signaalinkäsittelyn ja akustiikan laitos

Distribution:
Helsinki University of Technology
Department of Signal Processing and Acoustics
P.O. Box 3000
FI-02015 TKK
Tel. +358-9-451 3211
Fax. +358-9-452 3614
E-mail: Mirja.Lemetyinen@hut.fi
Web page: <http://signal.hut.fi>

© Jussi Salmi

ISBN 978-952-248-018-7 (Printed)
ISBN 978-952-248-019-4 (PDF)
ISSN 1797-4267

Multiprint Oy
Espoo 2009



ABSTRACT OF DOCTORAL DISSERTATION		HELSINKI UNIVERSITY OF TECHNOLOGY P. O. BOX 1000, FI-02015 TKK http://www.tkk.fi	
Author Jussi Salmi			
Name of the dissertation Contributions to Measurement-based Dynamic MIMO Channel Modeling and Propagation Parameter Estimation			
Manuscript submitted May 15, 2009		Manuscript revised July 18, 2009	
Date of the defence August 14, 2009			
<input type="checkbox"/> Monograph		<input checked="" type="checkbox"/> Article dissertation (summary + original articles)	
Faculty		Faculty of Electronics, Communications and Automation	
Department		Department of Signal Processing and Acoustics	
Field of research		Signal Processing for Communications	
Opponent(s)		Prof. Claude Oestges and Dr. Juha Laurila	
Supervisor		Prof. Visa Koivunen	
Instructor		Prof. Visa Koivunen	
<p>Abstract</p> <p>Multiantenna (MIMO) transceivers are a key technology in emerging broadband wireless communication systems since they facilitate achieving the required high data rates and reliability. In order to develop and study the performance of MIMO systems, advanced channel modeling that captures also the spatial characteristics of the radio wave propagation is required. This thesis introduces several contributions in the area of measurement-based modeling of wireless MIMO propagation channels. Measurement based modeling provides realistic characterization of the space, time and frequency dependency of the physical layer for both MIMO transceiver design and network planning.</p> <p>The focus in this thesis is on modeling and parametric estimation of mobile MIMO radio propagation channels. First, an overview of MIMO channel modeling approaches is given. A hybrid model for characterizing the spatio-temporal structure of measured MIMO channels consisting of a superposition of double-directional, specular-like propagation paths, and a stochastic process describing the diffuse scattering is formulated. State-space modeling approach is introduced in order to capture the dynamic channel properties from mobile channel sounding measurements. Extended Kalman filter (EKF) is employed for the sequential estimation problem and also statistical hypothesis testing for adjusting the model order are introduced. Due to the improved dynamic model of the mobile radio channel, the EKF approach outperforms maximum likelihood (ML) based batch solutions both in terms of lower estimation error as well as computational complexity.</p> <p>Finally, tensor representation for modeling multidimensional MIMO channels is considered and a novel sequential unfolding SVD (SUSVD) tensor decomposition is introduced. The SUSVD is an orthogonal tensor decomposition having several important applications in signal processing. The advantages of applying the SUSVD instead of other well known tensor models such as parallel factorization and Tucker-models, are illustrated using application examples in channel sounding data processing.</p>			
Keywords array signal processing, MIMO, radio propagation modeling, sequential estimation, tensors			
ISBN (printed) 978-952-248-018-7		ISSN (printed) 1797-4267	
ISBN (pdf) 978-952-248-019-4		ISSN (pdf)	
Language English		Number of pages 90 p. + app. 94 p.	
Publisher Helsinki University of Technology, Department of Signal Processing and Acoustics			
Print distribution Helsinki University of Technology, Department of Signal Processing and Acoustics			
<input checked="" type="checkbox"/> The dissertation can be read at http://lib.tkk.fi/Diss/2009/isbn9789522480194			



VÄITÖSKIRJAN TIIVISTELMÄ		TEKNILLINEN KORKEAKOULU PL 1000, 02015 TKK http://www.tkk.fi	
Tekijä Jussi Salmi			
Väitöskirjan nimi Dynaamisen MIMO radiokanavan mittauspohjainen mallinnus ja radiotie-etenemisen parametrien estimointi			
Käsikirjoituksen päivämäärä 15.5.2009		Korjatun käsikirjoituksen päivämäärä 18.7.2009	
Väitöstilaisuuden ajankohta 14.8.2009			
<input type="checkbox"/> Monografia		<input checked="" type="checkbox"/> Yhdistelmäväitöskirja (yhteenveto + erillisartikkelit)	
Tiedekunta	Elektroniikan, tietoliikenteen ja automaation tiedekunta		
Laitos	Signaalinkäsittelyn ja akustiikan laitos		
Tutkimusala	Tietoliikenteen signaalinkäsittely		
Vastaväittäjä(t)	Prof. Claude Oestges ja TkT Juha Laurila		
Työn valvoja	Prof. Visa Koivunen		
Työn ohjaaja	Prof. Visa Koivunen		
Tiivistelmä			
<p>Moniantenniset (MIMO) radiopäätelaitteet ovat avainteknologia tulevaisuuden langattomien laajakaistaisten tietoliikennejärjestelmien kehityksessä, sillä ne mahdollistavat suuren tiedonsiirtonopeuden sekä yhteyden luotettavuuden. MIMO tekniikoiden tutkimus- ja kehitystyö edellyttää kehittyneitä kanavamalleja, jotka kuvaavat radiotie-etenemisen ominaisuuksia myös tilan suhteen. Tässä työssä esitetään useita parannuksia langattomien MIMO radiotie-etenemiskanavien mittauspohjaiseen mallintamiseen. Mittauspohjainen mallinnus mahdollistaa radiojärjestelmien fyysisen rajapinnan tila-, aika- ja taajuusriippuvuuden realistisen kuvauksen, mikä on tärkeää sekä lähetin-vastaanotin että verkkosuunnittelussa.</p> <p>Väitöskirjassa keskitytään mobiilin MIMO radiotie-etenemiskanavan mallinnukseen ja parametriseen estimointiin. Työ sisältää katsauksen kirjallisuudessa esitettyihin malleihin. Lisäksi työssä kehitetään hybridimalli esittämään MIMO radiokanavien tila-aika rakennetta. Malli koostuu äärellisestä määrästä kaksisuuntaisesti mallinnettuja radiotie-etenemispolkuja, sekä radiokanavan diffuusua sirontaa kuvaavasta satunnaismuuttujasta. Radiokanavan dynaamiset ominaisuudet saadaan hyödynnettyä soveltamalla tila-avaruus-mallinnusta mobiilien radiokanavaluotainmittausten tietojenkäsittelyssä. Mallin parametrien rekursiivinen estimointi suoritetaan laajennetulla Kalman suotimella (EKF) ja mallin laajuutta arvioidaan tilastollisten hypoteesintestausmenetelmien avulla. Mobiileja mittauksia varten kehitetty parannettu dynaaminen malli ja siihen sovellettu EKF tuottavat sekä tarkempia estimaatteja että pienentävät laskennallista kuormaa verrattuna staattiseen malliin perustuviin suurimman todennäköisyyden (ML) estimaattoreihin.</p> <p>Lopuksi työssä esitetään MIMO kanavamalli tensorihajotelmamuodossa. Lisäksi johdetaan uusi hierarkinen tensorimalli sekä sen tehokkaaseen laskentaan soveltuva tensorihajotelma. Saavutetulla ortogonaalisella tensorihajotelmalla on monia tärkeitä sovelluskohteita signaalinkäsittelyssä. Uuden menetelmän etuja suhteessa hyvin tunnettuihin PARAFAC (parallel factorization) ja Tucker tensorimalleihin havainnollistetaan radiokanavaluotaimen mittaustietojen käsittelyesimerkkien avulla.</p>			
Asiasanat antenniryhmien signaalinkäsittely, MIMO, radiokanavamallinnus, rekursiivinen estimointi, tensorit			
ISBN (painettu)	978-952-248-018-7	ISSN (painettu)	1797-4267
ISBN (pdf)	978-952-248-019-4	ISSN (pdf)	
Kieli	Englanti	Sivumäärä	90 s. + liit. 94 s.
Julkaisija Teknillinen korkeakoulu, Signaalinkäsittelyn ja akustiikan laitos			
Painetun väitöskirjan jakelu Teknillinen korkeakoulu, Signaalinkäsittelyn ja akustiikan laitos			
<input checked="" type="checkbox"/> Luettavissa verkossa osoitteessa http://lib.tkk.fi/Diss/2009/isbn9789522480194			

Acknowledgements

The research work for this doctoral thesis has been carried out at the Department of Signal Processing and Acoustics, Helsinki University of Technology (TKK) under the supervision of Prof. Visa Koivunen. The Statistical Signal Processing group, led by Prof. Koivunen, is part of SMARAD (Smart and Novel Radio Research Unit), a Centre of Excellence nominated by the Academy of Finland.

I would like to express my gratitude to my supervisor Prof. Koivunen for his continuous support in terms of providing excellent working environment and well-grounded and tireless guidance during my doctoral research. Also, I would like to warmly thank Dr. Andreas Richter, who has been an invaluable asset throughout the course of my work as well as a good friend. He has provided me close guidance and endless clues for solving any issues — both scientific and less scientific ones. I am indebted to both Prof. Koivunen and Dr. Richter for the technical quality and results of my research.

I would like to thank the pre-examiners of this thesis, Prof. Claude Oestges and Dr. Terhi Rautiainen for their invaluable efforts in carefully examining the thesis. Many thanks belong also to all my colleagues at the part of the Department of Signal Processing and Acoustics formerly known as the Signal Processing Laboratory. It has been truly a pleasure to work in such an inspiring scientific environment. In particular, I would like to acknowledge the colleagues who have been stimulating my every day research at the office the most, including Dr. Traian Abrudan, Dr. Fabio Belloni, Sachin Chaudhari, Mei Yen Cheong, Mario Costá, Dr. Mihai Enescu, Azadeh Haghparast, Pekka Jänis, Dr. Maarit Melvasalo, Alexandra Oborina, Jan Oksanen, Dr. Cássio Ribeiro, Dr. Timo Roman, Karol Schober, and Eduardo Zacarias. Special thanks go to the department secretaries Mirja Lemetyinen and Anne Jääskeläinen (former) for support in any practical matters.

I would like to thank the two main sponsors of my post graduate studies, the Graduate School in Electronics, Telecommunications and Automation (GETA, 2007-2009) and the Graduate School of Electrical and Communications Engineering (Faculty Grad School, 2005–2007) for financial support. Especially, I would like to acknowledge the GETA secretary Marja Leppäharju as well as the directors Prof. Ari Sihvola and Prof. Iiro Hartimo (former). The research was also partly funded by the Nordite WILATI

project. Furthermore, I would like to thank Finnish Foundation for Technology Promotion (TES), Emil Aaltosen säätiö, Elektroniikkainsinöörien säätiö (EIS), HPY Tutkimussäätiö, and Nokia Foundation for financial support in terms of post graduate study scholarships.

The efforts of the parties who have provided the necessary measurement data used in this thesis are highly acknowledged. These include the group of Prof. Pertti Vainikainen at TKK, the group of professors Andreas Molisch and Fredrik Tufvesson at Lund University, as well as the group of Prof. Reiner Thomä at TU Ilmenau.

I would like to express my gratitude to all my family and friends — past and present — to whom I am indebted for too much for words to express. I apologize to them for the occasional periods of mental absence for reasons related to the wondering mind of a dedicated researcher. Many thanks for returning my feet to the ground from time to time.

Finally — thank you Monica and Samuel for your love, trust, and sharing all the joys and hardships of life. You complete me.

Järvenpää, July 18, 2009

A handwritten signature in black ink, appearing to read 'J. Salmi', with a stylized, cursive script.

Jussi Salmi

To Monica and Samuel

Contents

Acknowledgements	v
List of original publications	xi
List of abbreviations	xiii
List of symbols	xvii
1 Introduction	1
1.1 Motivation of the thesis	1
1.2 Scope of the Thesis	2
1.3 Contributions	3
1.4 Structure of the Thesis	4
1.5 Summary of Publications	5
2 MIMO Radio Channel Modeling	7
2.1 MIMO System Model	8
2.1.1 MIMO Principle	8
2.1.2 Multipath Propagation	8
2.1.3 MIMO System in a Fading Channel	11
2.2 MIMO Channel Models — a Review	12
2.2.1 Physics-based Models	13
2.2.2 Analytical Models	16
2.2.3 Mixed models	19
2.3 Measurement-Based Channel Modeling	20
2.3.1 Motivation	20
2.3.2 Channel Sounding Measurement Methodology	22
2.3.3 The Hybrid Channel Model	25
2.4 Summary and Discussion	28
3 Estimation of Propagation Model Parameters	31
3.1 Estimation Problem	31
3.2 Estimation of Static Model Parameters	33

3.2.1	Methods Based on Second Order Statistics of the Channel	33
3.2.2	Deterministic Maximum Likelihood Methods	37
3.3	Estimation of a Dynamic Model	39
3.3.1	State-Space Modeling Principle	39
3.3.2	Sequential Estimation Techniques	40
3.4	State-Space Modeling for Propagation Path Tracking	42
3.4.1	Dynamic Model	43
3.4.2	EKF Formulation	44
3.4.3	Model Order Selection	46
3.5	Estimation Examples	48
3.5.1	Measurement Setup	48
3.5.2	Goodness of Fit	48
3.5.3	Path Parameter Estimates	49
3.6	Summary and Discussion	49
4	Tensor Decompositions and Modeling for High Dimensional Data	57
4.1	Tensor Models	58
4.1.1	PARAFAC Model	58
4.1.2	Tucker/HOSVD Model	59
4.2	PARATREE/SUSVD	60
4.2.1	PARATREE Model	60
4.2.2	Sequential Unfolding SVD	61
4.3	Application Examples of Tensor Models	63
4.3.1	Tensor Valued MIMO Channel Modeling	63
4.3.2	Applications for PARATREE/SUSVD in Array Signal Processing	65
4.4	Summary and Discussion	66
5	Summary	69
	Bibliography	73

List of original publications

- I** J. Salmi, A. Richter, M. Enescu, P. Vainikainen, and V. Koivunen, “Propagation parameter tracking using variable state dimension Kalman filter,” in *The 63rd IEEE Vehicular Technology Conference (VTC 2006-spring)*, vol. 6, Melbourne, Australia, May 7–10, 2006, pp. 2757–2761.
- II** J. Salmi, A. Richter, and V. Koivunen, “Enhanced tracking of radio propagation path parameters using state-space modeling,” in *The 14th European Signal Processing Conference (EUSIPCO 2006)*, Florence, Italy, Sep. 4–8, 2006.
- III** J. Salmi, A. Richter, and V. Koivunen, “State-space modeling and propagation parameter tracking: Multitarget tracking based approach,” in *The 40th Asilomar Conference on Signals, Systems, and Computers*, Pacific Grove, CA, Oct. 29–Nov. 1, 2006, pp. 941–945.
- IV** J. Salmi, A. Richter, and V. Koivunen, “Tracking of MIMO propagation parameters under spatio-temporal scattering model,” in *The 41st Asilomar Conference on Signals, Systems, and Computers*, Pacific Grove, CA, Nov. 4–7, 2007, pp. 666–670.
- V** J. Salmi, A. Richter, and V. Koivunen, “Detection and tracking of MIMO propagation path parameters using state-space approach,” *IEEE Transactions on Signal Processing*, vol. 57, no. 4, pp. 1538–1550, Apr. 2009.
- VI** J. Salmi, A. Richter, and V. Koivunen, “Sequential Unfolding SVD for Low Rank Orthogonal Tensor Approximation,” in *Proc. The 42nd Asilomar Conference on Signals, Systems, and Computers*, Pacific Grove, CA, Oct. 26–29, 2008, pp. 1713–1717.
- VII** J. Salmi, A. Richter, and V. Koivunen, “Sequential Unfolding SVD for Tensors with Applications in Array Signal Processing,” accepted to *IEEE Transactions on Signal Processing*, 2009.

List of abbreviations

3G	Third Generation
3GPP	Third Generation Partnership Project
4G	Fourth Generation
ALS	alternating Least Squares
AoA	Angle of Arrival
AoD	Angle of Departure
BF	Beam Forming
BIC	Bayesian Information Criterion
BPSK	Binary Phase Shift Keying
BS	Base Station
CANDECOMP	Canonical Decomposition
COST	COoperation européenne dans le domaine de la recherche Scientifique et Technique
CRB	Cramér-Rao Bound
CUSUM	Cumulative Sum (detection scheme)
DFT	Discrete Fourier transform
DMC	Dense Multipath Components
DoA	Direction of Arrival (at receiver)
DoD	Direction of Departure (at transmitter)
DSL	Digital Subscriber Line
EADF	Effective Aperture Distribution Function
EKF	Extended Kalman Filter
EM	Expectation maximization
ESPRIT	Estimation of Signal Parameters via Rotational Invariance Technique
EVD	EigenValue Decomposition
FDTD	Finite Difference in Time Domain
FIM	Fisher Information Matrix
FSM	Finite Scatterer Model
GSCM	Geometrical Stochastic Channel Model
HOSVD	Higher Order SVD
HSDPA	High Speed Downlink Packet Access
i.i.d.	independent and identically distributed
IEEE	Institute of Electrical and Electronics Engineers

ISIS	Initialization and Search Improved SAGE Algorithm
JADE	Joint Angle and Delay Estimation
KF	Kalman Filter
LOS	Line-Of-Sight
LS	Least Squares
LTE	Long Term Evolution
MBCM	Measurement-Based Channel Modeling
MDL	Minimum Description Length
MIMO	Multiple-Input Multiple-Output
MISO	Multiple-Input Single-Output
ML	Maximum Likelihood
MoM	Method of Moments
MS	Mobile Station
MUSIC	MUltiple Signal Classification
MVDR	Minimum Variance Distortionless Response
NLOS	Non-Line-Of-Sight
NWLS	Nonlinear Weighted Least Squares
PARAFAC	Parallel Factorization
PARATREE	Tree structured tensor model
PAP	Power-Angular Profile
PDF	Probability Density Function
PDP	Power-Delay Profile
PF	Particle Filter
PSSA	Polarimetric Semi-Spherical Array
PULA	Polarimetric Uniform Linear Array
RARE	RANk REDuction estimator
RF	Radio Frequency
RIMAX	Parameter Estimation Algorithm
RT	Ray Tracing
Rx	Radio Receiver
SAGE	Space-Alternating Generalized Expectation- Maximization
SCM	Stochastic Channel Model
SIMO	Single-Input Multiple-Output
SISO	Single-Input Single-Output
SNR	Signal-to-Noise Ratio
SP	Semi-Parallel architecture
SPUCA	Stacked Polarimetric Uniform Circular Array
SSD	Simultaneous Schur Decomposition
SUSVD	Sequential Unfolding SVD
SV	Saleh-Valenzuela model
SVD	Singular Value Decomposition
TDM	Time Division Multiplexing
TDoA	Time Delay of Arrival

Tx	Radio Transmitter
UCA	Uniform Circular Array
UKF	Unscented Kalman Filter
ULA	Uniform Linear Array
VA	Virtual Array architecture
VCR	Virtual Channel Representation
WB	Weischelberger Model
WiMAX	Worldwide Interoperability for Microwave ACceSs
WLAN	Wireless Local Area Network
w.r.t.	with respect to

List of symbols

\diamond	Khatri-Rao (column-wise Kronecker) product
\otimes	Kronecker product
\times_n	n^{th} -mode tensor product
\circ	Outer product
\odot	Schur-Hadamard (element-wise) product
$a^*, \mathbf{a}^*, \mathbf{A}, \mathcal{A}$	a scalar, a vector, a matrix, and a tensor \mathbf{A}
\mathbf{A}^*	Complex conjugate of \mathbf{A}
\mathbf{A}^H	Hermitian (complex conjugated) transpose of \mathbf{A}
\mathbf{A}^T	Transpose of matrix \mathbf{A}
$\Re\{\mathbf{A}\}$	Real part of \mathbf{A}
$\Im\{\mathbf{A}\}$	Imaginary part of \mathbf{A}
$\hat{\theta}$	An estimate of θ
$\text{diag}(\mathbf{A})$	Vector of the diagonal elements of \mathbf{A}
$\text{vec}(\mathbf{A})$	Stacks all the elements of \mathbf{A} into a vector
$a_i(t)$	complex coefficient for the i^{th} signal component at time t
$\mathbf{a}_r^{(n)}$	r^{th} basis vector of n^{th} mode (dimension)
$\mathbf{A}^{(n)}$	matrix of n^{th} mode basis vectors
$\mathbf{b}(\varphi, \vartheta)$	steering vector
\mathbf{B}	matrix of steering vectors
\mathbf{B}_f	frequency response
$\mathbf{B}_{R_{H/V}}$	Rx-array response for horizontal/vertical polarizations
$\mathbf{B}_{T_{H/V}}$	Tx-array response for horizontal/vertical polarizations
\mathbb{C}	set of complex numbers
\mathbf{D}	matrix of first order differentials (Jacobian matrix)
f	frequency
f_c	carrier frequency
f_s	sampling frequency
$G_{T/R}(f)$	frequency response of the Tx/Rx (excluding antennas)
$\mathcal{G}_{T_{pol}R_{pol}}$	super diagonal path weight core tensor
$h_{m_R m_T}$	channel coefficient between m_T^{th} Tx and m_R^{th} Rx antenna
$\mathbf{h}_S, \mathbf{h}_D, \mathbf{h}_N$	model vector for specular paths, DMC, and receiver noise
\mathbf{H}	MIMO channel matrix, or KF measurement matrix

\mathbf{H}_w	MIMO channel matrix with i.i.d $\mathcal{N}_C(0, 1)$ elements
\mathcal{H}	MIMO channel tensor
\mathbf{I}_M	$M \times M$ identity matrix
j	imaginary number $j = \sqrt{-1}$
$\mathbf{J}(\boldsymbol{\theta}, \mathbf{R})$	Fisher information matrix
k	discrete time (snapshot) index
\mathbf{K}	Kalman gain matrix
\mathcal{K}	channel tensor in eigendomain
\mathcal{L}	log-likelihood function
M	total number of samples in an observation
$M_{f/R/T}$	number of frequency samples/Rx/Tx antenna ports
\mathbf{n}	noise vector
N	number of data dimensions
N_{pol}	number of polarization (path weight) components
$\mathcal{N}(\mu, \sigma^2)$	normal distribution with mean μ and variance σ^2
$\mathcal{N}_C(\mu, \sigma^2)$	complex normal distribution with mean μ and variance σ^2
p	propagation path index
$p(x y)$	conditional probability of x given y
P	number of propagation paths
$\mathbf{P}^{(k k-1)}$	prediction error covariance matrix
$\mathbf{P}^{(k k)}$	filtering error covariance matrix
\mathbf{P}_S	signal covariance matrix
$\mathbf{q}(\mathbf{y} \boldsymbol{\theta}, \mathbf{R})$	score function
\mathbf{q}^{μ_i}	state noise variance for parameter μ_i
\mathbf{Q}	state noise covariance matrix
R	number of factors in a tensor decomposition
R_{pol}	Rx polarization (H or V)
\mathbf{R}	covariance matrix
\mathbf{R}_D	covariance matrix of the DMC
$\mathbf{R}_{f/T/R}$	covariance matrix for frequency/Tx/Rx dimensions
\mathcal{S}	Tucker model core tensor
t	time
T_m	time duration for measuring a single snapshot
T_{pol}	Tx polarization (H or V)
T_s	sample interval
\mathcal{T}	auxiliary tensor in SUSVD
\mathbf{u}	unitary vector
\mathbf{U}	(left-hand) unitary matrix
\mathbf{v}	state noise vector
\mathbf{V}	(right-hand) unitary matrix
\mathbf{w}	weight vector (normalized steering vector)
\mathcal{W}	power coupling tensor
\mathbf{x}	vector of transmitted signal

\mathcal{X}	a tensor-valued variable
\mathbf{y}	vector of received/measured signal
α	logarithm of path weight magnitude parameter
$\gamma_{HH/HV/VH/VV}$	complex path weight for H-H/H-V/V-H/V-V polarization
$\boldsymbol{\gamma}$	vector of all complex path weights
$\boldsymbol{\Gamma}_p$	complex path weight matrix for propagation path p
$\delta(\tau)$	Dirac delta function
Δt	Snapshot interval
$\Delta\mu$	Dynamic (rate of change) parameter
$\vartheta_{T/R}$	elevation angle of departure/arrival at Tx/Rx
$\boldsymbol{\theta}, \hat{\boldsymbol{\theta}}$	general model parameter vector and its estimate
$\boldsymbol{\lambda}$	vector of eigenvalues (diagonal elements of $\boldsymbol{\Lambda}$)
$\boldsymbol{\Lambda}$	diagonal matrix of eigenvalues
$\boldsymbol{\mu}$	structural (nonlinear) parameter vector
π	number Pi
$\boldsymbol{\Pi}_n^\perp$	projection matrix
σ	singular value
σ^2	variance
τ	time delay of arrival
ϕ	path weight phase
$\varphi_{T/R}$	azimuth angle of departure/arrival at Tx/Rx
$\boldsymbol{\Phi}$	state transition matrix
$\boldsymbol{\Omega}, \tilde{\boldsymbol{\Omega}}$	power coupling matrix and its element-wise square root

Chapter 1

Introduction

1.1 Motivation of the thesis

In recent years, the available data rates in wireless systems have grown by several orders of magnitude, and the demand for higher rates continues to increase in the future. The increasing data rates in wireless communications enable new emerging services. A shift of general Internet traffic from wired broadband access (DSL) to wireless networks is inevitably taking place as well. Already the amount of data traffic in cellular networks is locally exceeding the voice traffic.

While providing enabling technologies to the ever growing demands for increasing data rates, the researchers and system designers are, at the same time, required to take into consideration several issues such as reliability of the connection, reception coverage, interference among wireless systems and/or users, spectrum allocation, power management, cost effectiveness etc. One key technology considered for future wireless systems is the utilization of multiple antennas at both ends of a communication link [149]. These MIMO (Multiple-Input-Multiple-Output), MISO (Multiple-Input-Single-Output), or SIMO (Single-Input-Multiple-Output) systems provide improved performance in several different aspects [19, 98]. Multiantenna techniques rely on multipath propagation phenomenon in the radio channel. While for a conventional, single antenna radio link the multipath channel is considered disadvantageous, for multiantenna radio links the multipath can be exploited to gain improved performance. A MIMO system in combination with a rich multipath channel allows to separate signals in space, in addition to traditional time, frequency and code division multiplexing. This feature can be utilized in order to either increase data rate of a single communication link, increase the reliability of the link, or allow multiple user to share the same radio resources. Hence, a multiantenna system can improve the utilization of the scarce radio resources locally. Other advantages of wireless multiantenna communications include improved link reliability

and extended coverage (spatial diversity), interference management (cooperative MIMO) as well as new services such as direction finding for indoor positioning. The MIMO concept has already been adopted in recent and ongoing wireless standardization, including IEEE 802.11n (WLAN) [56], IEEE 802.16 (WIMAX) [57], MIMO HSDPA (3/3.5G) [2], IMT-Advanced [58] and 3GPP Long Term Evolution (LTE) [1]. So far, these standards deal with very limited MIMO configurations. Utilization of the full potential of MIMO requires further research in several aspects.

1.2 Scope of the Thesis

One of the important research fields in the area of multiantenna communications is the measurement-based modeling of the space-, time-, and frequency dependent wireless channels. Realistic channel models are important for studying the theoretical gains of multiantenna communications, transceiver development and design, as well as network planning. The approach of building models based on measurements provides realistic tools for analyzing the potential of new technological solutions. This is crucial in order to compare the performance of real systems in simulations, without the need of implementing everything in a prototype hardware.

This doctoral thesis deals with measurement-based modeling of propagation channels. The focus is on the estimation of the space, time, frequency, and polarization dependent double directional mobile MIMO radio channel model parameters [136, 137] from dynamic channel sounding measurements [5, 62–64, 68, 70, 73, 74, 90, 142, 144, 145]. The term double directional refers to the fact that the channel is characterized by directional properties at both ends of the radio link, revealing the overall spatiotemporal multipath structure of the MIMO propagation channel. An advanced channel sounding measurement setup along with sophisticated estimation techniques allows separation of the influence of the measurement equipment from the properties of the wireless channel itself. Such methodology provides a general characterization of the radio channel at a certain signal bandwidth and specified carrier frequency, without imposing any restrictive assumptions on a specific communication scheme or antenna configuration. The obtained results of such a *measurement-based channel modeling* (MBCM) scheme can be later applied for analyzing specific, realistic systems with given antennas and other operational parameters [51, 84, 140, 143, 147, 151, 155].

In mobile communications the channels are always time-varying and understanding the dynamic behavior of channel is crucial in order to obtain a realistic view on the performance of the system. Conventional techniques for obtaining estimates of the double directional propagation parameters are based on models which do not utilize the time dependence in the measured radio channel conditions. In this thesis the focus is on sequential estimation

techniques and state-space modeling of the dynamic radio channel. The proposed Extended Kalman filter (EKF) solution provides improvements both in terms of accuracy of the parameter estimates, as well as computational efficiency due to recursive operation. The approach to track the propagation paths over time also captures the evolution of individual paths over time providing further insight essential for the development of dynamic channel models.

Another important aspect in wireless channel characterization is to have the underlying measurement model as realistic as possible. At the same time the identifiability of the parametrization should be maintained. In this thesis the physical channel model includes both the contribution of deterministic, dominant propagation paths — characterized by the double directional path model [136, 137] — as well as a stochastic model for the distributed diffuse scattering, or the dense multipath component (DMC) [108]. It is shown that having both of these components in the channel model provides a better fit to the physical reality.

Part of the thesis focuses on methods, which enable computationally tractable solutions to the sequential estimation problem. These techniques are necessary in order to reduce the computational complexity, which results from processing high-dimensional data sets. At the same time it is important to avoid making simplistic assumptions on the channel model. For this purpose, a novel decomposition technique for multidimensional data arrays (tensors) has been developed. This so-called Sequential Unfolding SVD (SUSVD) has several applications in array signal processing. An important application — especially relevant in the context of this thesis — is the low rank tensor approximation. The PARATREE/SUSVD low rank approximation is applied to reduce computational complexity in the sequential estimation algorithm (EKF). Tensor decompositions also allow to reveal relevant information from very high dimensional data.

As the scope of this thesis is on characterization and estimation of the physical radio channel, it does not deal with communication theoretical or implementation aspects of MIMO systems. These subjects are comprehensively considered in [43, 96, 98, 149]. The discussion on the estimation of the MIMO propagation channel is also limited to the estimation of the parameters of the double directional propagation path model. Hence, the stochastic model for the DMC is treated as an underlying colored noise process and its estimation is out of the scope of this thesis. Further discussion on the DMC and its estimation can be found in [108, 111, 112, 114, 115, 117].

1.3 Contributions

The main contribution of the thesis is a novel framework for dynamic modeling and sequential estimation of the MIMO propagation path param-

ters from channel sounding measurements. The proposed approach has several advantages compared to current state-of-the-art methods such as SAGE [38, 39] or RIMAX [108–110] especially in terms of improved dynamic modeling and computational performance. The individual contributions of the thesis are the following:

1. Derivation of a state-space model for describing the dynamics of double directional propagation paths.
2. Developing a sequential estimation method stemming from EKF for tracking propagation parameters over time.
3. Expressing the EKF in a form that is computationally tractable even in the case of very large data dimensions and a large number of parameters tracked within the state vector.
4. Developing a method for adjusting the model order using statistical hypothesis testing for path detection and evaluation of the significance of the estimates.
5. Employing the hybrid channel model comprised of the propagation paths and a generalized model for the dense multipath component (DMC). The generalized DMC model relies on Kronecker model with unconstrained structure of the individual covariance matrices in different data dimensions.
6. Introducing a novel tensor decomposition having several applications in signal processing. An example application is a low rank approximation, employed to facilitate efficient computation of specific expressions in the EKF — a problem that has been emphasized by the generalization of the DMC model.
7. Identifying and expressing MIMO channel models in terms of well known tensor decompositions.

1.4 Structure of the Thesis

This compendium-type thesis is divided into an introductory part, and a collection of the seven original publications. The introductory part of the thesis is structured as follows. Chapter 2 provides a literature review of different approaches to wireless MIMO channel modeling. The measurement based channel modeling approach is described in detail, and the hybrid channel model characterizing the underlying physical propagation phenomena based on channel sounding measurements is introduced. Chapter 3 gives an overview of the state-of-the-art in the field of multidimensional parameter estimation for propagation models. The author’s contributions in

state-space modeling of propagation path parameters are described, as well as illustrative estimation examples are provided to demonstrate the benefits of the proposed method. Chapter 4 gives a brief introduction into tensor modeling and decompositions. A novel PARATREE model and the SUSVD technique developed in this thesis work are described, with application examples in array signal processing involving low rank tensor approximation. Chapter 5 summarizes the thesis.

1.5 Summary of Publications

This section provides a summary of the original publications listed on page xi. In all the listed publications the derivations, the programming and the writing has been performed by the author, whereas the co-authors have contributed to the development of the system model, estimation methods and designing the experiments.

In publication [I], the state-space model for the complete double directional propagation path model is derived. The Extended Kalman filter (EKF) is applied to sequentially estimate (track) the propagation path parameters. The issue of varying the state dimension, i.e., the number of paths to track is also addressed. The algorithms are implemented in MATLAB computing software [89]. The performance of the proposed solution is compared by simulation against a state-of-the-art iterative maximum likelihood (ML) solution, namely RIMAX [108, 109]. Also real world measurements from the TKK's channel sounder [74] are evaluated. In addition, it is shown by simulation that the proposed solution is very fast in computation time compared to RIMAX.

In publication [II] the dynamic model is extended by including the rate of change variables to improve the prediction performance. Also the model order reduction problem is formulated in the form of the Wald test [66]. Simulations results are provided to confirm the usefulness of the model extension. Real world data from a RUSK channel sounder [90] measured by TU Ilmenau is used in the analysis [146]. The publication [II] was awarded the "Best Student Paper Award" at EUSIPCO 2006 conference in Florence, Italy.

In publication [III] the main contribution is the derivation of a CUSUM [47] path detection scheme in order to increase the model order in the sequential estimation when necessary. The proposed path detection technique is based on statistical evaluation of the whiteness of the residual sequence after subtracting the estimated paths and pre-whitening the data. The method provides further savings in computational cost compared to an exhaustive Maximum Likelihood (ML) based grid search.

In publication [IV] the model for the diffuse scattering is extended to a Kronecker model with unconstrained structure of the individual covariance

matrices in different data dimensions. Compared to earlier solutions where the diffuse scattering was assumed to be spatially white, this more general model adds computational complexity in the EKF expressions. A low rank tensor approximation is proposed in order to reduce the computational cost of the solution. This tensor decomposition has been later refined and studied in detail in publications [VI] and [VII].

Publication [V] is a comprehensive description of the state-space modeling approach discussed in publications [I–IV]. Additional contributions include the derivation of the dynamic model and its parametrization, especially focusing on the prediction model of the complex-valued path polarization coefficients. The state dimension adjustment is also described in detail and several illustrations on the estimation results with real world channel sounding data are provided.

In publication [VI] the low rank approximation introduced in publication [IV] is formulated in detail. The new tensor model is named PARATREE. The name stems from having close relation to PARAFAC [54, 79] family of tensor models. Moreover it relies on a hierarchical tree structure resulting from the proposed Sequential Unfolding Singular Value Decomposition (SUSVD) — a method to form the PARATREE model from orthogonal rank-1 tensors. An application example in noise suppression for channel sounding data is provided.

Publication [VII] is an extended description of the PARATREE/SUSVD decomposition. The proposed solution is compared against well known PARAFAC [54, 79] and Tucker [150] (HOSVD [29]) tensor models. The advantages of the proposed solution are illustrated through two application examples, the complexity reduction in algorithms [IV] and the measurement noise suppression [VI].

Chapter 2

MIMO Radio Channel Modeling

This chapter discusses modeling of Multiple-Input Multiple-Output (MIMO) Radio Channels. MIMO systems has been an increasingly popular research area in the wireless communications community during the last 10–15 years [41]. Wireless MIMO systems are based on the spatial degrees of freedom that arise from the utilization of multiantenna transceivers. MIMO offers improvements in terms of increased capacity, link reliability, interference mitigation, and SNR gain. However, not all of these benefits can be obtained simultaneously. Only recently MIMO has been adopted in technology standardization as well (IEEE 802.11n [56], WiMAX [57], 3GPP LTE [1]). The proposed MIMO configurations in these standards use only few transmit and receive antennas. This is partly due to hardware limitations, especially lack of space, manufacturing cost, as well as constraints on power consumption in battery operated mobile terminals. Another aspect is that the formulation of proper channel models to support the development of MIMO terminals, and related network planning, is still under development. Realistic modeling is necessary in order to fully understand and exploit all the gains available in MIMO systems.

The focus in this chapter is in MIMO channel modeling. For further reading on MIMO communications in general, including detailed description on information theoretic aspects, different space-time coding techniques, and fundamental tradeoffs in MIMO communications, see [96, 98, 149]. A thorough description of wireless communications in general can be found in [93].

This chapter is structured as follows. Section 2.1 introduces the MIMO communication system model. Also the concept of multipath propagation is introduced to facilitate the description of MIMO channel modeling approaches. Section 2.2 provides a review of various approaches to model the MIMO radio channel. Section 2.3 is dedicated to the measurement-based

channel modeling approach, which is one of the main topics of this thesis. Furthermore, the underlying propagation model, which is considered as the measurement model in the parameter estimation in Chapter 3, is introduced. Section 2.4 concludes the discussion on MIMO modeling.

2.1 MIMO System Model

2.1.1 MIMO Principle

The principle of a MIMO communication system [98, 149] is illustrated in Figure 2.1. The system in Figure 2.1 has multiple (M_T) transmit (Tx) antennas and multiple (M_R) receive (Rx) antennas. The coefficients $h_{m_R m_T}$ of the spatial channel between each Tx-Rx antenna pair are typically represented by a narrowband MIMO channel matrix

$$\mathbf{H} = \begin{bmatrix} h_{11} & \cdots & h_{1M_T} \\ \vdots & \ddots & \vdots \\ h_{M_R 1} & \cdots & h_{M_R M_T} \end{bmatrix}. \quad (2.1)$$

The input-output relation of a MIMO system may be given by the linear model

$$\mathbf{y} = \mathbf{H}\mathbf{x} + \mathbf{n}, \quad (2.2)$$

where the vector $\mathbf{y} \in \mathbb{C}^{M_R \times 1}$ denotes the received signal sampled at M_R Rx antenna ports, the vector $\mathbf{x} \in \mathbb{C}^{M_T \times 1}$ contains the samples of the transmitted symbols transmitted from M_T Tx antenna ports, and the vector $\mathbf{n} \in \mathbb{C}^{M_R \times 1}$ denotes samples of the receiver noise. Note that the coefficients in (2.1) include the influence of both the physical wireless propagation medium as well as the response of individual antennas and the corresponding RF (radio frequency) parts. The main driver for MIMO technology is the fact that MIMO systems have the potential to increase the capacity of a communication system as a linear function of $\min(M_R, M_T)$ without increasing transmit power or expanding bandwidth. This requires that the channel matrix \mathbf{H} in (2.1) has full rank [149].

2.1.2 Multipath Propagation

Radio communications are based on transmitting signals via electromagnetic wave propagation through a given medium. Before reaching the receiver, the signal is subjected to various physical propagation phenomena. These interactions include reflections, diffraction, scattering, absorption etc. [126]. The result is that each of the receiving antennas observes multiple realizations of the transmitted signal having individual delays, magnitudes, polarization behavior, as well as directional characteristics. In wireless communications

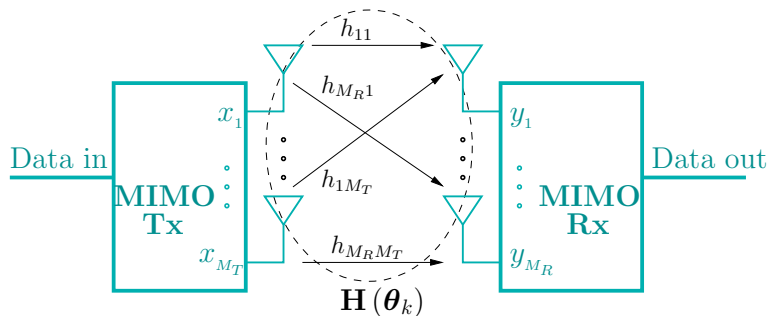


Figure 2.1: Description of the multiantenna communication, i.e., MIMO principle.

these mechanisms are commonly classified under the term *multipath* propagation, which is illustrated in Figure 2.2. Multipath propagation has a deteriorating influence on the received signal due to the constructive and destructive superposition of incoherent signal components leading to *fading*. Therefore, in conventional radio systems it has been considered as an impairment. Furthermore, the information carrying signal has some bandwidth. In a multipath environment the result is that all the frequencies in the signal band reach the receiver along each of the propagation *paths*, and the observed phase shift of the signal at different frequencies depends on the electric length of the individual signal paths. As a result, the fading of the received signal is frequency dependent due to either destructive or constructive effect from the combination of the individual components. In addition the channel may not be static, i.e., either the Tx or the Rx (or both) may be mobile, or interacting objects in the environment may be moving. Hence, the channel is also varying over time, which translates to Doppler shift. This kind of dynamic wireless channel is called *selective*. The time-frequency-space selectivity of the channel is commonly characterized by respective measures of coherence time, coherence bandwidth, and coherence distance. Without going into details, these measures describe the correlation of the channel in each domain, i.e., how rapidly the channel changes in each dimension, respectively (see e.g. [93, 149] for details).

Double Directional Propagation Path Model

The effects of different electromagnetic propagation mechanisms leading to multipath fading are commonly modeled by considering the channel as a sum of discrete propagation paths. This model assumes that the paths result from interactions in the far-field of the antennas. Hence, the signal components can be modeled as plane waves and the propagation interactions can be described through ray-optical simplifications. An illustration of a propagation path is shown in Figure 2.3. A path is characterized by

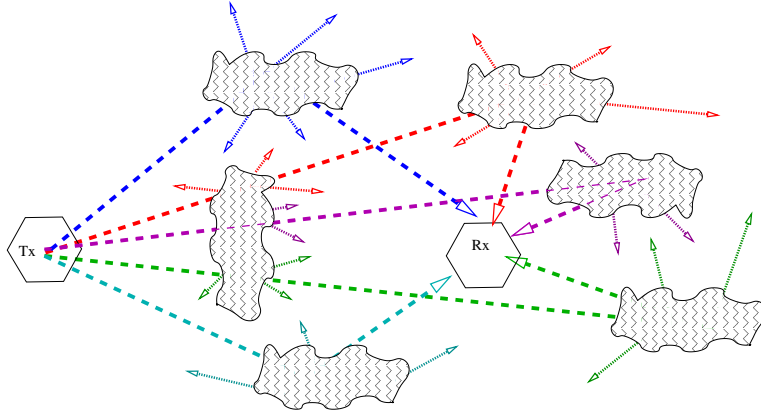


Figure 2.2: Illustration of multipath propagation. Different electrical path lengths not only yield different signal amplitudes, but result in a received signal having frequency dependent phase. The superposition of such signal components yields frequency dependent fading.

geometrical parameters such as time delay of arrival τ (TDoA), direction of arrival (DoA) in φ_R (azimuth), ϑ_R (elevation), direction of departure (DoD) in φ_T (azimuth), $\vartheta_{T,p}$ (elevation), as well as complex coefficients γ_{HH} , γ_{HV} , γ_{VH} , and γ_{VV} , describing co- and cross polarimetric properties of the path. The instantaneous MIMO channel transfer function as a superposition of such propagation paths can be written as

$$\mathbf{H}(f, \boldsymbol{\theta}) = G_R(f) \sum_{p=1}^P \left\{ \mathbf{B}_R(\varphi_{R,p}, \vartheta_{R,p}) \mathbf{\Gamma}_p \cdot \mathbf{B}_T^T(\varphi_{T,p}, \vartheta_{T,p}) e^{-j2\pi f \tau_p} \right\} G_T(f), \quad (2.3)$$

where $G_R(f)$ and $G_T(f)$ denote the frequency responses of the receiver and transmitter RF-chains, and $\mathbf{B}_R(\varphi_R, \vartheta_R) = [\mathbf{b}_{RH}(\varphi_R, \vartheta_R) \ \mathbf{b}_{RV}(\varphi_R, \vartheta_R)] \in \mathbb{C}^{M_R \times 2}$ and $\mathbf{B}_T(\varphi_T, \vartheta_T) = [\mathbf{b}_{TH}(\varphi_T, \vartheta_T) \ \mathbf{b}_{TV}(\varphi_T, \vartheta_T)] \in \mathbb{C}^{M_T \times 2}$ model the response of each port in the antenna arrays for two polarizations as a nonlinear function of the signal direction φ_i, ϑ_i . The antenna responses can be modeled using, e.g., the Effective Aperture Distribution Function (EADF) [62, 82, 83, 108] or spherical harmonics [33, 52]. These models can be obtained either through analytical description of the array geometry or based on calibration measurements. The matrix $\mathbf{\Gamma}_p$ contains the polarization coefficients of the p^{th} path, and is defined as

$$\mathbf{\Gamma}_p = \begin{bmatrix} \gamma_{HH,p} & \gamma_{VH,p} \\ \gamma_{HV,p} & \gamma_{VV,p} \end{bmatrix}. \quad (2.4)$$

It should also be noted that this double-directional superposition of propagation paths model (2.3) is a wideband model. However, it is valid as

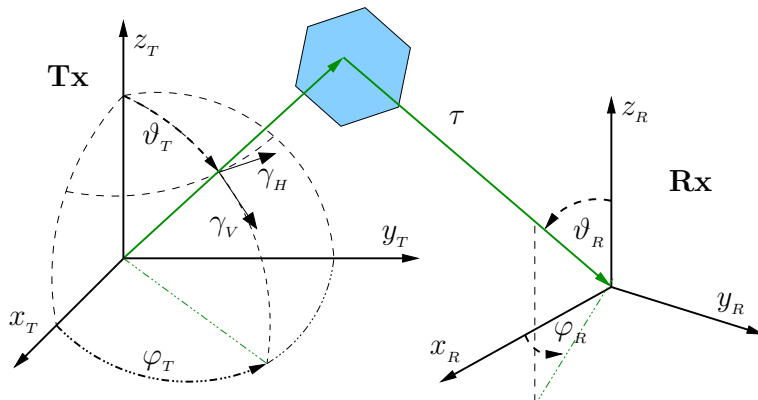


Figure 2.3: An illustration of a discrete propagation path and the geometrical and polarimetric parameters characterizing it.

such only over a limited frequency band, as the response of the antenna arrays as well as the interaction of the propagating waves with objects in the environment should be uniform within the signal bandwidth. The instantaneous realization of the *propagation channel* itself is characterized by the parameters

$$\boldsymbol{\theta}_S = [\boldsymbol{\tau}^T \boldsymbol{\varphi}_T^T \boldsymbol{\vartheta}_T^T \boldsymbol{\varphi}_R^T \boldsymbol{\vartheta}_R^T \boldsymbol{\gamma}_{HH}^T \boldsymbol{\gamma}_{HV}^T \boldsymbol{\gamma}_{VH}^T \boldsymbol{\gamma}_{VV}^T]^T, \quad (2.5)$$

whereas the *complete MIMO channel* is comprised of the system specific responses, i.e., $G_i(f)$ and \mathbf{B}_i in (2.3). The mapping of the parameters (2.5) to the basis functions \mathbf{B}_i is defined in [V], and a more comprehensive description may be found in [108]. The MIMO channel modeled as a superposition of propagation paths is often referred as the double directional channel model [91, 136, 137]. The model (2.3) has a very nice property of isolating the influence of the measurement system, including the antenna arrays, from the propagation channel. This is crucial for the measurement-based channel modeling approach, discussed in Section 2.3. The beauty of such framework is that after obtaining the propagation path parameters in (2.5) from measurements or simulation, one can reconstruct the channel for arbitrary antenna configurations, whose description \mathbf{B}_i can equally be obtained either by simulation or calibration measurement. This approach is extremely powerful for analyzing the performance of a MIMO system.

2.1.3 MIMO System in a Fading Channel

As it has been illustrated in the previous section, the wireless MIMO channel varies over frequency. Relating this into the system level MIMO description, the time and frequency dependent version of the MIMO channel matrix

in (2.1) can be written as

$$\mathbf{H}(t, \tau) = \begin{bmatrix} h_{11}(t, \tau) & \cdots & h_{1M_T}(t, \tau) \\ \vdots & \ddots & \vdots \\ h_{M_R1}(t, \tau) & \cdots & h_{M_R M_T}(t, \tau) \end{bmatrix}. \quad (2.6)$$

Note that each of the coefficients $h_{m_R m_T}$ can be expressed as a linear time-varying channel filter

$$h_{m_R m_T}(t, \tau) = \sum_i a_i(t) \delta(\tau - \tau_i(t)), \quad (2.7)$$

where δ denotes the Dirac delta function and a_i are complex coefficients for delays τ_i . Hence, the effect of mobile users, arbitrary propagation mechanisms of (possibly moving) scatterers, and all the complexities of solving Maxwell's equations can be reduced to a sum of complex coefficients a_i at different delays τ_i in (2.7). The frequency dependence under multipath fading is evident from the equivalent frequency domain presentation of (2.7), given by the Fourier transform of h as

$$H_{m_R m_T}(t, f) = \int_{-\infty}^{\infty} h_{m_R m_T}(t, \tau) e^{-j2\pi f \tau} d\tau = \sum_i a_i(t) e^{-j2\pi f \tau_i(t)}. \quad (2.8)$$

To conclude, the input-output relation in (2.2) for a fading channel (2.6) is given by the convolution of the channel and the transmitted signal as

$$\mathbf{y}(t) = \int_{\tau} \mathbf{H}(t, \tau) \mathbf{x}(t - \tau) d\tau + \mathbf{n}(t). \quad (2.9)$$

For a frequency flat channel, i.e., if the signal bandwidth is less than the coherence bandwidth, a single delay tap is sufficient to describe the channel, and $\mathbf{H}(t, \tau)$ in (2.9) simplifies to $\mathbf{H}(t)$ in (2.2). If the channel is constant over time, i.e., the channel coherence time is larger than the time span of interest, then the channel simplifies to \mathbf{H} .

In the following section different approaches to model the MIMO channel (either only the spatial MIMO matrix (2.1) or the wideband MIMO channel (2.6)) are reviewed.

2.2 MIMO Channel Models — a Review

There are several types of models available for characterizing the spatio-temporal wireless medium for multiantenna communications. The models can also be classified in various ways. The choice of a model — as well as the classification among them — depends on given objectives and system assumptions. A convenient classification of MIMO channel models is

MIMO Channel Models

Physics-based	Analytical
<u>Deterministic:</u> <ul style="list-style-type: none"> - Ray tracing (TR) - Finite difference time domain (FDTD) - Method of moments (MoM) 	<ul style="list-style-type: none"> - Full correlation - Spatially white (i.i.d.) - Kronecker model - Weischelberger (WB) model
<u>Stochastic:</u> <ul style="list-style-type: none"> - Geometry based stochastic models (GSCM) <ul style="list-style-type: none"> • COST273, IST-WINNER, 3GPP - Nongeometrical stochastic models <ul style="list-style-type: none"> • Extended Saleh-Valenzuela (SVA), Zwick model 	<div style="text-align: center; padding: 5px;">Mixed</div> <ul style="list-style-type: none"> - Finite scatterer model (FSM) - Virtual channel representation (VCR) - Maximum entropy model
<u>Measurement based:</u> <ul style="list-style-type: none"> - Measurement system independent - Application specific 	

Figure 2.4: Classification of MIMO channel modeling approaches.

given in [4] along with a comprehensive model survey. A modification of that classification that suits better for the purpose of this thesis is given in Figure 2.4. The fundamental distinction of models is made among *physics-based*, *analytical*, and *mixed models*. However, it should be noted that many alternative classifications are possible, such as narrowband vs. wideband, field measurements vs. scatterer models [163]. Even for the classification in Figure 2.4, it is possible to argue about a particular model belonging to one class or another. The details of the models classified in Figure 2.4 will be discussed in the following.

2.2.1 Physics-based Models

The term *physics-based model* refers to the fact that such a model explicitly characterizes the electromagnetic propagation environment between the transmitter and receiver locations. This allows separate description of the antenna (array) structure at the transceivers and the description is also independent of the signal bandwidth. The characterization is typically based on the double directional multipath propagation model (2.3) [91, 136, 137], which constitutes an important part of the underlying measurement model in this thesis as well. The physics-based models can be further classified into *deterministic models*, *stochastic models*, and *measurement-based models*. Stochastic models can be further divided into *geometrical stochastic channel models* (GSCM) and *nongeometrical stochastic models*. Measurement-based modeling is discussed in detail in Section 2.3, whereas the others are summarized in the following.

Deterministic Propagation Models

Deterministic propagation models seek to characterize a specific radio environment in a predetermined level of detail. They can be very accurate and physically meaningful, but on the other hand they are only representative for a specific propagation environment of interest. In order to apply deterministic models, a detailed description of the environment is required. Depending on the approach, these requirements may include accurate descriptions of the geometry (2D/3D), material properties, weather conditions, people etc. The most widely used deterministic modeling approach is so-called *ray tracing* (RT) [18, 42, 80]. RT is typically based on the *uniform geometrical theory of diffraction* [75]. The idea is to find all possible paths that the signal can travel between the Tx and the Rx, and then apply a set of rules on the interactions between the propagating wave and the environment along each of the signal paths. In this way a good prediction of the received signal can be formed. The deterministic models may also include a statistical component to account for uncertainties such as diffuse scattering from surface roughness etc. [32]. RT tools are computationally very expensive. Therefore several methods have been developed in order to reduce the complexity [19]. RT modeling is best applicable in man made environments, where also the structural database can be assumed to exist. Other deterministic modeling approaches include the *method of moments* (MoM) [53], and the *finite difference time domain* (FDTD) [159]. These are very accurate field prediction models, but due to computational complexity, their applicability is constrained to structures with limited dimensions, e.g. antennas and their close vicinity.

Stochastic Propagation Models

Stochastic propagation models can be further divided into *geometry-based stochastic channels models* (GSCM) [10, 91, 92, 94, 95, 101] and *nongeometrical stochastic models* [156, 164]. The idea in GSCM is to determine the locations of terminals and scatterers in a random fashion according to some probability distributions, and apply simplified models for the interactions of the propagating wave with the scatterers. GSCM facilitates describing a physically meaningful time-evolution of the channel, as the time-varying behavior is determined by the motion of the transmitters, receivers, as well as the interacting objects. The influence of different scatterers can be controlled by employing visibility regions, i.e., not all of the generated scatterers necessarily contribute to the channel at all time instants. The parameters of the GSCM models are typically derived based on measurements, and are expected to represent typical values for each defined model scenario. The scattering in GSCM may be modeled as a single-bounce [10, 91, 94, 101, 157] (one interaction per path component) or double bounce [19, 92]. Single

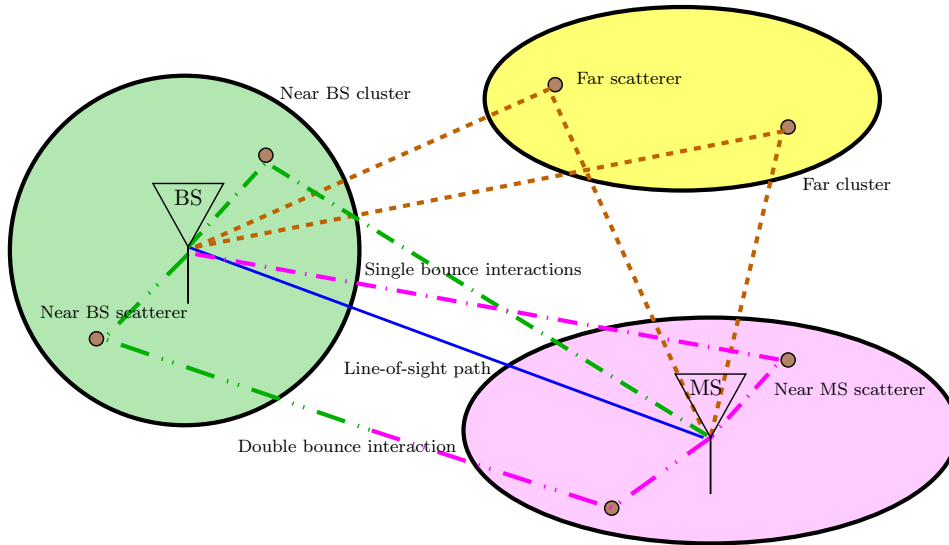


Figure 2.5: The GSCM principle. The channel is modeled as a superposition of paths interacting with different types of geometrically specified clusters of scatterers.

bounce models are suitable in macrocellular environment, where the scattering typically occurs only in vicinity of the mobile station (base station antennas are typically on a high mast). Double bounce models are valid also in micro- and picocell environments, such as indoors. Different GSCM models differ mainly in the way the scatterers are placed and how their interactions with the propagating radio wave are defined and parameterized. An illustration of the GSCM principle is shown in Figure 2.5 [19].

An example of a recent standardized GSCM type model is the *COST273 channel model* [19, 23]. The COST273 model is based on three types of clusters of scatterers. These include *i*) the *local cluster*, which is a ring of scatterers around mobile station (MS), basestation (BS), or both. *ii*) The *single-interaction cluster*, which is a single-bounce model representing a group of scatterers. *iii*) The *multiple-interaction cluster*, which describes the angular distribution of a cluster seen from the BS and mobile station MS independently. The COST273 model defines a large number of (in total 22) different environments. Although the number of parameters required for applying the model is limited, one of the remaining problems is to find realistic parameters for the clusters for each scenario [23]. Other popular, standardized GSCM type models include the WINNER models [8, 81] and their implementations [55, 124], which are based on the 3GPP Spatial Channel Model (SCM) [3, 125].

Nongeometrical stochastic models differ from the geometrical ones in that they do not explicitly model the geometry of the scattering environ-

ment. Instead, the channel realizations are based on paths, which are drawn from some statistical distributions of the parameters. Hence, the time evolution of the MIMO channel does not have a direct physical interpretation. An example of such model is the *Saleh-Valenzuela angular extended* (SVA) model [156], which extends the well known Saleh-Valenzuela (SV) model [120] by including angle of arrival (AoA) and angle of departure (AoD) information. The original SV model [120] uses doubly exponential decaying power model. The first profile models the power of each cluster and the second profile models the decaying power of the multipaths within clusters. The SVA model [120] includes additionally a uniform angular distribution of the clusters, and assumes a Laplacian distribution for the multipaths within each cluster [135]. Another example of a nongeometrical stochastic channel model is the so-called *Zwicky* model [164]. The main difference to the SVA model is that the multipath components are not clustered, i.e., each component is treated independently.

Measurement-Based Channel Modeling

Measurement-based channel modeling (MBCM) refers to the method where a measurement system along with parameter estimation techniques are employed in order to characterize the MIMO channel. A detailed discussion of the approach is given in Section 2.3. The approach differs from the other *physical modeling* approaches as follows:

- The results are specific to the measured environment as in deterministic modeling, but no environment database is explicitly required.
- Measurement-based modeling is often needed for determining the cluster/multipath parameter statistics for the stochastic models.
- The applied measurement system limits the generality of the results (bandwidth, antenna arrays, carrier frequency etc.).

An example of a physical modeling framework, which combines the SCM approach with the MBCM approach, has recently been introduced in [22]. The Random-Cluster Model [22] is based on the COST273 [19], and its cluster parameters are automatically estimated from channel sounding measurements. The model does not specify the geometry, but is solely based on cluster parametrization. Hence, the results of the model are specific to the measured environment.

2.2.2 Analytical Models

The purpose of the analytical models is to characterize the MIMO channel matrix (either (2.1) or (2.6)) without explicitly accounting for the propagation channel or having a detailed description of the array geometry. This

simplifies the simulation complexity significantly, which is especially desirable for large scale system level simulations. This subsection focuses on analytical modeling of the spatial MIMO matrix $\mathbf{H} \in \mathbb{C}^{M_R \times M_T}$ (2.1), i.e., the time- and frequency selectivity is ignored for now.

Correlation-Based Analytical Models

Correlation-based analytical models typically assume that the coefficients of the MIMO channel matrix \mathbf{H} (2.1) are zero-mean, complex circularly symmetric, normal distributed random variables. Then the second order statistics, i.e., the covariance matrix¹

$$\mathbf{R}_{full} = \text{E}[\text{vec}(\mathbf{H})\text{vec}(\mathbf{H})^H] \quad (2.10)$$

completely characterizes the spatial MIMO channel [19]. A realization of the channel can be simply drawn as

$$\text{vec}(\mathbf{H}_{full}) = \mathbf{R}_{full}^{\frac{1}{2}} \text{vec}(\mathbf{H}_w), \quad (2.11)$$

where \mathbf{H}_w denotes a matrix having each of its values drawn from $\mathcal{N}_C(0, 1)$, and $\mathbf{R}_{full}^{\frac{1}{2}}$ denotes any square root of a full rank matrix \mathbf{R}_{full} , e.g., given by Cholesky Factorization [44], satisfying $\mathbf{R}_{full}^{\frac{1}{2}} \mathbf{R}_{full}^{\frac{1}{2}H} = \mathbf{R}_{full}$. This is the most general form of a correlation model. However, as the array dimensions grow, the number of elements in the covariance matrix (2.10) increases quadratically, which can be an issue in terms of complexity and identifiability.

Spatial Whiteness

Spatial whiteness is the simplest analytical correlation-based model. In that model all the elements of the MIMO matrix \mathbf{H} are assumed to be *independent and identically distributed* (i.i.d.) with variance σ^2 . The full covariance matrix for this model is given by

$$\mathbf{R}_{i.i.d.} = \sigma^2 \mathbf{I}, \quad (2.12)$$

which yields a trivial realization of the channel as $\mathbf{H}_{i.i.d.} = \sigma \mathbf{H}_w$. Physical interpretation of this model is that the MIMO channel branches would be uncorrelated. Obviously this assumption is unrealistic, but the simplicity of the expression allows to derive closed form expressions for e.g. information theoretic analysis of MIMO systems [141]. The i.i.d. model has also been used for describing the spatial covariance matrices of a stochastic part of the radio channel model, namely the diffuse scattering component in [84, 108, 111, 145], as well as in publications [I–III].

¹The operation $\mathbf{h} = \text{vec}(\mathbf{H})$ stacks all the columns of a matrix \mathbf{H} as $\mathbf{h} = \text{vec}([\mathbf{h}_1 \cdots \mathbf{h}_{M_T}]) = [\mathbf{h}_1^T \cdots \mathbf{h}_{M_T}^T]^T$ as in the respective MATLAB [89] command.

Kronecker Model

The Kronecker model is a popular analytical correlation-based model [131]. It assumes that the spatial channel is separable at both link ends, yielding a model for the covariance matrix as²

$$\mathbf{R}_{kron} = \mathbf{R}_T \otimes \mathbf{R}_R. \quad (2.13)$$

A realization of the Kronecker modeled MIMO channel matrix is given by

$$\mathbf{H}_{kron} = \mathbf{R}_R^{\frac{1}{2}} \mathbf{H}_w \mathbf{R}_T^{\frac{1}{2}\text{T}}. \quad (2.14)$$

A physical interpretation of the Kronecker model is that the spatial distribution of the scattering at both link ends is independent. The implication of this is that the transmitted signal at any DoD contributes to the received signal at each DoA (having nonzero angular power spectrum). Note that this independence is also assumed in the COST273 multiple-interaction cluster description [19, 23]. However, although single clusters have this Kronecker separability, this property does not hold for the complete channel which is a superposition of several clusters of scatterers [23]. The Kronecker model (2.10) has significantly fewer parameters than the full covariance model (2.10). This reduces memory requirements and complexity of the model. Moreover, it increases model identifiability from measured data as the matrices can be estimated with less parameters, and from fewer realizations of the MIMO channel matrix. The Kronecker model is considered for the diffuse scattering of the measurement model in publications [I–V, VII], which is discussed in detail in Section 2.3.3.

Weichselberger Model

The Weichselberger model (WB) [158] can be viewed as a generalization of the Kronecker model. It is based on the eigenvalue decomposition of the Tx and Rx correlation matrices

$$\mathbf{R}_T = \mathbf{U}_T \mathbf{\Lambda}_T \mathbf{U}_T^H, \quad (2.15)$$

$$\mathbf{R}_R = \mathbf{U}_R \mathbf{\Lambda}_R \mathbf{U}_R^H, \quad (2.16)$$

where $\mathbf{U}_{T/R}$ are unitary matrices having the eigenvectors of $\mathbf{R}_{T/R}$ at their columns, and $\mathbf{\Lambda}_{T/R}$ is a diagonal matrix containing the corresponding eigenvalues. The Weichselberger model introduces a power coupling matrix $\mathbf{\Omega}$

²The Kronecker product of \mathbf{A} ($m \times n$) and \mathbf{B} ($p \times q$) is a $mp \times nq$ matrix defined as

$$\mathbf{A} \otimes \mathbf{B} = \begin{bmatrix} a_{11}\mathbf{B} & \cdots & a_{1n}\mathbf{B} \\ \vdots & \ddots & \vdots \\ a_{m1}\mathbf{B} & \cdots & a_{mn}\mathbf{B} \end{bmatrix} \in \mathbb{C}^{mp \times nq}$$

connecting different Tx and Rx eigenmodes. Hence, a realization of the WB MIMO channel is given by

$$\mathbf{H}_{WB} = \mathbf{U}_R \left(\tilde{\mathbf{\Omega}}_{WB} \odot \mathbf{H}_w \right) \mathbf{U}_T^T, \quad (2.17)$$

where \odot denotes Schur (element-wise) product, and $\tilde{\mathbf{\Omega}}_{WB}$ is the element-wise square root of $\mathbf{\Omega}_{WB}$, defined as $\mathbf{\Omega}_{WB} = \tilde{\mathbf{\Omega}}_{WB} \odot \tilde{\mathbf{\Omega}}_{WB}$. In Section 4.3.1 the WB model is described using tensor notation, and the approach described in [158] for computing the coupling matrix is extended for the coupling tensor. It should be also noted that the Kronecker model is obtained as a special case of the WB with a rank-1 coupling matrix $\mathbf{\Omega} = \boldsymbol{\lambda}_R \boldsymbol{\lambda}_T^T$, where³ $\boldsymbol{\lambda}_{T/R} = \text{diag}(\boldsymbol{\Lambda}_{T/R})$.

2.2.3 Mixed models

The term *mixed models* refers to a class of (spatial) MIMO models, which have some characteristics of both physical and analytical models. In [4] these were referred to as *propagation motivated analytical models*, since they have a stronger relation to the physics of the radio wave propagation than the purely analytical models. Mixed models include the *finite scatterer model* [13], the *virtual channel representation* [127], as well as the *maximum entropy model* [31].

Finite Scatterer Model

The Finite Scatterer Model (FSM) [13] describes the MIMO channel as a superposition of a finite number of multipath components, that are treated according to ray-optical concepts (plane waves). In [4, 19] the FSM model is classified among analytical models, although it explicitly allows for the separation of the physical propagation channel from the antenna arrays and other system responses. The formulation of the FSM for the spatial MIMO matrix is given as [19]

$$\mathbf{H}_{FSM} = \mathbf{B}_R \left(\tilde{\mathbf{\Omega}}_{FS} \odot \mathbf{H}_w \right) \mathbf{B}_R^T, \quad (2.18)$$

where $\mathbf{B}_{T/R} \in \mathbb{C}^{M_{T/R} \times P}$ denotes the matrices of Tx/Rx steering vectors corresponding to P multipaths, and $\tilde{\mathbf{\Omega}}$ is defined as for the WB model. The coupling matrix $\mathbf{\Omega}_{FS}$ is always diagonal if single bounce scattering is assumed, and it can be formulated as a diagonal matrix for multiple scattering as well by increasing P . The multipath parameters defining the steering vectors may be drawn from, e.g., assumed statistical distributions.

³The operation $\mathbf{a} = \text{diag}(\mathbf{A})$ extracts the elements on the diagonal of \mathbf{A} into a column vector \mathbf{a} .

Virtual Channel Representation

The Virtual Channel Representation (VCR) [127] models the MIMO channel in beamspace, which effectively means that the channel is transformed from the domain of the antenna elements to the angular domain. The spatial coupling is then modeled using *virtual DoAs and DoDs*. This is done by combining contributions from predefined, unitary steering matrices $\tilde{\mathbf{B}}_{T/R}$ as

$$\mathbf{H}_{VCR} = \tilde{\mathbf{B}}_R \left(\tilde{\mathbf{\Omega}}_{VCR} \odot \mathbf{H}_w \right) \tilde{\mathbf{B}}_T^T. \quad (2.19)$$

Hence, the matrices $\tilde{\mathbf{B}}_{T/R}$ represent the virtual DoAs and DoDs, and the coupling matrix $\tilde{\mathbf{\Omega}}$ determines their connections. The linearity of the model in the fixed virtual directions facilitates convenient expressions for information theoretical analysis, but the physical relation of the representation to the actual DoAs and DoDs is not explicit in the model.

Maximum Entropy Model

The Maximum Entropy Model [31] is based on formulating the MIMO channel model from an information theoretic point of view. The model is based on maximum entropy principle, i.e., for any given state of knowledge on the physical constraints, the model is expressed through probability distributions maximizing the model entropy. This approach avoids any limiting model assumptions that are not supported by prior information. The model is hence given in as general form as possible, and additional prior information, such as bandwidth, angular distributions or specific DoAs etc., can be flexibly incorporated in the model as necessary. Any unknown parameters can be treated through marginal probability distributions [31].

2.3 Measurement-Based Channel Modeling

This section is dedicated to the concept of measurement-based channel modeling (MBCM). The approach is motivated in Section 2.3.1. The channel sounding measurement methodology is introduced in Section 2.3.2. Section 2.3.3 describes the MIMO propagation channel measurement model applied in the parameter estimation in Chapter 3.

2.3.1 Motivation

In this thesis, the MBCM is considered to be an approach to model the time-, frequency- and space-dependent MIMO radio channel using measured data. The goal is to derive and estimate the parameters of a MIMO propagation channel model, that are independent of the applied measurement system. These model parameters can then be utilized for various purposes. An

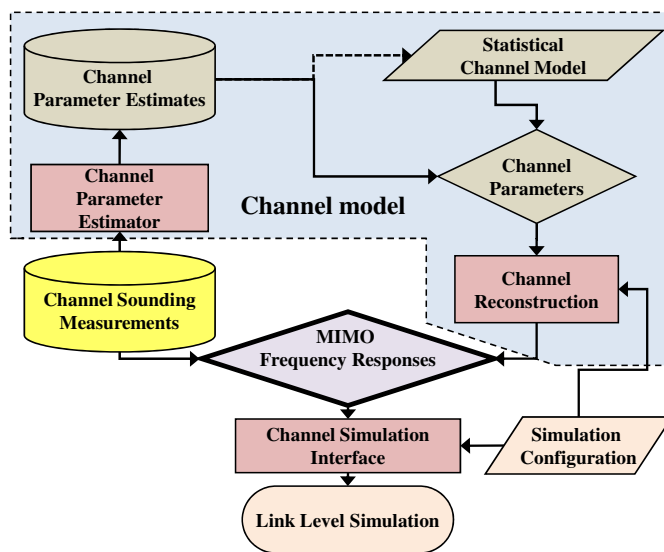


Figure 2.6: Measurement-based channel modeling (MBCM) framework.

illustration of the MBCM framework is given in Figure 2.6. The MBCM framework includes (either requires or enables) the following procedures

- Conducting MIMO channel sounding measurements (necessary requirement),
- Estimating the channel model parameters from measurement data,
- Deriving model statistics for parameterizing and improving current channel models,
- Reconstructing channel realizations for simulation purposes using measurement-based parameters or, alternatively,
- Applying the measured channels directly in simulations (propagation effects remain coupled with the antennas used in the measurements).

Also the quality of the parameter estimates should be evaluated for model refinement and estimator development purposes.

The measurement-based channel modeling approach allows ideally to separate the influence of the measurement antenna system from the MIMO propagation channel. This requires that the measurement equipment is properly calibrated, both in terms of the system frequency response as well as the directional and polarimetric response of the antenna arrays, see (2.3). If these requirements are met, then the estimation results obtained by employing a proper high resolution parameter estimator along with a realistic channel model, can achieve a valid description the propagation environment. However, the applicability of such results is limited in several ways, including

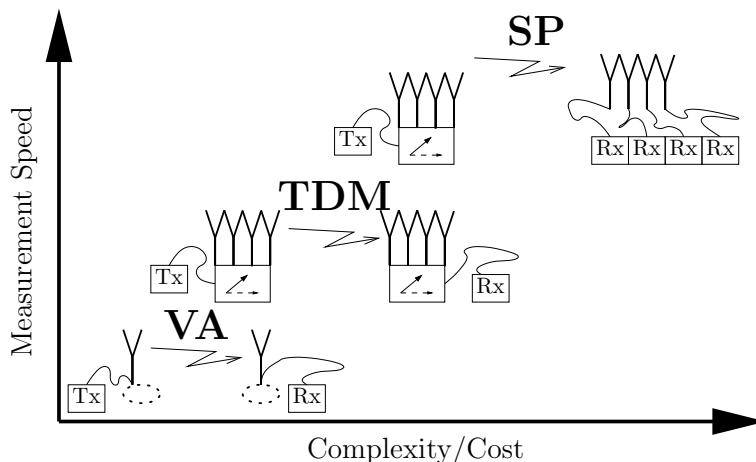


Figure 2.7: MIMO channel sounding architectures: virtual arrays (VA), switched architecture (TDM), and semi-parallel (SP) architecture.

- *Carrier frequency* — the interaction of radio waves with the propagation environment is typically very different at different frequencies, e.g., 100 MHz, 1 GHz, or 5 GHz.
- *Signal bandwidth* — influences especially the delay resolution, but has influence also on model assumptions such as frequency selectivity of the antennas and other propagation interactions.
- *Transmit power* — regulated by standards or licenses in order to avoid interference with other systems.
- *Angular and polarimetric resolution* — depends on the employed antenna arrays and their calibration.

The results are also specific to the measurement location. For further discussion on MBCM limitations, see [83]. The advantage of the MBCM approach is that the obtained results of such a scheme can be later applied for analyzing specific, realistic systems with given antennas and other operational parameters (see, e.g., [51, 84, 140, 143, 147, 151, 155]).

2.3.2 Channel Sounding Measurement Methodology

There are three basic architectures for measuring the MIMO radio channels: virtual arrays (VA), switched architecture (or time division multiplexed, TDM), and semi-parallel (SP) architecture. The classification of these in terms of implementation cost vs. measurement speed is illustrated in Figure 2.7.

Table 2.1: Typical parameter values for the TKK channel sounder [74].

	Label	Value
Frequency samples	M_f	193
Transmitter ports	M_T	32
Receiver ports	M_R	32
Bandwidth	$B = \frac{1}{T_s}$	120 MHz
Snapshot duration	T_m	~ 3 ms
Snapshot interval	Δt	~ 40 ms

Virtual Array

The virtual array (VA) approach refers to a setup where a single antenna at both ends of the link is mechanically moved by a scanner [104]. The pattern of movement can be modified to form an arbitrary *virtual MIMO array* configuration. This approach is cost effective. However, the measurement of a single MIMO channel matrix takes a very long time. Hence, only completely static environments can be considered. Other drawbacks in the VA approach include: 1) The coupling of the antenna elements is not captured as there is only a single element present. This is good from a channel measurement point of view, but it limits the applicability of the data as such in a MIMO system simulation. 2) The phases of the local oscillators at Tx and Rx must be stable.

Switched Array

The switched array (TDM) architecture is probably the most widely applied technique, especially among the commercial channel sounders [36,90]. In the TDM approach an antenna array is employed at both link ends, and the orthogonality of the measured channels between each Tx-Rx antenna pair is achieved by synchronized switching of the antenna ports. The structure of a snapshot of data from a TDM sounder is illustrated in Figure 2.8. The achievable measurement rate $1/\Delta t$ is limited by the number of channels to measure $M_T \cdot M_R$, the sampling frequency $f_s = 1/T_s$ and sampling duration $M_f \cdot T_s$, as well as data buffering capacity and storage speed ($\Delta t = N \cdot T_m$). Additionally, each channel is typically measured twice to ensure sufficient guard time to avoid any effects from antenna switching. To conclude, achieving sufficient temporal sampling rate while conducting TDM MIMO channel sounding measurements, involves making a tradeoff between the number of channels to measure vs. mobility of the environment or transceivers (the maximum Doppler frequency should be less than $1/(2\Delta t)$). Table 2.1 lists the parameters of a typical measurement configuration used for the TKK channel sounder [74].

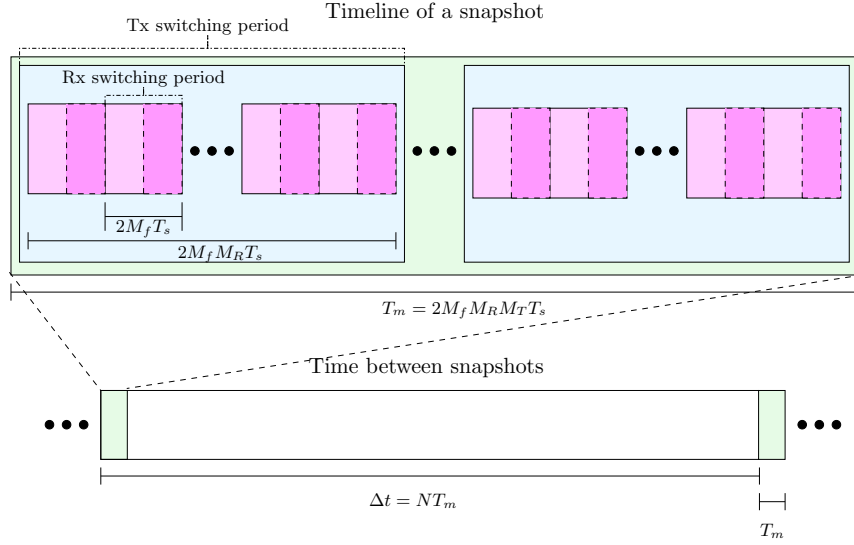


Figure 2.8: The structure of a snapshot obtained by switched channel sounder.

Figure 2.9 shows an example of three antenna arrays along with their switches. The Stacked Polarimetric Uniform Circular Array (SPUCA) [85] has in total $4 \cdot 16 = 64$ elements ($2 \cdot 64 = 128$ ports), but the switch seen in Figure 2.9 limits the operability to 32 ports. Also the Polarimetric Semi-Spherical Arrays (PSSA) have 20 elements (40 ports), but the switches limit the operability to 32 ports.

Semi-Parallel Architecture

The semi-parallel architecture in Figure 2.7 refers to a setup where the Tx uses time-division to separate the channels, whereas all the Rx elements measure at the same time. As switching is conducted only at one link end, this approach allows significantly faster measurements speeds. However, the measurement rate is also limited by the data buffering and storage capabilities. Also the cost of such system is much higher due to M_R receivers required at the Rx.

Recently, channel sounding measurements have been conducted using a dual-sounder setup (one Tx and two Rx units) for multi-link characterization [5, 70, 73]. This setup allows to capture the truly simultaneous channel conditions for two interfering radio links. The approach can be viewed as something between the TDM and SP approaches, as both Rx units measure simultaneously (although individually the switching is purely TDM-based).

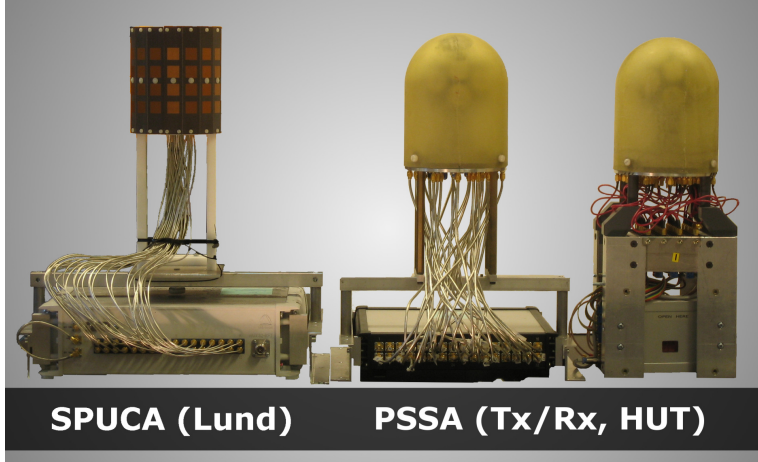


Figure 2.9: Three antenna arrays applied in dual link channel sounding measurements [5, 70, 73]: Stacked Polarimetric Uniform Circular Array (SPUCA) [85] and two Polarimetric Semi-Spherical Arrays (PSSA) [72, 74].

2.3.3 The Hybrid Channel Model

The MIMO propagation channel model employed for characterizing the *measured* MIMO channel transfer functions in [I–VII] is comprised of three model components: 1) Dominant propagation paths (\mathbf{h}_S), 2) Dense Multipath Component (DMC, or diffuse scattering, \mathbf{h}_D), and 3) Measurement noise (\mathbf{h}_N). The model is called a *hybrid channel model*, as it contains both a deterministic component, i.e., the propagation paths, as well as a random component, i.e., the DMC (and measurement noise). The vector form of the discretized, time-invariant version of the model with M_f frequency samples, M_R Rx ports and M_T Tx ports is defined as⁴

$$\mathbf{h} = \mathbf{h}_S + \mathbf{h}_D + \mathbf{h}_N \in \mathbb{C}^{M \times 1}, \quad (2.20)$$

where $M = M_f M_T M_R$. The individual model components are described in the following.

Dominant Propagation Paths

The dominant propagation paths component \mathbf{h}_S is a superposition of discrete multipaths obeying the double directional path model (2.3). The sampled version of (2.3) is given by

$$\mathbf{h}_S = \sum_{T_{pol}=\{H,V\}} \sum_{R_{pol}=\{H,V\}} \mathbf{B}_{T_{pol}R_{pol}} \cdot \boldsymbol{\gamma}_{T_{pol}R_{pol}}, \quad (2.21)$$

⁴The tensor version of the model is described in [VII] and Chapter 4.

where the matrices⁵

$$\mathbf{B}_{T_{pol}R_{pol}} = \mathbf{B}_{R_{pol}} \diamond \mathbf{B}_{T_{pol}} \diamond \mathbf{B}_f \in \mathbb{C}^{M \times P} \quad (2.22)$$

contain the basis functions (including systems responses G_i in (2.3)) for different polarization configurations of P paths (see [V] for details). The paths are described by geometrical parameters (DoAs, DoDs, propagation delays) as well as polarization coefficients, which are defined with respect to some reference directions of the Tx and Rx arrays and are assumed to obey ray optical (plane wave) modeling principles. The model does not explicitly include details on the nature of the interactions from which the individual paths result from (reflection, scattering, diffraction), or the multitude of them (line-of-sight, single bounce, double bounce). However, the nature and source of multipath components may be determined in post-processing, see e.g. [103]. The estimation of the parameters of the dominant propagation paths from dynamic channel sounding measurements [I–V] is the topic of interest in this thesis, and it will be further discussed in Section 3.4.

Dense Multipath Component

The Dense Multipath Component (DMC) is a necessary part of the MIMO channel model in order to provide means to mathematically describe the contribution of the rich diffuse scattering in the propagation channel, which can not be modeled by the dominant propagation paths. Another way to distinguish between a propagation path and DMC is through their time varying nature. If a channel would be constant, one may be able to fully reconstruct the whole channel transfer function using a very high number of propagation paths. However, this model fails if the channel changes even slightly. This is due to the fact that most of the individually less significant channel contributions result from a superposition of signals having different spatio-temporal structure. Moreover, the *true* dominant propagation paths will prevail within a larger spatial region. Especially in a dynamic channel while either one of the terminals, or possibly a source of propagation mechanism is moving, it is evident that, regardless of the measurement system, only part of the radio channel can be modeled using the dominant propagation paths. Figure 2.10 illustrates the influence of the DMC in a Power-Angular-Delay spectrum of a measured MIMO channel. After removing the estimated propagation paths (the peaks in Figure 2.10a), it is evident that a significant amount of energy in the channel remains unaccounted for. It should be noted that the profile in Figure 2.10b also contains measurement noise, which hides part of the DMC profile (as well as some weak propagation paths).

The DMC, i.e., the vector \mathbf{h}_D in (2.20), is assumed to be comprised of a large number of individually weak signal components. Therefore, owing to

⁵Operator \diamond denotes the Khatri-Rao product (column-wise Kronecker-product).

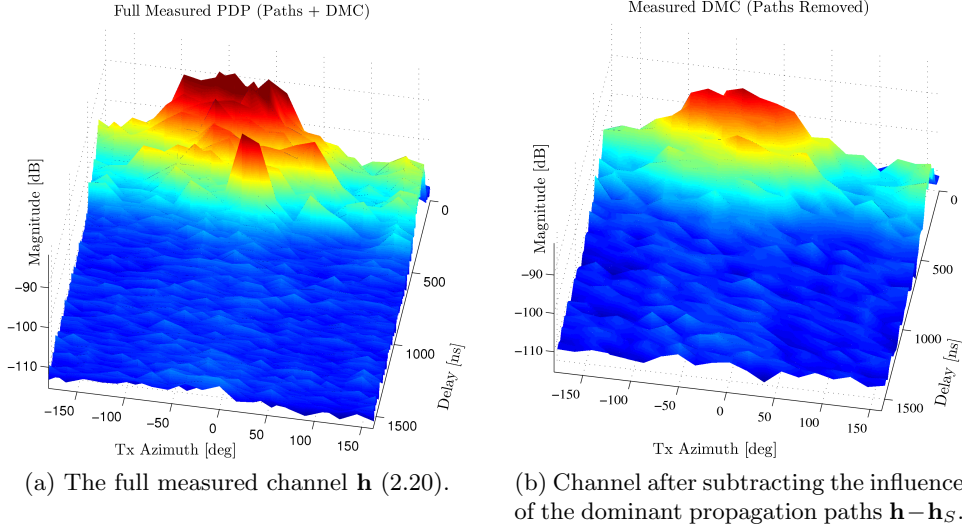


Figure 2.10: Instantaneous Power-Tx Azimuth-Delay-Profile from a MIMO measurement with 16 element circular array in a street scenario. The data is averaged over all receiver elements.

the central limit theorem, it can be modeled as a zero-mean complex circular symmetric normal distributed random vector

$$\mathbf{h}_D \sim \mathcal{N}_C(\mathbf{0}, \mathbf{R}_D), \quad (2.23)$$

with a covariance matrix $\mathbf{R}_D \in \mathbb{C}^{M \times M}$. As this matrix can become very large (see Table 2.1 for typical dimensions) it is necessary to enforce some structure for the DMC model. This is crucial for *i*) ensuring the identifiability (estimation) of the model, and *ii*) constraining computational complexity and memory requirements. The DMC is assumed to have structure both in delay as well as in angular domain, see publication [IV], [112]. In addition, the DMC is assumed to obey the Kronecker model (2.13), and the covariance matrix is defined as

$$\mathbf{R}_D = \mathbf{R}_R \otimes \mathbf{R}_T \otimes \mathbf{R}_f. \quad (2.24)$$

Estimation of the DMC covariance matrices is out of the scope of this thesis. An algorithm to estimate (2.24) is introduced in [115], whereas estimation of a simplified, spatially white ($\mathbf{R}_R = \mathbf{I}_{M_R}$, $\mathbf{R}_T = \mathbf{I}_{M_T}$) DMC model (applied also in publications [I–III]) is described in [105, 107, 108, 111, 113]. Further discussion on modeling the DMC can be found in [V], [112] and its contribution to MIMO capacity is analyzed in [114].

Measurement Noise

The measurement noise \mathbf{h}_N in (2.20) is assumed to be a white complex circular symmetric normal distributed random vector

$$\mathbf{h}_N \sim \mathcal{N}_C(\mathbf{0}, \sigma_N^2 \mathbf{I}), \quad (2.25)$$

with variance σ_N^2 . The measurement noise results from both thermal noise from the receiver electronics as well as ambient noise not induced by the transmitted signal.

2.4 Summary and Discussion

This chapter provides an overview of MIMO radio channel modeling. Table 2.2 summarizes the discussion on different modeling approaches by considering their applicability for specific purposes. The differences in the use of models depends on many factors, and the choice of a proper model depends on the task at hand. Typically higher level simulations require a model for the physical layer to be valid for a wide variety of environments, simple to implement and fast to compute, such as SCM or ACM. On the other hand, link level studies can afford a more detailed model having physical relevance, such as DCM or MBCM. Such models are also necessary for network coverage and transceiver design. On the other hand, ACM type of models are well suited for studying theoretical MIMO performance gains as they often facilitate establishing information theoretical results even in a closed form. To obtain similar statistically relevant results based on DCM or MBCM may require a large set of possible channel conditions to be representative, which can turn out to be very tedious in practice.

Table 2.2: Summary of MIMO channel modeling approaches.

Applicability	Approach			
	DCM ^a	SCM ^b	MBCM ^c	ACM ^d
System level simulations	-	++	+	+++
Network coverage	+	-	+	-
Link level analysis	+	(+)	++	-
Statistical analysis	(+)	-	(+)	++
Physical relevance	++	-	+++	--
Simplicity	--	+	+	+++
Generality	--	+	--	++

^aDeterministic Channel Models [18, 32, 42, 80]

^bStochastic Channel Models [8, 10, 19, 81, 91, 92, 94, 95, 101, 156, 157, 164]

^cMeasurement-Based Channel Models [22, 51, 84, 140, 143, 147, 151, 155]

^dAnalytical (and mixed) Channel Models [13, 31, 127, 131, 141, 158]

Measurement-based modeling is somewhat coupled with all the other modeling approaches as all models should be based on observations of the physical phenomena. On the other hand, MBCS also employs some underlying model(s), which typically belong to some of the other model categories. The hybrid channel model described in Section 2.3.3 is a combination of a deterministic propagation path model and a stochastic model for the diffuse scattering. This modeling approach is a good tradeoff between limiting the model dimensionality in terms of the number of parameters in the model vs. compliance with physical reality. It is also well suited for dynamic modeling and the related sequential estimation method introduced in the next chapter.

Chapter 3

Estimation of Propagation Model Parameters

This chapter addresses the problem of parameter estimation in the context of extracting the parameters of deterministic propagation paths of the hybrid channel model introduced in Section 2.3.3 from MIMO channel sounding measurements (see Section 2.3.2). The estimation problem is first defined in Section 3.1. Sections 3.2 and 3.3 provide a review of the estimation techniques developed for this application. Section 3.4 introduces the proposed state-space model and the sequential estimator. Some estimation examples are provided in Section 3.5. The discussion in Section 3.6 concludes this chapter.

3.1 Estimation Problem

The measurement model for MIMO channel sounding data observed at discrete time instances $k \in \{1, \dots, K\}$ is based on the hybrid channel model introduced in Section 2.3.3, and is given by

$$\mathbf{y}_k = \mathbf{h}_S(\boldsymbol{\theta}_{S,k}) + \mathbf{h}_D(\boldsymbol{\theta}_{D,k}) + \mathbf{h}_{N,k} \in \mathbb{C}^{M \times 1}. \quad (3.1)$$

The vectors \mathbf{h}_S , \mathbf{h}_D and $\mathbf{h}_{N,k}$, denote the model components for the dominant (specular-like) propagation paths, the diffuse scattering (DMC), and the measurement noise, respectively. The estimation problem boils down to finding the respective parameters $\boldsymbol{\theta}_{S,k}$, $\boldsymbol{\theta}_{D,k}$, (and σ_N^2) that minimize a given cost function while fitting the model to the observations $\mathbf{y}_{1,\dots,k}$. The parametrization depends on the choice of models for the individual components in (3.1), the employed measurement setup, as well as the dynamic nature of the model.

This thesis focuses on the estimation of the deterministic part \mathbf{h}_S (2.21) only, i.e., the parameters $\boldsymbol{\theta}_S$ of the dominant propagation paths. Hence, the parameters $\boldsymbol{\theta}_{D,k}$ and σ_N^2 of the distribution functions of the random

vectors \mathbf{h}_D (2.23) and \mathbf{h}_N (2.25) are assumed to be known, i.e., in practice they are estimated from the same set of data. From the estimation of the dominant propagation paths point of view, the measurement model can thus be reformulated as

$$\mathbf{y}_k = \mathbf{h}_S(\boldsymbol{\theta}_{S,k}) + \mathbf{n}_k \in \mathbb{C}^{M \times 1}, \quad (3.2)$$

where $\mathbf{n}_k \sim \mathcal{N}_C(\mathbf{0}, \mathbf{R}_k)$, with $\mathbf{R}_k = \mathbf{R}_{D,k} + \sigma_{N,k}^2 \mathbf{I}$, and $\mathbf{R}_{D,k}$ is defined in (2.24). The probability density of (3.2) is given by $\mathbf{y}_k \sim \mathcal{N}_C(\mathbf{h}_S(\boldsymbol{\theta}_{S,k}), \mathbf{R}_k)$. Hence, the DMC is treated as a colored normal distributed noise in the measurement model for the propagation paths.

The vector $\mathbf{h}_S(\boldsymbol{\theta}_S)$ models the propagation paths, see (2.3) and (2.21). The propagation path parameters $\boldsymbol{\theta}_S$ defined in (2.5) can be further divided into *structural* parameters

$$\boldsymbol{\mu} = [\boldsymbol{\tau}^T \boldsymbol{\varphi}_T^T \boldsymbol{\vartheta}_T^T \boldsymbol{\varphi}_R^T \boldsymbol{\vartheta}_R^T]^T \in \mathbb{R}^{5 \cdot P \times 1} \quad (3.3)$$

and weight parameters

$$\boldsymbol{\gamma} = [\boldsymbol{\gamma}_{HH}^T \boldsymbol{\gamma}_{HV}^T \boldsymbol{\gamma}_{VH}^T \boldsymbol{\gamma}_{VV}^T]^T \in \mathbb{C}^{4 \cdot P \times 1}, \quad (3.4)$$

yielding

$$\boldsymbol{\theta}_S = [\boldsymbol{\mu} \boldsymbol{\gamma}]. \quad (3.5)$$

The relationship of these parameters with the observation model for \mathbf{h}_S is revealed as the model (2.21) can be simplified to

$$\mathbf{h}_S = \mathbf{B}(\boldsymbol{\mu}) \cdot \boldsymbol{\gamma}, \quad (3.6)$$

where $\mathbf{B}(\boldsymbol{\mu}) = [\mathbf{B}_{HH}(\boldsymbol{\mu}) \mathbf{B}_{HV}(\boldsymbol{\mu}) \mathbf{B}_{VH}(\boldsymbol{\mu}) \mathbf{B}_{VV}(\boldsymbol{\mu})] \in \mathbb{C}^{M \times 4 \cdot P}$, see (2.22). The model (3.6) is nonlinear w.r.t. the structural parameters $\boldsymbol{\mu}$ (3.3). These real valued parameters describe the geometry of the double directional propagation paths and they are mapped to the observation through complex shift operations, see publication [V]. On the other hand, the complex valued polarization weights $\boldsymbol{\gamma}$ (3.4) are linear in the model. This is useful since it allows for minimizing a given cost function w.r.t. $\boldsymbol{\mu}$ only, as an estimate of $\boldsymbol{\gamma}$ can be computed in closed form for any $\boldsymbol{\mu}$ using a linear (weighted) least squares method.

To conclude, the problem of estimating the propagation path parameters is very demanding since it involves colored normal distributed noise, high data dimensionality, possibly correlated and closely spaced sources, polarization aspects, arbitrary array configurations as well as model order selection. In addition, as the channel sounding measurements are often acquired in mobile scenarios, there is typically only a single snapshot of data available for estimating the parameters of a channel realization.

Static Model		Dynamic Model
<u>Spectral-based</u>	<u>Maximum likelihood</u>	<u>Kalman filters</u>
- Beamforming (Bartlett, MVDR)	Stochastic ML	- Extended Kalman filter (EKF)
<u>Subspace-based</u>	Deterministic ML	- Unscented Kalman filter (UKF)
- MUSIC (spectral)	- SAGE	<u>Sequential Monte Carlo</u>
- ESPRIT (parametric)	- RIMAX	- Particle filter

Figure 3.1: Classification of nonlinear parameter estimation techniques based on different modeling assumptions.

A classification of nonlinear parameter estimation techniques is given in Figure 3.1, where the main distinction is made between *static* and *dynamic* modeling of the time evolution. In the following sections 3.2 and 3.3, a literature review is given covering different approaches for solving the propagation parameter estimation problem described in this section. The considered methods vary in several aspects, including underlying modeling assumptions. These differences are pointed out along with the description. The applicability of different methods for the given problem is also addressed.

3.2 Estimation of Static Model Parameters

Parameter estimators relying on the static model assume that the parameters of interest remain unchanged over the observation period. The classification of the static parameter estimation techniques in Figure 3.1 follows mainly the one presented already over 10 years ago in [77]. Since then, the interest in the context of MIMO radio channel parameter estimation has focused on ESPRIT-type algorithms, such as UNITARY-ESPRIT [50] and R-D-ESPRIT [48], as well as maximum likelihood (ML) based approaches including stochastic ML methods [59,97,106], and deterministic ML methods such as SAGE [38,39] and RIMAX [108–110]. The ML-based *high-resolution parametric estimators* are capable of estimating also the parameters of coherent signals, unlike the spectral-, or subspace-based techniques, whose performance may suffer drastically under such conditions. An overview of these techniques may be found also in [160].

3.2.1 Methods Based on Second Order Statistics of the Channel

The methods discussed in this subsection are based on the assumption that the measurement model, denoted by $\tilde{\mathbf{y}}_k$ to distinguish from \mathbf{y}_k in (3.2), is defined as

$$\tilde{\mathbf{y}}_k = \tilde{\mathbf{h}}_S(\boldsymbol{\theta}_{S,k}) + \tilde{\mathbf{n}}_k \in \mathbb{C}^{\tilde{M} \times 1}, \quad (3.7)$$

where $\tilde{\mathbf{h}}_{S,k} \sim \mathcal{N}_C(\mathbf{0}, \tilde{\mathbf{B}}(\boldsymbol{\mu})\mathbf{P}_S\tilde{\mathbf{B}}^H(\boldsymbol{\mu}))$, and $\tilde{\mathbf{n}}_k \sim \mathcal{N}_C(\mathbf{0}, \sigma_N^2\mathbf{I})$. The matrix $\mathbf{P}_S \in \mathbb{C}^{P \times P}$ in (3.8) is called the signal covariance matrix, and $\tilde{\mathbf{B}}(\boldsymbol{\mu}) \in \mathbb{C}^{\tilde{M} \times P}$ is defined as in (3.6), with the exception that $\tilde{\mathbf{B}}(\boldsymbol{\mu})$ here may denote only a subset of the model $\mathbf{B}(\boldsymbol{\mu})$ defined in (3.6) and (2.22). In fact, the $\tilde{\bullet}$ notation is used here to point out the fact that the model in (3.7) may represent only a subset of the full model in (3.2). This model dimensionality reduction can be in terms of number of measurement apertures, e.g., $\tilde{M} = M_R$, or polarization, e.g., $\tilde{\mathbf{B}}(\boldsymbol{\theta}_S) = \mathbf{b}_{R_V}(\varphi_R, \vartheta_R)$. Furthermore, it is assumed that $\mathbb{E}[\tilde{\mathbf{h}}_{S,k}\tilde{\mathbf{h}}_{S,l}^H] = 0$, for $k \neq l$. Hence, contrary to (3.2) where \mathbf{h}_S is considered as a deterministic mean, the model (3.7) indicates that $\tilde{\mathbf{y}}_k$ is a zero-mean circularly symmetric normal distributed random vector with the covariance matrix

$$\tilde{\mathbf{R}} = \tilde{\mathbf{B}}(\boldsymbol{\mu})\mathbf{P}_S\tilde{\mathbf{B}}^H(\boldsymbol{\mu}) + \sigma_N^2\mathbf{I}. \quad (3.8)$$

The methods described in this subsection are essentially based on these modeling assumptions.

Beamforming

Beamforming (BF) [152] is a basic spectral-based estimation method. In fact, it can be viewed as the direct spatial extension of the periodogram [139]. The idea is to mathematically steer the radiation main lobe of the antenna array in each direction and measure the corresponding energy level. Beamforming methods rely on an estimate of the covariance matrix (3.8), which is given by the sample covariance matrix as

$$\hat{\mathbf{R}} = \frac{1}{K} \sum_{k=1}^K \tilde{\mathbf{y}}_k \tilde{\mathbf{y}}_k^H. \quad (3.9)$$

The classical form of BF is the so-called *Bartlett* beamformer, and its power spectrum is given by

$$P_{BF}(\varphi, \vartheta) = \mathbf{w}^H(\varphi, \vartheta) \hat{\mathbf{R}} \mathbf{w}(\varphi, \vartheta), \quad (3.10)$$

where the weight vectors are defined as the normalized steering vectors (response of the antenna array)

$$\mathbf{w}(\varphi, \vartheta) = \mathbf{b}(\varphi, \vartheta) / \sqrt{\mathbf{b}^H(\varphi, \vartheta) \mathbf{b}(\varphi, \vartheta)}. \quad (3.11)$$

As a BF example, let us consider a reduced model $\tilde{\mathbf{y}}_k = \mathbf{y}_R \in \mathbb{C}^{M_R \times 1}$ for a vector of samples corresponding to the Rx array elements obtained from the transmitted signal of a single Tx antenna at a single frequency. Then

$\mathbf{b}(\varphi, \vartheta) = \mathbf{b}_{R_{H/V}}(\varphi_R, \vartheta_R)$, i.e., one also needs to consider the polarizations independently. The advantage of BF is that the obtained spectrum can be interpreted as the signal power of the channel in each DoA/DoD. The BF is simple to implement, and it also represents the maximum likelihood estimate for a signal direction in case of a single source [77]. Furthermore, BF in (3.10) does not require $\hat{\mathbf{R}}$ to be full rank. The downside is that the resolution is very limited and — regardless of the signal quality — the resolution can only be enhanced by increasing the number of sensors, which is often not possible due to physical limitations. This essentially prevents beamforming from providing statistically consistent DoA estimates for multiple-signal case [139].

The *minimum variance distortionless response* (MVDR) beamformer, also known as Capon's BF [14], is a modification of BF, and its spectrum is defined as

$$P_{MVDR}(\varphi, \vartheta) = \frac{1}{\mathbf{w}^H(\varphi, \vartheta) \hat{\mathbf{R}}^{-1} \mathbf{w}(\varphi, \vartheta)}, \quad (3.12)$$

The MVDR maintains a fixed gain in the direction of interest while minimizing the power contributed from any other direction. This leads to a significant improvement in the resolution compared to conventional BF. However, the MVDR has a requirement for the sample covariance matrix (3.9) to be invertible. The BF solutions do not scale well with an increasing number of parameters. Therefore, their applicability is mainly limited to a grid search to obtain an (initial) estimate of a single or a few parameters related to a specific measurement aperture, e.g., Rx/Tx data vector.

Subspace-Based Methods

The subspace-based methods include the *MUSIC* (Multiple Signal Classification) [9, 129, 130], different types of ESPRIT (Estimation of Signal Parameters via Rotational Invariance Techniques) algorithms [99, 119], as well as the RARE (RANK Reduction estimator) [100]. The subspace methods are based on the model (3.7). They rely on the eigenvalue decomposition of the covariance matrix (3.8), which may be defined as

$$\tilde{\mathbf{R}} = \mathbb{E}[\tilde{\mathbf{y}}\tilde{\mathbf{y}}^H] = \mathbf{U}\mathbf{\Lambda}\mathbf{U}^H = \mathbf{U}_s\mathbf{\Lambda}_s\mathbf{U}_s^H + \mathbf{U}_n\mathbf{\Lambda}_n\mathbf{U}_n^H, \quad (3.13)$$

where $\mathbf{U}_s \in \mathbb{C}^{\tilde{M} \times P}$ and $\mathbf{\Lambda}_s \in \mathbb{R}^{P \times P}$ denote the eigenvectors and eigenvalues associated with the signal subspace with P sources, whereas $\mathbf{U}_n \in \mathbb{C}^{\tilde{M} \times (\tilde{M}-P)}$ and $\mathbf{\Lambda}_n \in \mathbb{R}^{(\tilde{M}-P) \times (\tilde{M}-P)}$ denote those of the noise subspace, which is orthogonal to the signal subspace. The model (3.13) of the covariance matrix (3.8) is the basis of the subspace-based techniques.

The idea in the *MUSIC* algorithm [9, 129, 130] is to find the $P < M$ directions that minimize the projection of the steering vector to the whole

noise subspace. The so-called MUSIC pseudo-spectrum is then defined as

$$P_{MUSIC}(\varphi, \vartheta) = \frac{1}{\mathbf{w}^H(\varphi, \vartheta) \hat{\mathbf{U}}_n \hat{\mathbf{U}}_n^H \mathbf{w}(\varphi, \vartheta)}, \quad (3.14)$$

where $\mathbf{w}^H(\varphi, \vartheta)$ is defined in (3.11). The MUSIC pseudospectrum (3.14) should exhibit high peaks at P angles corresponding to the steering vectors orthogonal to the noise subspace. In general, the resolution of MUSIC is significantly better than beamforming methods. However, the performance of the MUSIC algorithm depends on the quality of the subspace estimates. This can be very limiting in high dimensional dynamic measurements where availability of independent realizations is scarce. Degraded performance occurs also if the weights $\boldsymbol{\gamma}$ in (3.6) for the signals of different directions are highly correlated [76]. The MUSIC algorithm can be extended for joint estimation of parameters in multiple dimensions, as in the *JADE* (Joint Angle and Delay Estimation) [153, 154].

The *ESPRIT* algorithm [99, 119] and its extensions [48, 50] rely on the rotational invariance property of the signal subspace induced by a translational invariance in the array used in the measurement. This means that it is only applicable for parameter estimation with array geometries, where the array may be divided into a number of equidistantly spaced and identical subarrays. However, ESPRIT doesn't require knowledge of the specific antenna responses, as long as the radiation patterns are identical for all the antenna elements. If these requirements are met, the parameters related to the dimensions for which the translational invariance property of the array applies can be estimated in a closed form.

The subspace methods require that there is a sufficient amount of realizations available to obtain reliable estimates of the subspaces. In dynamic channel sounding measurements the parameter estimation is typically based on a single snapshot of the measured data. *Spatial smoothing* [102] is a method that can be used to build up the rank of the covariance matrix for applying subspace-based techniques for multidimensional parameter estimation in such scenarios. However, this method decreases the effective measurement aperture dimensions, which translates to lowering the maximum number of separable signals, as well as degrading the accuracy of the estimates. Unlike for beamforming methods, the accuracy of both ESPRIT and MUSIC increases significantly with increasing number of available measurements or signal-to-noise ratio (SNR).

Stochastic Maximum Likelihood Methods

Stochastic ML methods [59, 97, 105, 106] are based on modeling the measured signal as a zero-mean normal distributed random vector as in (3.7) and (3.8). The estimation of the parameters is then based on maximizing the likelihood

function

$$p(\mathbf{y}|\boldsymbol{\theta}_S) = \frac{1}{\pi^M \det(\mathbf{R}(\boldsymbol{\theta}_S))} e^{-\mathbf{y}^H \mathbf{R}^{-1}(\boldsymbol{\theta}_S) \mathbf{y}}. \quad (3.15)$$

For estimating the propagation path parameters, the stochastic ML approach typically leads to a solution, which is computationally more demanding than the one relying on deterministic ML model discussed in the next subsection, see also discussion in [139, Appendix B]. However, it provides a natural means to estimate the parameters of the DMC [108]. Such an approach has been investigated for simplified model in [105], where the DMC was modeled using a mixture of Von Mises distributions [87] in azimuth direction.

3.2.2 Deterministic Maximum Likelihood Methods

Given the measurement model (3.2), the likelihood function, i.e., the probability distribution associated with an observation \mathbf{y} resulting from the deterministic model $\mathbf{h}_S(\boldsymbol{\theta}_S)$ (3.6) and a known noise covariance matrix \mathbf{R} , is given by

$$p(\mathbf{y}|\boldsymbol{\theta}_S, \mathbf{R}) = \frac{1}{\pi^M \det(\mathbf{R})} e^{-(\mathbf{y} - \mathbf{h}_S(\boldsymbol{\theta}_S))^H \cdot \mathbf{R}^{-1} \cdot (\mathbf{y} - \mathbf{h}_S(\boldsymbol{\theta}_S))}. \quad (3.16)$$

Then a maximum likelihood estimate of $\boldsymbol{\theta}_S$ would be obtained as the parameter vector $\hat{\boldsymbol{\theta}}_{S,ML}$ maximizing the likelihood (3.16). However, maximizing (3.16) is essentially a nonlinear weighted least-squares (NWLS) problem, and it is straightforward to show that, using the relation (3.6), an optimal solution is found by minimizing the cost function

$$\hat{\boldsymbol{\mu}} = \arg \max_{\boldsymbol{\mu}} \left[(\mathbf{y}^H \mathbf{R}^{-1} \mathbf{B}(\boldsymbol{\mu})) (\mathbf{B}^H(\boldsymbol{\mu}) \mathbf{R}^{-1} \mathbf{B}(\boldsymbol{\mu}))^{-1} (\mathbf{B}^H(\boldsymbol{\mu}) \mathbf{R}^{-1} \mathbf{y}) \right], \quad (3.17)$$

and

$$\hat{\boldsymbol{\gamma}} = (\mathbf{B}^H(\hat{\boldsymbol{\mu}}) \mathbf{R}^{-1} \mathbf{B}(\hat{\boldsymbol{\mu}}))^{-1} \mathbf{B}^H(\hat{\boldsymbol{\mu}}) \mathbf{R}^{-1} \mathbf{y}. \quad (3.18)$$

Minimizing the cost function (3.17) is, however, a difficult and computationally demanding task due to high dimensionality and multiple local maxima. This becomes more evident by recalling the dimensions of $\mathbf{B} \in \mathbb{C}^{M \times P}$, $\mathbf{R} \in \mathbb{C}^{M \times M}$, and $\mathbf{y} \in \mathbb{C}^{M \times 1}$, where the (unknown) number of paths $P \sim 10^1 - 10^2$, and the dimension of the observation $M = M_R \cdot M_T \cdot M_f \sim 10^4 - 10^6$, can be very high, see also Table 2.1 and the discussion in publication [V].

SAGE

The Space-Alternating Generalized Expectation-maximization (SAGE) [38] is a popular numerical technique to find ML estimates. It has been introduced in the context of propagation parameter estimation for a SIMO configuration in [39], and since then it has been extensively applied in the estimation

of parameters from MIMO configuration as well [40]. The principle in SAGE is to evaluate the likelihood function (3.16) iteratively using the current parameter estimates. Then, a subset of the parameters is kept fixed while the likelihood is maximized w.r.t. a complementary subset of the parameters. These new estimates are then fixed and employed in the computation of the likelihood while it is being maximized w.r.t. to another subset of the parameters. The convergence to a (possibly local) maximum is guaranteed as in the conventional EM. The advantage of SAGE is that the computational cost of maximizing the likelihood function in a single iteration can be scaled as the subsets of simultaneously updated parameters can be chosen arbitrarily small. However, the rate of convergence can depend significantly on the choice of the parameter subsets. Examples of the parameter subsets include *i*) the parameters of each of the individual paths, or *ii*) parameters of all paths related to specific measurement aperture. In principle, SAGE would also be suitable for including the DMC in the measurement model, either as the colored measurement noise as in (3.2), or even having the parameters of the DMC θ_D in (3.1) estimated within the SAGE algorithm. However, such an approach has not been pursued in the literature.

In [148] it is shown that both the Unitary ESPRIT and the SAGE both provide reliable results in terms of finding the correct estimates in practice in a 3-D (azimuth, elevation and delay) parameter estimation example. However, the performance of the algorithms, also in terms of computational complexity and memory requirements, depends on how the subarrays are chosen in Unitary ESPRIT, and on the other hand on the discretization of the parameter space in SAGE.

RIMAX

The RIMAX [108–110] estimation method is the first known approach to model the channel using both the superposition of specular propagation paths (2.21) as well as DMC (2.23). The estimation of the parameters belonging to these two model components is performed in an alternating fashion similarly to SAGE. However, the core of the algorithm is a gradient-based iterative optimization method, namely Levenberg-Marquardt algorithm [86, 88]. The parameter estimates are initialized by a SAGE-like grid search (or a subspace-based technique when applicable), but the ML-iterations are performed by alternating between jointly optimizing all the parameters belonging either to the specular propagation paths or the DMC. RIMAX also addresses the reliability of the path estimates. This assessment is based on the estimates of the estimation error variance of the path weights, which is provided by the diagonal elements of the inverse of the Fisher Information Matrix (FIM) approximated using the Hessian [128].

As both SAGE and RIMAX rely on the deterministic ML assumption, their statistical performance can be very close to optimal, see e.g. discussion

in [139, Appendix-B]. However, both SAGE and RIMAX suffer from the fact that they neglect the dynamic nature of the problem. Hence, significant computational effort is spent on iterations for maximizing the likelihood function (3.16) based on noisy measurements without utilizing the time-evolution of the parameters. All the *batch* solutions based on the static model suffer from the fact that everything needs to be recomputed at the arrival of a new observation.

3.3 Estimation of a Dynamic Model

This section provides a general overview of sequential estimation algorithms. A detailed discussion on the proposed state-space model for the propagation path parameter estimation is given in Section 3.4.

3.3.1 State-Space Modeling Principle

The estimation methods for static models described in Section 3.2 are derived under the assumption that the propagation path parameters remain constant during an observation period, and are independent from observation to observation. *Sequential* estimation techniques differ from the static methods by employing a state-space model to describe the time-evolution of the state of the system. Sequential estimation techniques stem from control engineering, but have been extensively applied in navigation and target tracking applications, where the state is typically defined as the position and velocity of the targets. The state in the context of this work consists of the propagation path parameters (3.5) and possibly their respective rates of change. The state is modeled as a Markov model, i.e., one is interested in estimating an unobservable discrete-time Markov sequence $\boldsymbol{\theta}_k$ at time instances $k \geq 1$, while the observations are given by a sequence \mathbf{y}_k .

State-space models are comprised of two model equations: the *state transition* equation, modeling the time evolution of the unobservable signal, and the *measurement* equation, describing the relation of the unobservable state to the observed signal. The state transition equation is defined as

$$\boldsymbol{\theta}_k = f(\boldsymbol{\theta}_{k-1}) + \mathbf{v}_k. \quad (3.19)$$

The relation $f(\boldsymbol{\theta}_{k-1})$ models the state transition, i.e., the expected evolution of the state between time instances, whereas \mathbf{v}_k is called the state noise, modeling the perturbations related to the state transition. The measurement equation is given by

$$\mathbf{y}_k = h(\boldsymbol{\theta}_k) + \mathbf{n}_k, \quad (3.20)$$

where $h(\boldsymbol{\theta}_k)$ denotes the mapping of the state variables to the observation \mathbf{y}_k , and \mathbf{n}_k models the underlying noise.

The modeling assumptions associated with (3.19) and (3.20), including the choice between linear vs. nonlinear models for $f(\boldsymbol{\theta})$ and $h(\boldsymbol{\theta})$ as well as forms of the respective noise distributions, have significant influence on the selection of the employed sequential estimation method and are discussed in the next subsection.

3.3.2 Sequential Estimation Techniques

Available sequential estimation techniques (also known as Bayesian tracking) include different Kalman filters (Kalman Filter (KF) [65], Extended Kalman Filter (EKF) [34], Unscented Kalman Filter (UKF) [60, 61]), as well as Sequential Monte-Carlo methods, commonly known as Particle Filters (PF) [6, 35, 45]. An overview of these methods and their applicability to propagation parameter estimation are discussed in the following.

Kalman Filter

The Kalman Filter [7, 12, 46, 65, 134] is the optimal solution in terms of minimizing the mean square error while recursively solving the conditional mean for $\boldsymbol{\theta}_k | \mathbf{y}_{1, \dots, k}$ in the case when the state transition (3.19) and the measurement equation (3.20) are linear, and all the associated probability densities are normal distributed. In such case the *linear* state transition equation for a vector-valued state $\boldsymbol{\theta}_k \in \mathbb{R}^{P \times 1}$ is given by

$$\boldsymbol{\theta}_k = \boldsymbol{\Phi} \boldsymbol{\theta}_{k-1} + \mathbf{v}_k, \quad (3.21)$$

where $\boldsymbol{\Phi}$ denotes the state transition matrix describing the time-evolution of the state, and $\mathbf{v} \sim \mathcal{N}(\mathbf{0}, \mathbf{Q})$ is the state noise. Hence, the probability density of the predicted state is given by $\boldsymbol{\theta}_{k|k-1} | \boldsymbol{\theta}_{k-1} \sim \mathcal{N}(\boldsymbol{\Phi} \boldsymbol{\theta}_{(k-1|k-1)}, \mathbf{Q})$. The *linear* measurement equation for a vector valued measurement $\mathbf{y}_k \in \mathbb{R}^{M \times 1}$ is defined as

$$\mathbf{y}_k = \mathbf{H} \boldsymbol{\theta}_k + \mathbf{n}_k, \quad (3.22)$$

where $\mathbf{H} \in \mathbb{R}^{M \times P}$ is the system matrix, and $\mathbf{n} \sim \mathcal{N}(\mathbf{0}, \mathbf{R})$ denotes the measurement noise. Assuming this linear state-space model (3.21)–(3.22), an optimal solution for the conditional mean is given by $\boldsymbol{\theta}_k | \mathbf{y}_{1, \dots, k} \sim \mathcal{N}(\boldsymbol{\theta}_{(k|k)}, \mathbf{P}_{(k|k)})$, where $\boldsymbol{\theta}_{(k|k)}$ as well as the associated filtering error covariance matrix $\mathbf{P}_{(k|k)}$ are estimated by the Kalman filter equations. Further details of the algorithm may be found in several textbooks [7, 12, 46] and are omitted here. Examples on how $\boldsymbol{\Phi}$ and \mathbf{Q} are constructed can be found in publication [V]. As the measurement equation in this thesis (3.2) mapping the propagation path parameters to channel sounding data is nonlinear, the linear Kalman filter is not directly applicable.

Extended Kalman Filter (EKF)

The Extended Kalman filter (EKF) [7, 12, 34, 46] is an extension of the linear Kalman filter to state-space models where either the state transition (3.19), the measurement equation (3.20) or both are nonlinear. It is based on the Taylor series approximation for linearizing the model about the current estimate and applying conventional Kalman filter equations on the linearized model. The associated probability densities are assumed to obey normal distributions. A typical *nonlinear* state-space model is formulated as

$$\boldsymbol{\theta}_k = f(\boldsymbol{\theta}_{k-1}) + \mathbf{v}_k, \quad (3.23)$$

$$\mathbf{y}_k = h(\boldsymbol{\theta}_k) + \mathbf{n}_k, \quad (3.24)$$

where the noise processes \mathbf{v}_k and \mathbf{n}_k are defined as in (3.21)–(3.22). To apply the Kalman filter equations the model is linearized using the, commonly first order, Taylor series approximation. Hence the state transition matrix Φ in the Kalman filter equations is replaced by the Jacobian matrix

$$\tilde{\Phi} = \left. \frac{\partial f(\boldsymbol{\theta}_{k-1})}{\partial \boldsymbol{\theta}_{k-1}} \right|_{\boldsymbol{\theta}_{k-1} = \hat{\boldsymbol{\theta}}_{(k-1|k-1)}}, \quad (3.25)$$

and the measurement matrix \mathbf{H} is replaced by the Jacobian matrix

$$\tilde{\mathbf{H}} = \left. \frac{\partial h(\boldsymbol{\theta}_k)}{\partial \boldsymbol{\theta}_k} \right|_{\boldsymbol{\theta}_k = \hat{\boldsymbol{\theta}}_{(k|k-1)}}. \quad (3.26)$$

A major benefit of the EKF is that, except for the differentiation required for the linearization, the complexity and memory requirements of the solution are in the same order as for the linear Kalman filter. A potential drawback is that the EKF may be sensitive to the linearization error and hence it can be prone to diverge. However, EKF has proven to suit well for the estimation of the propagation path parameters in channel sounding measurements [I–V], and the employed approach is described in detail Section 3.4.

Unscented Kalman Filter (UKF)

The Unscented Kalman Filter (UKF) [60, 61] is another approach to apply Kalman filtering framework for a nonlinear state-space model. The idea in UKF is to apply a nonlinear, normal distributed state-space model such as (3.23)–(3.24). The difference compared to EKF is that the estimation of the prediction and posterior means and covariances is based on deterministic sampling of the originating distribution. These samples, also known as *sigma points*, are then propagated through the nonlinear functions. With this approach, the conditional mean and covariance estimates can achieve accuracy comparable to third order Taylor series expansion (in comparison

to first order for EKF) for any nonlinearity. Furthermore UKF does not require explicit calculation of Jacobian or Hessian matrices. The main reason for which the UKF has not been applied in large-scale problems, such as the estimation of propagation path parameters from channel sounding data, is that it requires explicit computation of the cross-covariance matrices between the state and the observation. The dimensions of such matrices ($\sim 10^3 \times 10^5$) become prohibitively large in the application at hand.

Particle Filters (PF)

Particle Filters (PF) [6, 35, 45] can be applied to a state-space model of arbitrary level of nonlinearity or any assumed distribution. The idea in PF methods is to apply *sequential Monte Carlo methods* such as *importance sampling* and *resampling*, and estimate the distributions of interest based on a large number of particles sampled, propagated through the nonlinearities, and resampled in an (asymptotically) optimal fashion. The computational complexity of a particle filter can become prohibitively high if the state dimension is assumed to be high, as is the case for the estimation of propagation path parameters. Particle filtering has recently been applied to the problem of propagation path parameter estimation from channel sounding measurements as well [161, 162]. However, the PF in [161] is formulated essentially for a single path only (multiple paths tracked by separate PFs), and also the associated PDFs were assumed to obey normal distribution. As PF is most useful for estimating multimodal or asymmetric parameter distributions or highly nonlinear models, its use in the context of propagation path parameter estimation is questionable. Moreover, the number of particles required for tracking a large number of parameters can make the computational complexity of PF prohibitive. It is also doubtful how well the PF approach applies for detecting multiple paths, i.e., how to associate the particles with individual paths. Benefits over EKF in this case may be minor or nonexistent. On the other hand, PF may be suitable for the estimation of the parameters of a purely stochastic channel model with possibly multi-modal distribution, such as the DMC.

3.4 State-Space Modeling for Propagation Path Tracking

This section introduces the developed state-space model, the derived EKF, and the related model order selection techniques for the estimation of the propagation path parameters introduced in original publications [I–V]. The combination of the described methods constitute the main contribution of this thesis, namely a complete framework for the estimation of the propagation path parameters based on dynamic modeling.

3.4.1 Dynamic Model

The dynamic model is based on the assumption that the parameters of the propagation paths are correlated over subsequent measurement instances. The state vector $\boldsymbol{\theta}_k$ at time k is then defined as

$$\boldsymbol{\theta}_k = \left[\boldsymbol{\mu}_k^\top \ \Delta\bar{\boldsymbol{\mu}}_k^\top \ \boldsymbol{\alpha}_k^\top \ \boldsymbol{\phi}_k^\top \ \Delta\bar{\boldsymbol{\phi}}_k^\top \right]^\top. \quad (3.27)$$

The parameters $\boldsymbol{\mu}$ defined in (3.3) are called the *structural* parameters, as they define the spatial structure of the propagation paths. The vector $\Delta\bar{\boldsymbol{\mu}}$ contains their rate of change. The complex path weight parameters (3.4) are parameterized as $\boldsymbol{\alpha}_i = \Re\{\log(\boldsymbol{\gamma}_i)\}$, $\boldsymbol{\phi}_i = \Im\{\log(\boldsymbol{\gamma}_i)\}$ ($i \in \{T_{pol}, R_{pol}, p\}$), and $\Delta\bar{\boldsymbol{\phi}}$ denotes phase evolution common to all the path weight polarization components of each individual path.

The state transition is given by a linear model as in (3.21), i.e.,

$$\boldsymbol{\theta}_k = \boldsymbol{\Phi}\boldsymbol{\theta}_{k-1} + \mathbf{v}_k, \quad (3.28)$$

where $\mathbf{v}_k \sim \mathcal{N}(\mathbf{0}, \mathbf{Q})$ is the state noise. Details on how $\boldsymbol{\Phi}$ and \mathbf{Q} are structured are given in publication [V].

The measurement equation is identical to (3.2) and is defined as

$$\mathbf{y}_k = \mathbf{h}_S(\boldsymbol{\theta}_k) + \mathbf{n}_k, \quad (3.29)$$

where $\mathbf{h}_S(\boldsymbol{\theta}_k)$, defined in (3.6) and (2.21) denotes the nonlinear mapping of the propagation path parameters to the measured channel. The noise term $\mathbf{n}_k \sim \mathcal{N}_C(\mathbf{0}, \mathbf{R})$, with $\mathbf{R} = \mathbf{R}_D + \sigma_N^2 \mathbf{I}$ models the contribution of both the DMC and the measurement noise, see (2.23)–(2.25).

Some remarks on the dynamic model

It should be noted that the introduction of the *dynamic* parameters $\Delta\bar{\boldsymbol{\mu}}$ in publication [II] and $\Delta\bar{\boldsymbol{\phi}}$ in [V] essentially improves the prediction of the parameters in the dynamic model. In other words, neglecting the dynamic parameters would result in a requirement to increase the corresponding values in the state noise covariance matrix \mathbf{Q} in order to account for a deterministic change in the parameters. This fact has been illustrated in publication [V, Section III] for the phase evolution $\Delta\bar{\boldsymbol{\phi}}$, but similar conclusions could be drawn for the structural parameters $\Delta\bar{\boldsymbol{\mu}}$. In addition, it is shown in [II] that having $\Delta\bar{\boldsymbol{\mu}}$ in the state improves the estimator performance in terms of lower estimation error variance. The dynamic parameter $\Delta\boldsymbol{\alpha}_i$ for the path weight magnitudes, on the other hand, is not considered in the model since any deterministic temporal variation is assumed to be hidden by other sources of randomness. Therefore the tracking of the long term time evolution has not been considered. In low mobility measurements, also some or all of the

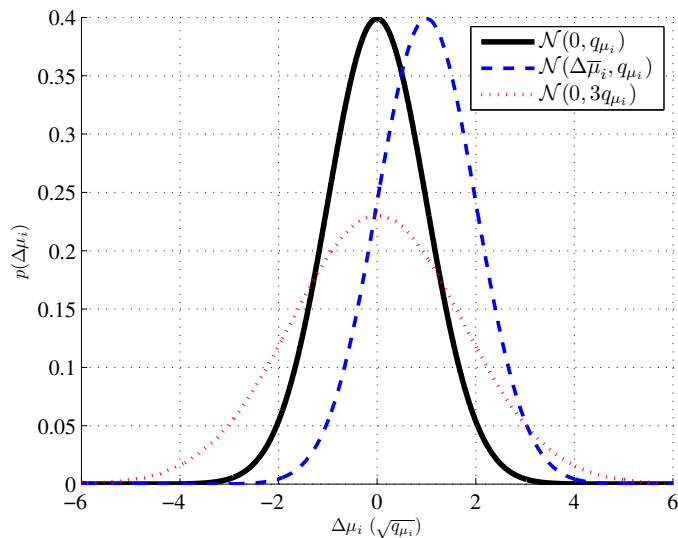


Figure 3.2: Interplay of the state noise model vs. dynamic parameters. The unit of the x-axis is normalized to $\sqrt{q_{\mu_i}}$. If a mean $\Delta\bar{\mu}_i$ of the true distribution, here $\Delta\mu_i \sim \mathcal{N}(\Delta\bar{\mu}_i, q_{\mu_i})$, of the change $\Delta\mu_i = \mu_{i,k} - \mu_{i,k-1}$ of a parameter μ_i over time is neglected, it has to be compensated by increasing the state noise variance. In this conceptual example the variance is tripled.

$\Delta\bar{\mu}$ parameters may be considered to be left out of the model in order to reduce the complexity.

Figure 3.2 shows a conceptual illustration for the interplay between the state noise and the dynamic modeling. Let us assume that the true distribution of $\Delta\mu_i = \mu_{i,k} - \mu_{i,k-1}$ is given by $\Delta\mu_i \sim \mathcal{N}(\Delta\bar{\mu}_i, q_{\mu_i})$. Then, if the mean $\Delta\bar{\mu}_i$ in the rate of change is neglected, a variance value higher than q_{μ_i} must be chosen for the state noise to ensure tracking is not lost. Increasing the state noise variance would, however, increase the estimation error as well.

Another important contribution, first introduced in publication [III], is the parametrization of the path magnitudes in a logarithmic scale $\alpha_i = \log(|\gamma_i|)$. It is shown in publication [V, Section III] that this parametrization results again in a normal distributed time evolution, see publication [V] for further discussion.

3.4.2 EKF Formulation

The EKF is a suboptimal solution for estimating the parameters of the dynamic model due to the employed Taylor series linearization. However, it has been selected as the method of choice for the sequential estimation in this work for the following reasons.

- The linear approximation of the nonlinear model is sufficient for the

problem at hand, as indicated by simulation results ,e.g., in publication [I].

- The assumption of the associated probability densities being normal distributed holds, see discussion in [V].
- The formulation of the EKF facilitates computationally efficient implementation [I–V].
- The implementation has turned out to produce reliable results in real world dynamic measurements [I–V], [73, 103, 121].

The formulation of the EKF employed in publications [I–V] is based on the *alternative form* of the Kalman filtering equations, see e.g., [12]. Replacing the linear system matrix \mathbf{H} in the Kalman filter by the Jacobian matrix $\mathbf{D}(\boldsymbol{\theta}) = \frac{\partial}{\partial \boldsymbol{\theta}^T} \mathbf{h}_S(\boldsymbol{\theta})$ yields equations for the EKF. From those one can identify some useful expressions, namely the Score function:

$$\begin{aligned} \mathbf{q}(\mathbf{y}|\boldsymbol{\theta}, \mathbf{R}) &= \frac{\partial}{\partial \boldsymbol{\theta}} \mathcal{L}(\mathbf{y}|\boldsymbol{\theta}, \mathbf{R}) \\ &= 2 \cdot \Re \{ \mathbf{D}^H(\boldsymbol{\theta}) \mathbf{R}^{-1} (\mathbf{y} - \mathbf{h}_S(\boldsymbol{\theta})) \}, \end{aligned} \quad (3.30)$$

and the Fisher Information Matrix (FIM):

$$\begin{aligned} \mathbf{J}(\boldsymbol{\theta}, \mathbf{R}) &= -\mathbb{E} \left\{ \frac{\partial}{\partial \boldsymbol{\theta}} \mathcal{L}(\mathbf{y}|\boldsymbol{\theta}, \mathbf{R}) \left(\frac{\partial}{\partial \boldsymbol{\theta}} \mathcal{L}(\mathbf{y}|\boldsymbol{\theta}, \mathbf{R}) \right)^T \right\} \\ &= 2 \cdot \Re \{ \mathbf{D}^H(\boldsymbol{\theta}) \mathbf{R}^{-1} \mathbf{D}(\boldsymbol{\theta}) \}, \end{aligned} \quad (3.31)$$

both of which are well known from estimation theory [128]. The EKF equations can be summarized as

$$\hat{\boldsymbol{\theta}}_{(k|k-1)} = \boldsymbol{\Phi} \hat{\boldsymbol{\theta}}_{(k-1|k-1)} \quad (3.32)$$

$$\mathbf{P}_{(k|k-1)} = \boldsymbol{\Phi} \mathbf{P}_{(k-1|k-1)} \boldsymbol{\Phi}^T + \mathbf{Q} \quad (3.33)$$

$$\mathbf{P}_{(k|k)} = \left(\mathbf{P}_{(k|k-1)}^{-1} + \mathbf{J}(\hat{\boldsymbol{\theta}}_{(k|k-1)}, \mathbf{R}_k) \right)^{-1} \quad (3.34)$$

$$\Delta \hat{\boldsymbol{\theta}}_k = \mathbf{P}_{(k|k)} \mathbf{q} \left(\mathbf{y}_k | \hat{\boldsymbol{\theta}}_{(k|k-1)}, \mathbf{R}_k \right) \quad (3.35)$$

$$\hat{\boldsymbol{\theta}}_{(k|k)} = \hat{\boldsymbol{\theta}}_{(k|k-1)} + \Delta \hat{\boldsymbol{\theta}}_k. \quad (3.36)$$

The advantage of this formulation for the EKF is that the Score function (3.30) and the FIM (3.31) can be solved in a computationally efficient manner. Similar expressions were derived for a simplified DMC model in [108]. An exact, as well as a computationally efficient approximate solution for the FIM (based on a novel SUSVD tensor decomposition) for the more general Kronecker model for the DMC in (2.23)–(2.24) have been derived in the original publications [IV] and [VII].

3.4.3 Model Order Selection

In dynamic channel sounding measurements the number of dominant propagation paths P is varying over time. This takes place especially at street or corridor crossings or at the transitions between line-of-sight (LOS) and non-line-of-sight (NLOS) channel conditions. The state-space model in Section 3.4.1 is formulated for joint estimation of the propagation path parameters. Consequently, it is necessary to adapt the state dimension within the EKF according to the number of significant paths present in the channel. An optimal solution for determining the correct number of components to estimate could be formulated based on the Minimum Description Length (MDL) [118], which is also related to Bayesian Information Criterion (BIC), see [138] for discussion. However, the computational complexity involved in evaluating these criteria renders them infeasible as they would require evaluation of likelihood functions for a very large number of path combinations and parameter values. The approach adopted in this work for detecting the number of paths is based on applying two one-sided statistical tests. The first one is used to determine if the channel contains paths which are not currently present in the state vector. The second one is used for testing the significance of current estimates and — if necessary — removing the insignificant paths from the state.

Detection of New Paths

The detection of new paths is performed in, [I]-[II], [122] by applying the RIMAX algorithm [108–110] on the residual

$$\mathbf{y}_k - \mathbf{h}_S(\boldsymbol{\theta}_k) \quad (3.37)$$

in order to search initial estimates for a fixed number of new paths at each snapshot. In publication [III] a cumulative sum (CUSUM) test [47] is proposed for this purpose. The idea in [III] is to apply a hypothesis test to evaluate the whiteness of the residual (3.37) to detect whether new paths were present. The whitening is based on the estimated DMC covariance matrix. In practice the CUSUM approach turned out to be rather sensitive to modeling errors, especially since the previously employed simplified model for the DMC was unable to produce reasonable whitening of the residual due to model mismatch.

Another approach that has turned out to work well in practice for detecting new paths is introduced in [V]. The idea is to form a grid in the space of the structural parameters, and evaluate the likelihood function at these points. The statistics of the proposed test follows a χ^2 distribution with degrees of freedom equal to the number of polarization components $N_{pol} \in \{1, 2, 4\}$. A detection threshold can be formed based on specifying a probability of false alarm, see [V]. If a detection threshold is exceeded

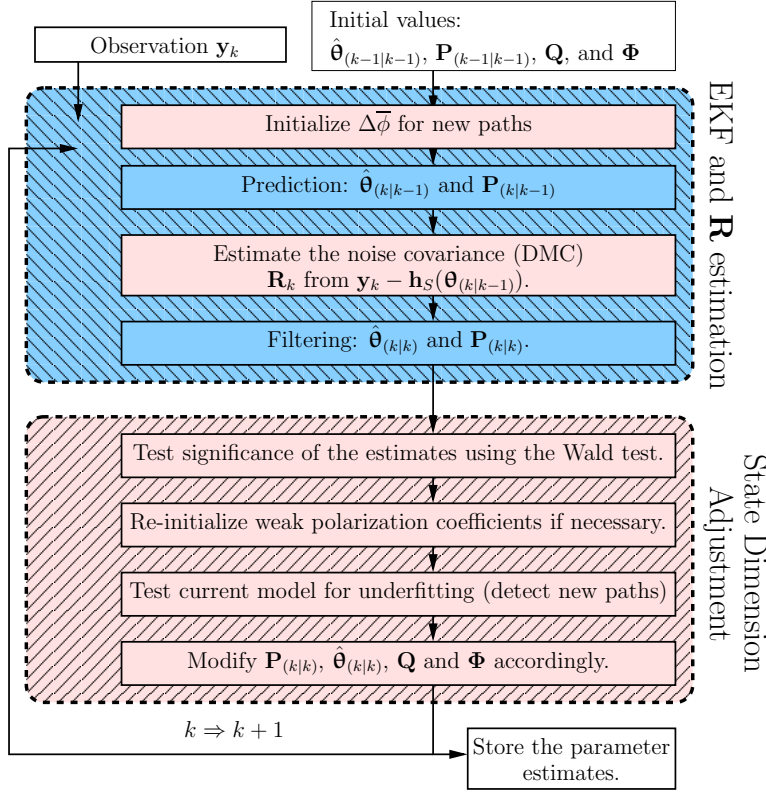


Figure 3.3: Complete estimation procedure (see [V] for details).

for any point, an initial estimate for a path is obtained by iteratively making the detection grid denser in the vicinity of that point until convergence is reached. The convergence criterion can be chosen individually for each parameter, see [V, Section V-C] for details.

Reduction of Paths

The reduction of paths from the state is proposed in [II], and it is based on a statistical test known as the Wald test [66]. The idea of the test is to evaluate the significance of each estimated path based on the validity of their respective polarization path weight estimates. These values can be shown to follow a χ^2 distribution with N_{pol} degrees of freedom, allowing to formulate a hypothesis test with a detection threshold for deciding whether a path should be removed from the state [V].

A flow chart of the estimation process for a single snapshot is shown in Figure 3.3.

3.5 Estimation Examples

3.5.1 Measurement Setup

The performance of the estimator introduced in Section 3.4 has been validated with measurement data. The estimation examples in this section are from a measurement campaign conducted by Institute of Communications and Measurement Engineering, Ilmenau University of Technology and Medav GmbH on August 12th 2004 at Ilmenau city center using the RUSK channel sounder [90]. The Tx antenna array is a 16 element UCA (Uniform Circular Array) placed on a measurement trolley. The receive Rx array is an 8 element dual polarized PULA (Polarimetric Uniform Linear Array) at 3.7 m height. The bandwidth of the sounding signal is 120 MHz at a carrier frequency of 5.2 GHz. The time separation between the snapshots is 20.48 ms. This setup enables the estimation of the propagation path parameters, excluding the elevation at the receiver (ϑ_R) due to elevation ambiguity of the PULA. Furthermore, only the polarization components (γ_{VH} and γ_{VV}) are estimated due to single (vertically) polarized elements in the Tx array. For a detailed description of the measurement, see [146].

3.5.2 Goodness of Fit

In order to describe how well the estimated model fits into the measured data, estimation results from two different measurement routes are presented, see [121] for a full description. Figure 3.4 and Figure 3.5 show a comparison of both Power-Angular Profiles (PAP) for Tx and Rx azimuth angles, as well as Power-Delay Profiles (PDP) over the measurement time. The plots show the aforementioned PAPs and PDPs for the measured channel \mathbf{h} (equal to \mathbf{y} in Section 3.4), estimated paths $\hat{\mathbf{h}}_S$, estimated DMC and noise $\hat{\mathbf{h}}_D + \hat{\mathbf{h}}_N \sim \mathcal{N}_C(\mathbf{0}, \mathbf{R})$ (using reconstructed realizations of $\mathbf{h}_D + \mathbf{h}_N$), and the reconstruction of the whole channel $\hat{\mathbf{h}} \sim \mathcal{N}_C(\hat{\mathbf{h}}_S, \hat{\mathbf{R}})$. The 0° azimuth angle is in the direction of the ULA broadside for the Rx, and in the direction of movement for the Tx.

From Figures 3.4–3.5 the following conclusions can be drawn:

- The path estimates together with the estimated DMC achieve a very good reconstruction of the channel in terms of visual evaluation of the power profiles.
- The DMC is the dominating component of the model in NLOS, whereas in LOS the radio link is dominated by the concentrated propagation paths.
- In many cases the DMC has a structured angular profile in addition to an exponentially decaying profile in the delay.

Another illustration of the estimators performance is provided by examining the PDP's of the whitened residual sequences, i.e., the PDP of

$$\hat{\mathbf{h}}_w = \hat{\mathbf{R}}^{-\frac{1}{2}} \left(\mathbf{h} - \hat{\mathbf{h}}_S \right), \quad (3.38)$$

where, ideally, $\mathbf{h}_w \sim \mathcal{N}_C(0, \mathbf{I})$. Figure 3.6 depicts the PDP's of the routes in Figures 3.4–3.5 in three dimensional plots. It can be observed that the PDP of the whitened residual resembles that of a normal distributed white noise with standard deviation equal to one. The sample estimates $\hat{\sigma}_w$ for the standard deviation of $\hat{\mathbf{h}}_w \sim \mathcal{N}_C(0, \hat{\sigma}_w^2 \mathbf{I})$ for the two considered routes are $\hat{\sigma}_{w, \#2} = 1.0011$ and $\hat{\sigma}_{w, \#3} = 1.0009$, respectively.

3.5.3 Path Parameter Estimates

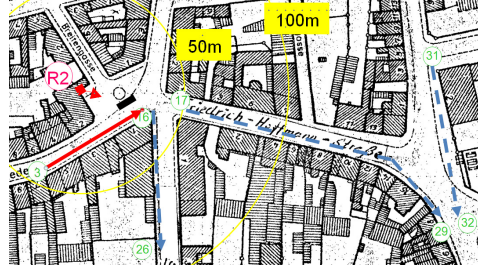
In this section examples of parameter estimates are illustrated for a selected path from each of the measurements described in the previous section. Figure 3.7 and Figure 3.8 include visualization of the magnitude of the path weights in dB ($20 \log_{10}(|\gamma_{HV/VV}|)$), the evolution of the path weight phases ($\phi_k - \phi_{k-1}$), and estimates for the delay (τ), Rx azimuth (φ_R) and Tx angles (φ_T) and (ϑ_T). The green line indicates the 90% confidence region of the estimates. An explanation of the observed path behavior is given in the figure captions.

3.6 Summary and Discussion

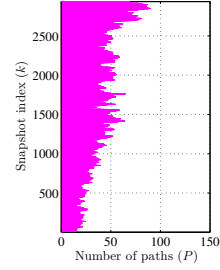
This chapter discusses the state-of-the-art in MIMO channel sounding parameter estimation techniques. The problem with methods relying on modeling the channel through the second order statistics is that it can be very difficult to obtain sufficient number of independent realizations to estimate the channel parameters. This is also related to the fact that the weights of the signals, i.e., the polarization coefficients, are coupled with the structural parameters, i.e., a change in the path weights typically results from a change also in the underlying structural parameters. The techniques such as beamforming, MUSIC and ESPRIT are also typically applicable for only a subset of the parameters. The deterministic maximum likelihood methods SAGE and RIMAX are probably the two most common methods for the task and can be considered as the best candidates if a batch estimator relying on a static model is desired.

As the underlying phenomenon in mobile radio channels is often dynamic, as in any cellular communication system, the proposed dynamical model along with the *sequential* estimation approach employing the EKF has several advantages over the ML-based *static* estimation methods.

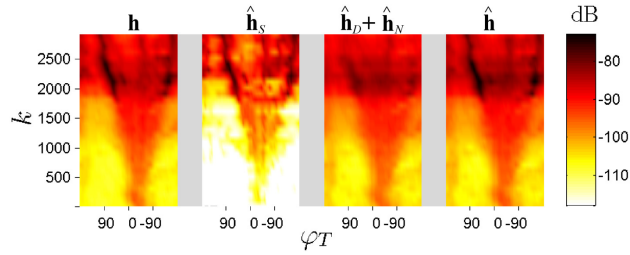
1. EKF, being sequential and non-iterative, has significantly lower computational complexity than SAGE or RIMAX, see, e.g., [I] and [II].



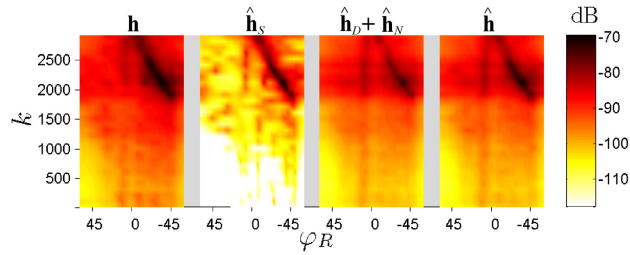
(a) Map of the measurement route #2 (3 to 16).



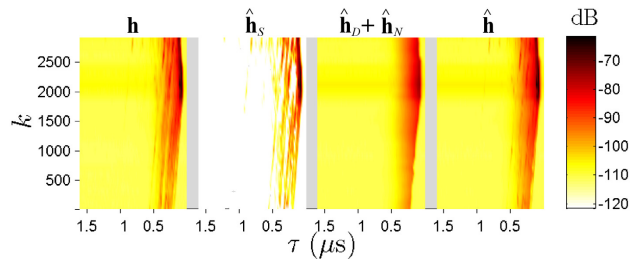
(b) Number of tracked paths.



(c) PAP at the Tx.

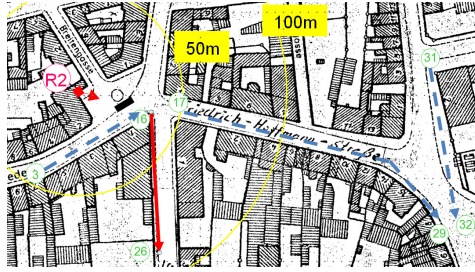


(d) PAP at the Rx.

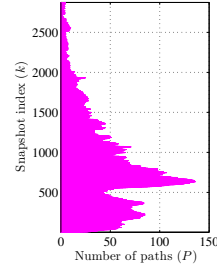


(e) PDP of the route.

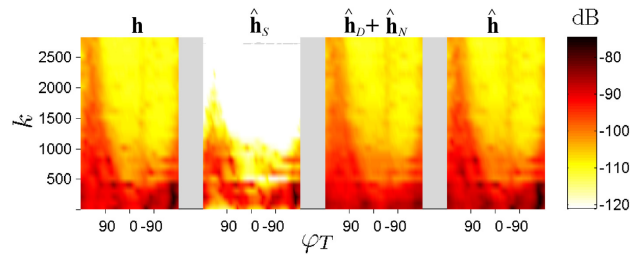
Figure 3.4: PAP and PDP plots for measured, estimated and reconstructed data for route from point 3 to point 16. The DMC (\mathbf{h}_D) clearly dominates in the NLOS region until $k \approx 1700$. Then the Tx enters LOS and the propagation paths (\mathbf{h}_S) begin to prevail.



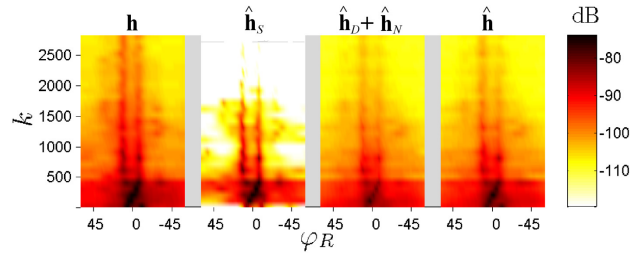
(a) Map of the measurement route #3 (16 to 26).



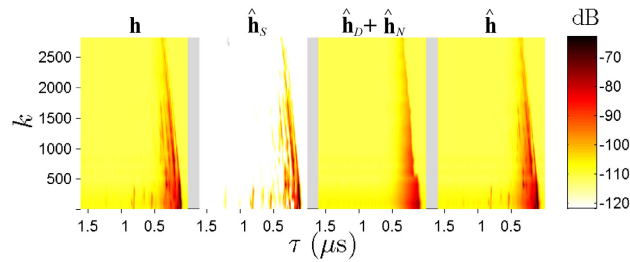
(b) Number of tracked paths.



(c) PAP at the Tx.

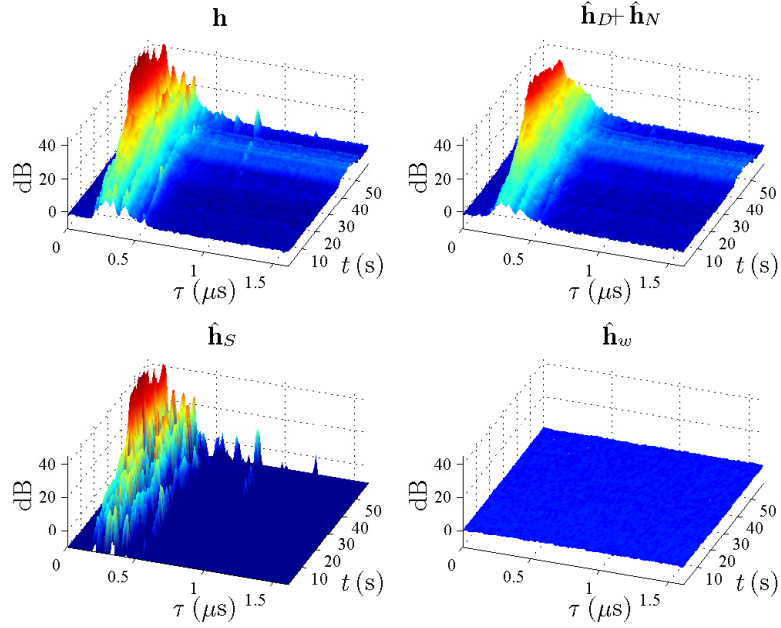


(d) PAP at the Rx.

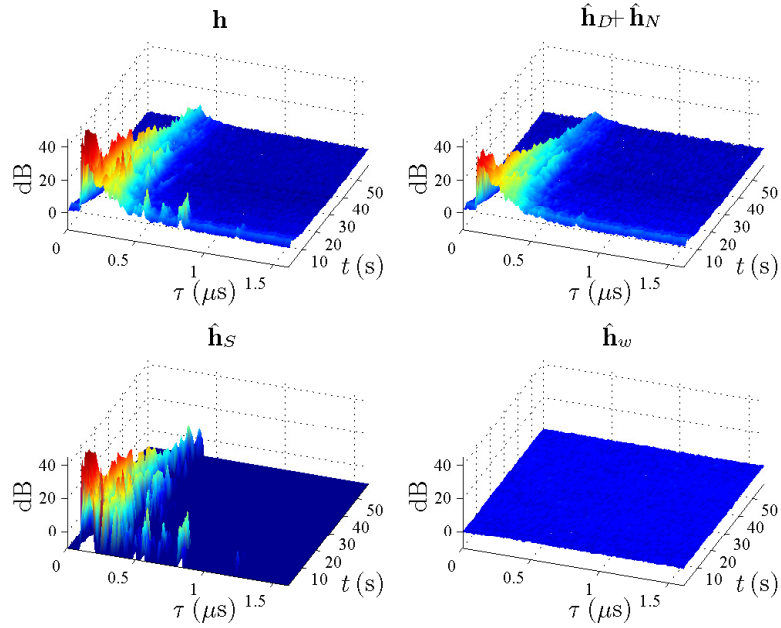


(e) PDP of the route.

Figure 3.5: PAP and PDP plots for measured, estimated and reconstructed data for route from point 16 to point 26. In the NLOS (after $k = 500$) it can be observed that the DMC has clearly a bimodal distribution in Rx azimuth, which should be taken into account while considering an angular model for the DMC.



(a) Route #2 (3 to 16) (Figure 3.4).



(b) Route #3 (16 to 26) (Figure 3.5).

Figure 3.6: PDP's of the measurement \mathbf{h} , estimated paths $\hat{\mathbf{h}}_S$, estimated DMC and measurement noise $\hat{\mathbf{h}}_D + \hat{\mathbf{h}}_N$, and the whitened residual $\hat{\mathbf{h}}_w \sim \mathcal{N}_C(0, \hat{\sigma}_w^2 \mathbf{I})$, defined in (3.38). The estimated standard deviations for the whitened residuals were $\hat{\sigma}_{w, \#2} = 1.0011$ and $\hat{\sigma}_{w, \#3} = 1.0009$, respectively.

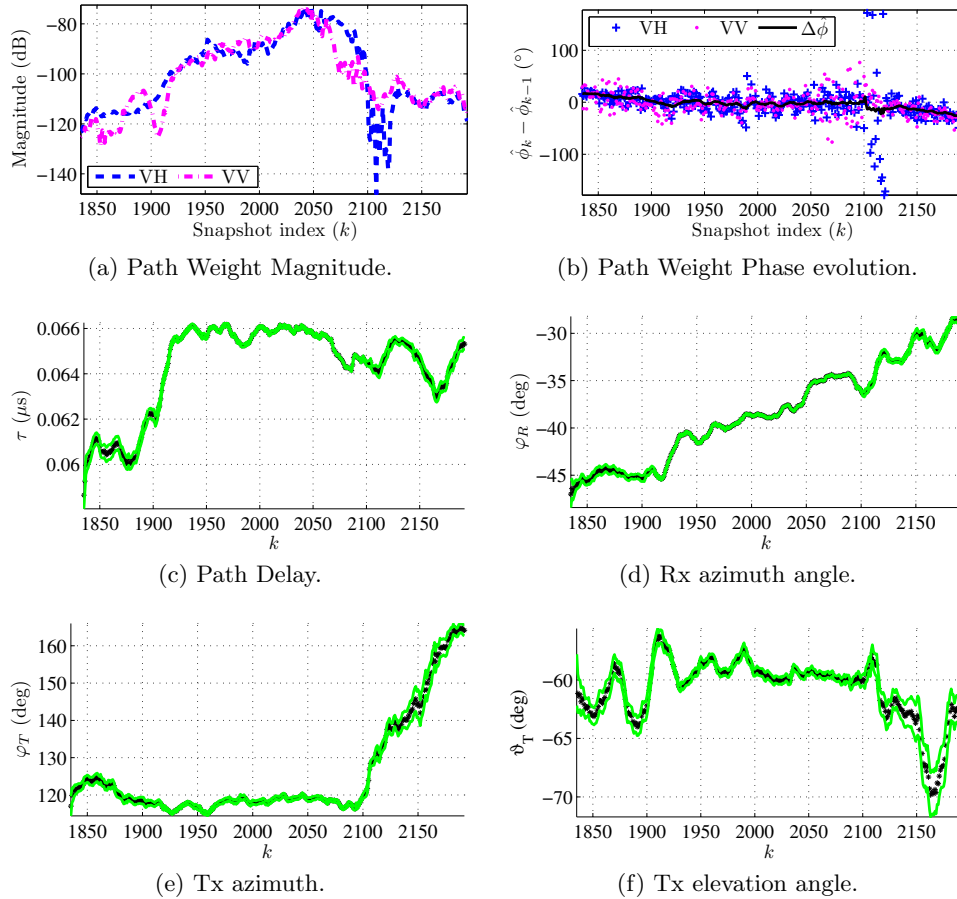


Figure 3.7: Example path parameters from route #2 (in Figure 3.4). The signal for this path propagates at a low elevation angle at the Tx and impinges a structure on the right hand side of the Rx. The path power decays while the Tx moves behind a van, causing changes also in Tx azimuth and elevation. The polarizations have mostly equal power levels, except at $k \approx 2100$, when the VH -coefficient is fading in (a). This fade also deteriorates the tracking of the VH -phase in (b).

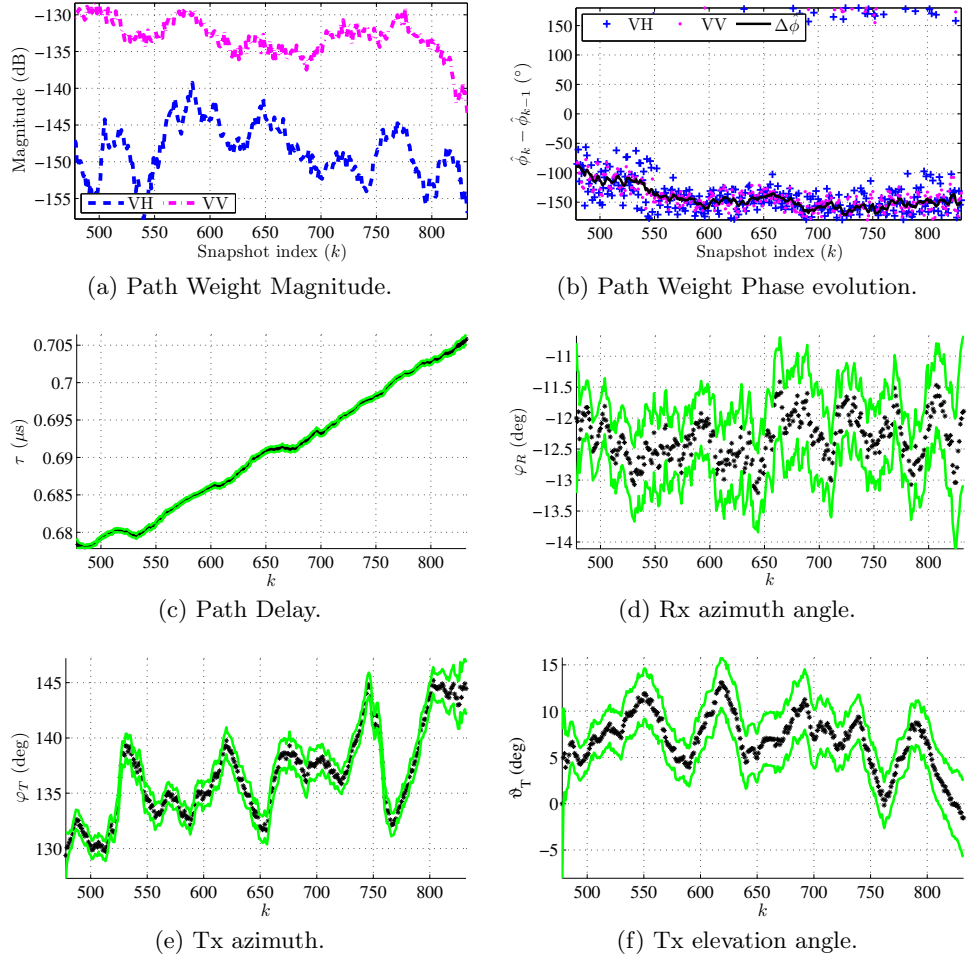


Figure 3.8: Example path parameters from route #3 (in Figure 3.5). The point of reflection seen from the Rx is very stable, see (d). The dominance of the VV -polarization implies that the main reflector or scatterer strongly supports the vertical electric field (e.g. a vertical metal structure such as a lamp post) or at least it does not mix the polarizations. The lengthening of the path in (c) can also be observed from (b) as a large negative rate of change of the phase (directly related to the Doppler shift).

2. Tracking the propagation paths maintains the identities of individual paths allowing, e.g., to study the time evolution and to identify the dominant propagation mechanism as well as type and source of radio wave interactions, as it has been shown in [103].
3. A better dynamic model provides better statistical performance in terms of lower estimation error, see publications [I] and [II].

Table 3.1 concludes the chapter on propagation path parameter estimation techniques by summarizing the features of different methods. This evaluation relies on the modeling assumptions associated with each technique, as presented in Sections 3.2 and 3.3. *Scalability* refers to both scalability in the number of parameter dimensions, as well as number of estimated paths. *Resolution* describes the ability to distinguish closely spaced paths. *Dynamic modeling* refers to the estimator’s applicability to process time-varying data and track time-varying parameters. *Computational complexity* gives an idea of the computational effort required to process the data. *Statistical performance* indicates the asymptotic (large sample) performance of the estimators. However, such a comparison is not important in the application at hand, as the estimation has to rely on relatively small number of realizations. Also the fundamental limits such as Cramér-Rao lower bound [21] are different depending on the modeling assumption and dimensionality. Finally, the last row in Table 3.1 indicates the suitability of the method for propagation parameter estimation from channel sounding measurements. The value of ESPRIT is bracketed due to requirement on translational invariance of the arrays.

Table 3.1: Summary of parameter estimation techniques suitable for estimation of propagation parameters from channel sounding measurements.

Feature	Approach				
	ESPRIT ^a	SAGE ^b	RIMAX ^c	EKF ^d	PF ^e
Scalability	(+)	+++	++	++	--
Resolution	(+)	++	++	++	+
Dynamic modeling	--	-	-	++	+++
Comp. complexity	+	--	-	++	--
Stat. Perf.	+	++	++	+	++
Suitability to MBCM	(+)	+	++	+++	-

^aEstimation of Signal Parameters via Rotational Invariance Technique [48, 50, 99, 119]

^bSpace-Alternating Generalized Expectation-Maximization [38–40]

^cRIMAX [108–110]

^dExtended Kalman Filter [I–V]

^eParticle Filter [161, 162]

Chapter 4

Tensor Decompositions and Modeling for High Dimensional Data

Tensor representation is a natural approach to model data having more than two variable dimensions. Tensor techniques stem from applications in psychometrics [16, 150], sociology, chromatography and chemometrics [37, 133], but have recently found their way into many signal processing problems as well [24, 25, 49, 132].

The data obtained from MIMO channel sounding measurements are a good example of tensor-valued data, as the samples of the channel transfer function are obtained for a set of frequencies, a number of Tx and Rx ports, and over time. Adopting a tensor representation for the data allows for applying tensor decomposition techniques [133], which are essentially generalizations of the well known matrix decompositions such as the Singular Value Decomposition (SVD) [44] for higher dimensional arrays of data. Tensor decompositions can be used, for example, for model identification, dimensionality reduction, compression of data, low rank approximation etc..

In publication [IV] a computationally efficient method for finding the Fisher Information Matrix based on a novel low rank tensor approximation is introduced. This approach is necessary in order to reduce the computational complexity of the developed EKF, introduced in Section 3.4.2. In fact, the proposed method was only later identified as a tensor decomposition technique, and it turned out to have several other interesting applications as well. The so-called PARATREE tensor model and Sequential Unfolding SVD (SUSVD) decomposition are refined in publication [VI] along with an application example for suppressing measurement noise from channel sounding data. A comprehensive treatment of the PARATREE/SUSVD approach including comparison to PARAFAC and HOSVD is given in publication [VII].

In this chapter, some basic tensor modeling approaches and concepts, namely the PARAFAC and the Tucker models, are reviewed in Section 4.1. In Section 4.2 the PARATREE model and the novel Sequential Unfolding SVD (SUSVD) [IV, VI, VII] are introduced. The presented tensor models are applied to MIMO channel modeling in Section 4.3. Section 4.3 also includes other application examples for the novel PARATREE/SUSVD approach.

4.1 Tensor Models

There are two major tensor model families, namely the PARAFAC [54, 79] (CANDECOMP [15]) and the Tucker [150] models. PARAFAC is based on modeling the N -dimensional tensor as a sum of R rank-1 tensors, whereas Tucker models decompose a tensor using a smaller dimensional core tensor and possibly orthonormal basis matrices for each mode. A good description of the properties and differences of the two approaches can be found in [71, 133], for example. A general model unifying the two approaches is introduced in [26].

4.1.1 PARAFAC Model

The PARAFAC model is essentially a description of the tensor as a sum of R rank-1 tensors. The rank of a tensor is defined as the minimum number of rank-1 components yielding the tensor as their linear combination. There are a number of ways to express a PARAFAC decomposition [71, 133]. Consider an N -dimensional tensor $\mathcal{X} \in \mathbb{C}^{M_1 \times M_2 \times \dots \times M_N}$ and N matrices $\mathbf{A}^{(n)} \in \mathbb{C}^{M_n \times R}$, where R is the number of factors that is ideally equal to the rank of the tensor. Then the matrices $\mathbf{A}^{(n)}$, $n \in [1, \dots, N]$, with columns $\mathbf{a}_r^{(n)}$, $r \in [1, \dots, R]$ can be formed such that the tensor \mathcal{X} is given by the sum of outer products

$$\mathcal{X} = \sum_{r=1}^R \mathbf{a}_r^{(1)} \circ \mathbf{a}_r^{(2)} \circ \dots \circ \mathbf{a}_r^{(N)}, \quad (4.1)$$

where each outer product of the vectors $\mathbf{a}_r^{(n)}$ is a rank-1 tensor. For the definition of the rank-1 tensor as well as the outer product of N vectors see publication [VII, Section II-A].

An illustration of the PARAFAC model for the case $N = 3$ is given in Figure 4.1, where the relation to (4.1) is obtained by setting $\mathbf{a}_r^{(1)} = \mathbf{a}_r$, $\mathbf{a}_r^{(2)} = \mathbf{b}_r$ and $\mathbf{a}_r^{(3)} = \mathbf{c}_r$. Each of the outer products of the three vectors forms a rank-1 tensor. For further discussion on the tensor rank, see [17, 30, 69].

The PARAFAC model is typically fitted to data by using an Alternating Least Squares (ALS) approach, see [71, 133], [VII, Section III-A]. Alternative

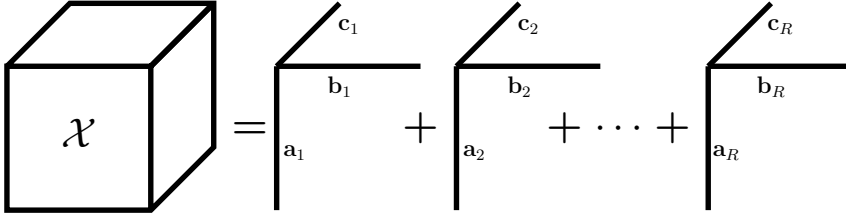


Figure 4.1: Illustration of the PARAFAC decomposition — a sum of R rank-1 tensors. The relation to (4.1) is established by setting the factors $\mathbf{a}_r^{(1)} = \mathbf{a}_r$, $\mathbf{a}_r^{(2)} = \mathbf{b}_r$ and $\mathbf{a}_r^{(3)} = \mathbf{c}_r$.

approaches are introduced in [27, 28], and a survey of several different methods is provided in [37]. In principle, the PARAFAC decomposition can not be deflated in contrary to the SVD for matrices. In general, the best rank $R - 1$ approximation of a tensor does not consist of the same rank-1 components as the rank R approximation [30, 69]. Consequently, the PARAFAC decomposition has to be evaluated for each rank $R = 1, \dots, R_{max}$ separately to obtain the best fit. Methods for finding a proper rank are discussed in [11, 17].

4.1.2 Tucker/HOSVD Model

Tucker models [71, 133, 150] are another commonly used way to represent a tensor decomposition. The idea is to form a limited set of basis vectors for each mode, and express the tensor as a linear combination of the outer products of different basis vectors of each mode. A tensor \mathcal{X} can be expressed using the Tucker model as

$$\mathcal{X} = \mathcal{S} \times_1 \mathbf{U}^{(1)} \times_2 \mathbf{U}^{(2)} \dots \times_N \mathbf{U}^{(N)}, \quad (4.2)$$

where $\mathcal{S} \in \mathbb{C}^{R_1 \times \dots \times R_N}$ is called *the core tensor*, and the matrices $\mathbf{U}^{(n)} \in \mathbb{C}^{M_n \times R_n}$ contain the basis vectors. The notation \times_n denotes the n^{th} -mode product and is defined in publication [VII, Section II-A]. The Tucker decomposition (for $N = 3$) is illustrated in Figure 4.2.

Several approaches for fitting a Tucker model to data have been proposed. Perhaps the most intuitive approach is the so-called Tucker’s “Method I” [150], later known as the HOSVD [29]. HOSVD is formed by computing the basis matrices $\mathbf{U}^{(n)}$ in (4.2) as the left singular vectors of the SVD of the n^{th} mode unfolding (defined in publication [VII, Section II-A]) of \mathcal{X} , see [VII, Section III-B]. The orthogonality property of this decomposition makes it convenient for deflation in order to form a low rank tensor approximation [67]. However, it should be again noted that, as opposed to the SVD for matrices, a low rank approximation through deflation is suboptimal for higher order tensors, albeit it may be a good one [30]. Also an

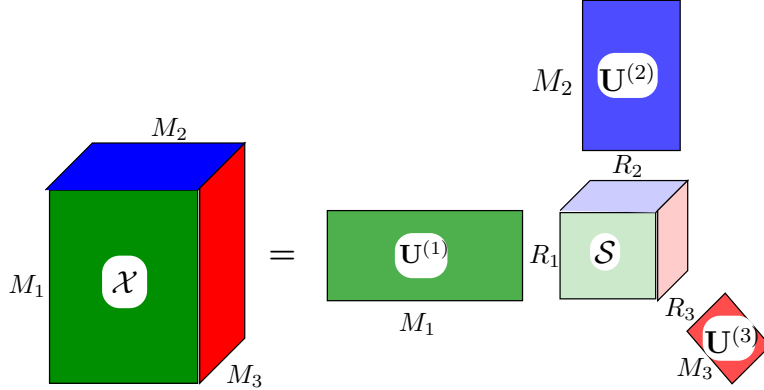


Figure 4.2: Illustration of the Tucker3 decomposition. The tensor is decomposed as a linear combination of basis vectors in different modes according to (4.2).

ALS solution exists for fitting a Tucker model [78, 133], but it requires that the number of factors in different modes R_n must be fixed.

4.2 PARATREE/SUSVD

4.2.1 PARATREE Model

In this subsection a novel PARATREE tensor decomposition studied in publications [IV, VI, VII] is introduced. It is based on a novel hierarchical formulation for a PARAFAC-type model having not only different number of factors in different modes, but additionally the number of factors in each mode can vary in each *branch* in the hierarchical tree structure. The term branch refers to a set of factors having common factor(s) in previous mode(s) (see Figure 4.3). The total number of factors used to form the decomposition depends on the magnitude of the factors of the previous modes of that branch. The product of the magnitudes indicates the significance of each branch.

The PARATREE model for an N -mode tensor can be expressed as a sum of outer products as

$$\mathcal{X} = \sum_{r_1=1}^{R_1} \mathbf{a}_{r_1}^{(1)} \circ \left(\sum_{r_2=1}^{R_2} \mathbf{a}_{r_1, r_2}^{(2)} \circ \cdots \circ \sum_{r_{N-1}=1}^{R_{N-1}} \left(\mathbf{a}_{r_1, \dots, r_{N-2}, r_{N-1}}^{(N-1)} \circ \mathbf{a}_{r_1, \dots, r_{N-2}, r_{N-1}}^{(N)} \right) \right). \quad (4.3)$$

The vector $\mathbf{a}_{r_1, \dots, r_n}^{(n)}$ above denotes the r_n^{th} column of the n^{th} mode matrix of basis vectors $\mathbf{A}_{r_1, \dots, r_{n-1}}^{(n)}$. The subscript r_1, \dots, r_{n-1} indicates the dependency of these matrices on the indexes of the previous factors of that branch in the decomposition tree. Also the number of factors R_n within each mode

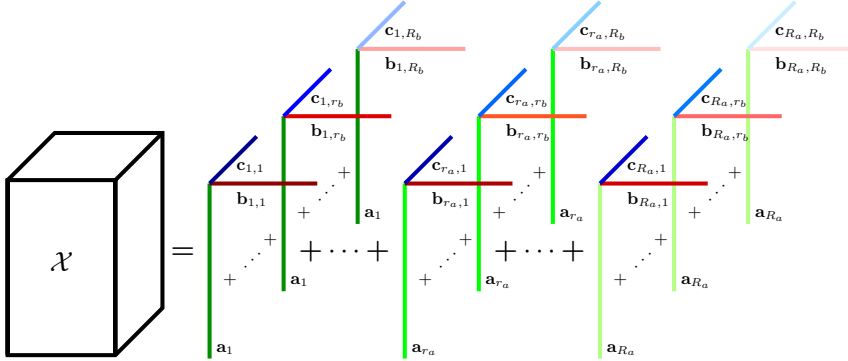


Figure 4.3: Illustration of the three-way PARATREE decomposition that is a hierarchical sum of R rank-1 tensors. The basis vector \mathbf{a}_{r_a} of the r_a^{th} factor in the first mode may be common for several factors in the remaining modes.

n can vary within different branches. Hence, R_n in (4.3) can be viewed as a shorthand notation for $R_{r_1, \dots, r_{n-1}}^{(n)}$.

The PARATREE model is illustrated for a three-way tensor in Figure 4.3. The difference to the PARAFAC model depicted in Figure 4.1 is seen in the r_a^{th} basis vector \mathbf{a}_{r_a} in the first mode, since it may be common for several factors in the remaining modes. To clarify the illustration in Figure 4.3, the notation of (4.3) can be simplified (for $N = 3$) to

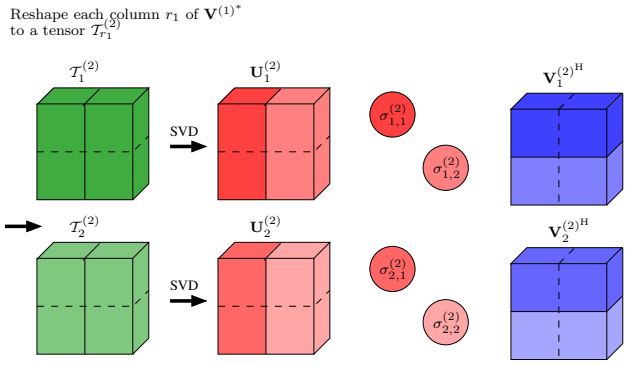
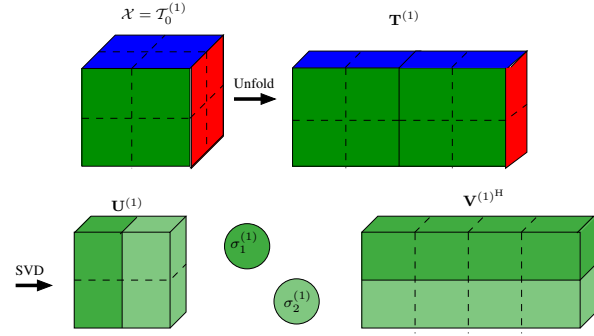
$$\mathcal{X} = \sum_{r_a=1}^{R_a} \mathbf{a}_{r_a} \circ \sum_{r_b=1}^{R_b} (\mathbf{b}_{r_a, r_b} \circ \mathbf{c}_{r_a, r_b}), \quad (4.4)$$

where the relation to (4.3) is obtained by setting $\{\mathbf{a}_{r_a}, \mathbf{b}_{r_a, r_b}, \mathbf{c}_{r_a, r_b}\} \equiv \{\mathbf{a}_{r_1}^{(1)}, \mathbf{a}_{r_1, r_2}^{(2)}, \mathbf{a}_{r_1, r_2}^{(3)}\}$.

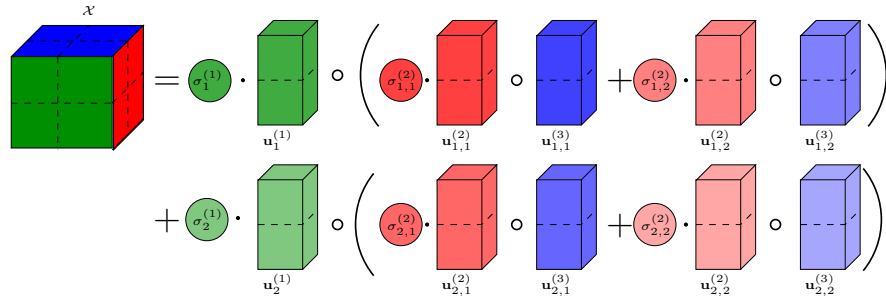
4.2.2 Sequential Unfolding SVD

SUSVD, introduced in this thesis, is a computational method for obtaining an orthogonal PARATREE model. It is based on the idea of sequentially applying the matrix SVD [44] on an unfolded tensor formed from each of the right singular vectors of the SVD in the previous mode. The SUSVD method and its reconstruction is visualized for a $2 \times 2 \times 2$ three-way tensor in Figure 4.4. The $2 \times 2 \times 2$ tensor in Figure 4.4a can be reconstructed with the PARATREE model as

$$\mathcal{X} = \sum_{r_1=1}^{R_1} \sigma_{r_1}^{(1)} \cdot \mathbf{u}_{r_1}^{(1)} \circ \sum_{r_2=1}^{R_2} \sigma_{r_1, r_2}^{(2)} \cdot \mathbf{u}_{r_1, r_2}^{(2)} \circ \mathbf{u}_{r_1, r_2}^{(3)}. \quad (4.5)$$



(a) Decomposition.



(b) Reconstruction.

Figure 4.4: The SUSVD for a $2 \times 2 \times 2$ tensor. Different colors refer to different dimensions of the tensor. A circled σ denotes a singular value, dashed blocks are elements of the tensors, and solid lines are used to separate the column vectors. (a) The tensor is first unfolded to a matrix $\mathbf{T}_0^{(1)}$. After applying SVD on this matrix, each of the right-hand singular vectors are reshaped and another SVD is applied on them. The procedure is repeated for each “branch” and “sub-branch”, until no additional dimensions remain in the right hand basis vectors, i.e., the matrix $\mathbf{V}^{(N-1)}$ has only M_N rows. (b) The tensor is reconstructed as a sum of outer products of weighted (by $\sigma_{r_1}, \sigma_{r_1, r_2}$) unitary basis vectors $\mathbf{u}_{r_1}^{(1)}, \mathbf{u}_{r_1, r_2}^{(2)}$ and $\mathbf{u}_{r_1, r_2}^{(3)}$.

The full ($R_1 = 2$, $R_2 = 2$) reconstruction is illustrated in Figure 4.4b. A detailed description of the algorithm is given in publication [VII, Section III-C].

It should be noted that all the rank-1 components in the PARATREE model given by the SUSVD are orthogonal to each other (see the proof in publication [VII, Appendix B]). This facilitates deflating the full decomposition and obtaining a low rank approximation having a precisely specified fitting error, which is a highly desirable feature in several applications.

4.3 Application Examples of Tensor Models

4.3.1 Tensor Valued MIMO Channel Modeling

To support the discussion in this section on the relations between the hybrid MIMO channel model (2.20) and tensor decompositions, let us first introduce the tensor equivalent to the vectorized channel model (2.20) as

$$\mathcal{H} = \mathcal{H}_S + \mathcal{H}_D + \mathcal{H}_N \in \mathbb{C}^{M_f \times M_T \times M_R}, \quad (4.6)$$

where \mathcal{H}_S , \mathcal{H}_D , and \mathcal{H}_N denote the tensor valued model parts for the propagation paths, DMC and measurement noise, respectively. The relation to the vector model (2.20) is simply given by $\mathbf{h} = \text{vec}(\mathcal{H})$.

Double Directional Propagation Path Model as a PARAFAC Model

An example of a PARAFAC model is obtained by expressing the double directional propagation path model (2.21) in tensor form as

$$\mathcal{H} = \sum_{p=1}^P \mathbf{b}_p^{(f)} \circ \left(\sum_{T_{pol}=\{H,V\}} \sum_{R_{pol}=\{H,V\}} \gamma_{T_{pol}R_{pol},p} \cdot \mathbf{b}_{T_{pol},p}^{(T)} \circ \mathbf{b}_{R_{pol},p}^{(R)} \right), \quad (4.7)$$

where the relation of the basis vectors $\mathbf{b}^{(i)}$ to (2.22) is given by $\mathbf{B}_{T/R_{pol}} = [\mathbf{b}_{T/R_{pol},1}^{(T/R)} \cdots \mathbf{b}_{T/R_{pol},P}^{(T/R)}]$ and $\mathbf{B}_f = [\mathbf{b}_{f,1}^{(f)} \cdots \mathbf{b}_{f,P}^{(f)}]$. Equation (4.7) can be further simplified to

$$\mathcal{H} = \sum_{p'=1}^{P'} \left(\gamma_{p'} \cdot \mathbf{b}_{p'}^{(f)} \circ \mathbf{b}_{p'}^{(T)} \circ \mathbf{b}_{p'}^{(R)} \right), \quad (4.8)$$

where the index p' includes also the polarization effects, i.e., $P' = N_{pol}P$.

Double Directional Propagation Path Model as a Tucker Model

As an example of a Tucker model, the instantaneous $M_f \times M_T \times M_R$ channel may be written as

$$\mathcal{H} = \left(\sum_{T_{pol}=\{H,V\}} \sum_{R_{pol}=\{H,V\}} \mathcal{G}_{T_{pol}R_{pol}} \times_2 \mathbf{B}_{T_{pol}}^{(T)} \times_3 \mathbf{B}_{R_{pol}}^{(R)} \right) \times_1 \mathbf{B}^{(f)}, \quad (4.9)$$

which is essentially a sum of four Tucker3-type tensor decompositions with super diagonal core tensors $\mathcal{G}_{T_{pol}R_{pol}}$, one for each polarization component (HH , HV , VH , and VV), and a common basis matrix $\mathbf{B}^{(f)}$ in the frequency dimension.

Realization of DMC as a Tucker Model

Another example of a Tucker model is provided by considering a random realization of the DMC in (2.23). The distribution of the vector valued DMC is given by $\mathbf{h}_D \sim \mathcal{N}_C(\mathbf{0}, \mathbf{R}_D)$. The eigenvalue decomposition (EVD) of the covariance matrix \mathbf{R}_D in (2.24) may be written as

$$\begin{aligned} \mathbf{R}_D &= \mathbf{U} \mathbf{\Lambda} \mathbf{U}^H \\ &= (\mathbf{U}^{(R)} \otimes \mathbf{U}^{(T)} \otimes \mathbf{U}^{(f)}) (\mathbf{\Lambda}^{(R)} \otimes \mathbf{\Lambda}^{(T)} \otimes \mathbf{\Lambda}^{(f)}) (\mathbf{U}^{(R)} \otimes \mathbf{U}^{(T)} \otimes \mathbf{U}^{(f)})^H \\ &= (\mathbf{U}'^{(R)} \otimes \mathbf{U}'^{(T)} \otimes \mathbf{U}'^{(f)}) (\mathbf{U}'^{(R)} \otimes \mathbf{U}'^{(T)} \otimes \mathbf{U}'^{(f)})^H, \end{aligned} \quad (4.10)$$

where $\mathbf{U}'^{(i)} = \mathbf{U}^{(i)} \mathbf{\Lambda}^{(i)1/2}$, $i \in \{f, T, R\}$. It can be seen from this relation that a realization of the DMC in a tensor form $\mathcal{H}_D \in \mathbb{C}^{M_f \times M_T \times M_R}$ can be written using a Tucker notation as

$$\mathcal{H}_D = \mathcal{H}_w \times_1 \mathbf{U}'^{(f)} \times_2 \mathbf{U}'^{(T)} \times_3 \mathbf{U}'^{(R)}, \quad (4.11)$$

where \mathcal{H}_w denotes a matrix having each of its elements drawn from $\mathcal{N}_C(0, 1)$. An alternative expression is given by

$$\mathcal{H}_D = \left(\mathcal{H}_w \odot (\boldsymbol{\lambda}^{(f)} \circ \boldsymbol{\lambda}^{(T)} \circ \boldsymbol{\lambda}^{(R)})^{\frac{1}{2}} \right) \times_1 \mathbf{U}^{(f)} \times_2 \mathbf{U}^{(T)} \times_3 \mathbf{U}^{(R)}, \quad (4.12)$$

where $\boldsymbol{\lambda}^{(i)} = \text{diag}(\mathbf{\Lambda}^{(i)})$, and \odot denotes an element-wise product. The form in (4.12) allows a simple way to include the measurement noise, see (2.25), as its variance can be directly summed with the DMC eigenvalue tensor, yielding

$$\mathcal{H}_D + \mathcal{H}_N = \left(\mathcal{H}_w \odot (\boldsymbol{\lambda}^{(f)} \circ \boldsymbol{\lambda}^{(T)} \circ \boldsymbol{\lambda}^{(R)} + \sigma_N^2)^{\frac{1}{2}} \right) \times_1 \mathbf{U}^{(f)} \times_2 \mathbf{U}^{(T)} \times_3 \mathbf{U}^{(R)}. \quad (4.13)$$

Tensor Generalization of the Weichselberger Model as a Tucker Model

The spatial Weichselberger model (WB) in (2.17) can be extended to include additional dimensions, such as frequency in our task at hand, using the Tucker notation. This extension for the wideband MIMO channel using tensor notation has been discussed also in [20]. A realization of the three dimensional channel is given by

$$\mathcal{H}_{WB} = \left(\mathcal{H}_w \odot \widetilde{\mathcal{W}}_{WB} \right) \times_1 \mathbf{U}^{(f)} \times_2 \mathbf{U}^{(T)} \times_3 \mathbf{U}^{(R)}, \quad (4.14)$$

where $\widetilde{\mathcal{W}}_{WB}$ denotes the element-wise square root of a power coupling tensor, which is the equivalent of the power coupling matrix $\mathbf{\Omega}_{WB}$ in (2.17). Following the derivation for the spatial model in [158], an estimate of the power coupling tensor can be obtained as follows. Let us define $\mathcal{K}(t)$ as the channel tensor at time t in the *eigendomain*, given by

$$\mathcal{K}(t) = \mathcal{H}(t) \times_1 \mathbf{U}^{(f)\text{H}} \times_2 \mathbf{U}^{(T)\text{H}} \times_3 \mathbf{U}^{(R)\text{H}}. \quad (4.15)$$

An estimate of the power coupling tensor is then obtained by

$$\widehat{\mathcal{W}}_{WB} = \frac{1}{T} \sum_{t=1}^T (\mathcal{K}(t) \odot \mathcal{K}^*(t)). \quad (4.16)$$

4.3.2 Applications for PARATREE/SUSVD in Array Signal Processing

Reduction of Computational Complexity

The SUSVD was first introduced in publication [IV] to facilitate computationally efficient approximate solution for the FIM used in the developed EKF, see Section 3.4.2. In earlier work [I–III] a simplified structure (spatial whiteness $\mathbf{R}_T = \mathbf{R}_R = \mathbf{I}$) was assumed for the Kronecker structured covariance matrix of the DMC model (2.24). However, as pointed out in publication [IV] and [112] this assumption may not be realistic in general. Nevertheless, the more general model (2.24) increases the computational complexity significantly (see [IV], [VII, Section IV-B]). Fortunately, the complexity can be reduced by rewriting the problem by using a low rank tensor approximation considered in publications [IV, VII].

Figure 4.5 shows an example comparison of computational complexity while computing the FIM for different low rank decompositions as a function of approximation error. The best performance is obtained using the PARATREE/SUSVD solution. The detailed description of the problem can be found in publication [VII, Section IV].

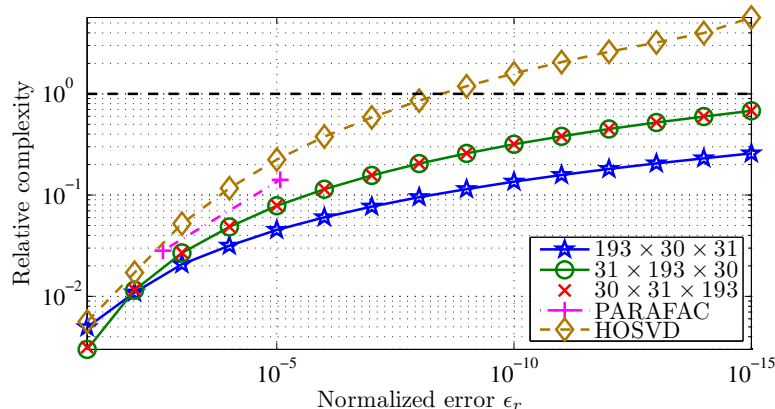


Figure 4.5: Complexity relative to an exact solution for computing the Fisher information matrix with PARATREE, PARAFAC, and HOSVD. PARATREE was applied for different ordering of the dimensions with $M_f = 193$, $M_T = 30$, and $M_R = 31$. Having the largest dimension first yields the most reduction in computational complexity with PARATREE. The PARAFAC-ALS failed to converge while fitting higher rank models. The considered HOSVD strategy has the highest complexity in this task, and the complexity can even grow higher than that of the exact solution.

Filtering of Channel Sounding Data

Another application utilizing the low rank tensor approximation is the filtering of the measurement noise in channel sounding data. This application was first proposed in [116], and it has been further analyzed in publications [VI] and [VII]. The basic idea is to compute the full SUSVD for a set of tensor valued MIMO channel sounding data. This decomposition is then deflated by subtracting the least significant orthogonal components that cumulatively contribute to noise energy present in the data.

Figure 4.6 illustrates the SNR gain obtained by using the proposed solution in a PDP averaged over all Tx-Rx channels of a measured MIMO snapshot. In this example the SNR improvement is in the order of 15 dB. Detailed description of the proposed method can be found in publications [VI, VII]. The latter also contains comparison against equivalent approach using HOSVD.

4.4 Summary and Discussion

In this chapter MIMO channel sounding data has been represented in tensor form. Well known tensor models such as PARAFAC [54, 79] and Tucker [150] are employed. Furthermore, a novel PARATREE tensor model and a non-iterative orthogonal decomposition technique SUSVD have been introduced

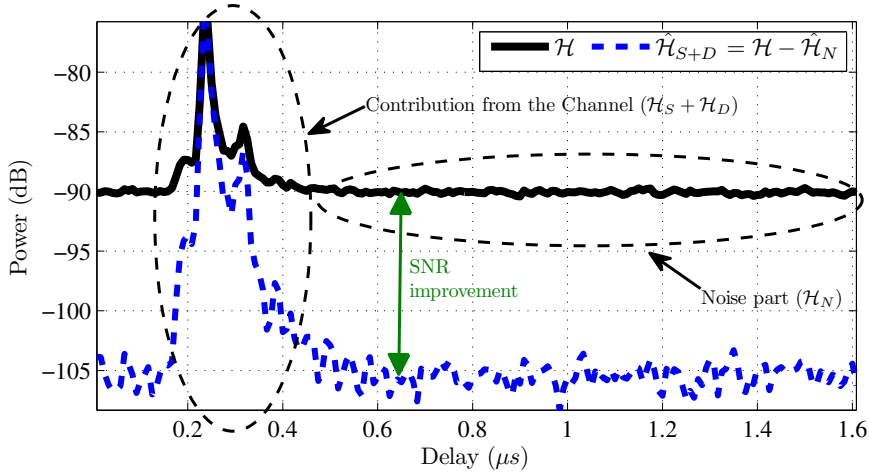


Figure 4.6: The SNR of a measured MIMO snapshot with poor initial SNR is improved by 15 dB by applying SUSVD-based noise removal method.

in publications [IV, VI, VII]. Application examples are provided in array signal processing and MIMO channel sounding. The proposed PARATREE/SUSVD method is very suitable for low rank tensor approximation in applications involving MIMO channel sounding data. Other applications and desirable features include, but may not be restricted to

- Reducing computational complexity in high dimensional problems (including the FIM computation for the EKF)
- Measurement noise suppression (subspace filtering)
- Data compression and analysis (similar to low rank matrix approximation)
- Fast and reliable computation and possibility to do adaptive selection of the rank
- Revealing hidden structures and dependencies in data.

Table 4.1 provides a comparison of the properties of different tensor decompositions. PARAFAC based models are most suitable for model identification, such as blind source separation or chemical analysis, whereas Tucker models provide an orthogonal decomposition best suitable for compression or low rank approximation. Also PARATREE possesses the orthogonality property through SUSVD, which makes it an attractive representation for low rank approximation. In addition, while fitting the model to data with a fixed fitting error, PARATREE allows an individual set of basis vectors for each branch yielding smaller rank compared to Tucker-based models such

Table 4.1: Summary of tensor decompositions.

Feature	Approach		
	PARAFAC	Tucker	PARATREE
Orthogonality	-	+	+
Identification	+	-	-
Compression	-	+	+
Low rank approx.	-	+	++
Computation	-	+	+

as HOSVD [29]. This property is very useful for example in the FIM computation example, see publication [VII].

As tensor representation provides natural means to express multidimensional problems it can be expected that tensor modeling will increase its popularity in the design and analysis of wireless communication systems and array signal processing. This claim is also supported by the growing dimensionality in wireless communications through introduction of diversity and multiantenna techniques. Seminal work in this area has already been conducted in e.g., [24, 25, 49, 123, 132].

Chapter 5

Summary

This thesis contains several contributions to measurement-based dynamic MIMO channel modeling and related propagation parameter estimation.

Modeling of the physical wireless MIMO channel is an important and necessary enabler for several tasks in the development of MIMO systems. These tasks include information theoretical studies, transceiver algorithm and hardware design, antenna design, and network planning, to name a few. However, different tasks impose different and often contradicting requirements for models. Chapter 2 provides an overview of different modeling approaches and their applicability and limitations in specific tasks. Special attention is given to measurement-based channel modeling (MBCM), which aims at modeling the measured MIMO channel independently of the measurement system, i.e., regardless of the transmitted waveform, antenna configuration and other properties of the employed hardware. The double directional propagation path channel model (2.3) is an example of a model capable of decoupling the MIMO channel from the radio front-ends. However, in practice it is necessary to model also the dense multipath component (DMC) of the channel resulting from the diffuse scattering in the environment. Together the superposition of concentrated propagation paths and the DMC constitute the hybrid channel model described in Section 2.3.3.

In mobile communication systems the channels are time-varying and studying the wireless MIMO channel for such systems requires dynamic channel sounding measurements. In order to obtain realistic characterization of such dynamic channel conditions it is necessary to formulate also the channel model in a dynamic form. Chapter 3 discusses the estimation of propagation parameters from channel sounding measurements. Conventional and state-of-the-art methods such as SAGE [38–40] and RIMAX [108–110] rely on a static channel model and fail to capture the dynamic properties of the mobile channel. Moreover, they rely on batch computation and everything needs to be re-computed at the arrival of new observation. In Section 3.4 the hybrid channel model is formulated as a dynamic state-space model in

order to track the parameters of the double directional propagation path model. The method of choice for the sequential estimation problem is the Extended Kalman filter (EKF) due to its suitability considering given modeling assumptions, along with its significantly lower computational complexity. Another important part of the estimation procedure is the model order adjustment since the number of significant propagation paths contributing to the overall MIMO channel varies over time. In this thesis an approach based on hypothesis testing is proposed. A detailed description of the state-space modeling approach summarized in Section 3.4 for propagation path tracking can be found in the original publications [I–V].

The last part of this thesis deals with tensor decomposition techniques. Tensor representation provides a natural means for expressing multidimensional data. Tensor decompositions have several applications in signal processing including rank and basis identification, data compression, dimensionality reduction through low rank approximation etc. In Section 4.2 a novel PARATREE/SUSVD method is introduced. The low rank tensor approximation obtained using this method provides significant reduction in computational complexity, for example, while solving the Fisher Information matrix (FIM), which is included in the formulation of the employed EKF in Section 3.4. The need for such complexity reduction arises from the underlying data covariance model comprised of the superposition of the general Kronecker model for the DMC (2.24) and the measurement noise (2.25). This general DMC model was employed in publications [IV, V], whereas in [I–III] the Tx and Rx covariance matrices were assumed to be spatially white — a fact that allowed significant computational simplification. In publications [VI, VII], the PARATREE/SUSVD is identified as a more general tensor decomposition and its performance is compared against well known PARAFAC and HOSVD decompositions. The SUSVD provides an orthogonal PARATREE decomposition, which makes it suitable for low rank approximation through deflation. Comparing against HOSVD with a similar deflation approach and a fixed approximation error, the SUSVD yields a smaller rank due to a richer set of basis functions, i.e., an individual set is computed for each branch in the PARATREE model.

Research work not only solves some research problems, but also leads to identifying new research topics and open problems. In the following is a list of some future research topics, which deserve to be further studied based on the findings made in this thesis:

- Analyzing the propagation parameter estimates obtained from various measurement campaigns in order to develop realistic dynamic MIMO channel models.
- Development of the dynamic model used in the estimator in terms of relating the state noise quantities more rigorously to different environmental variables such as velocity of the terminals.

- Comparing the estimation performance while applying different antenna models and array manifold representations, for example, EADF [62, 82, 83, 108] vs. spherical harmonics [33, 52].
- Improving the path detection scheme in terms of optimizing the multidimensional and possibly correlated detection grid.
- Development of the DMC model in terms of mixture modeling, time-evolution, and deriving realistic parametric models for the covariance matrices of the different data dimensions.
- Investigating the possibility to employ tensor techniques in MIMO communications. Prospective applications include multidimensional channel estimation, as well as low-rank approximation and compression to support channel state information (CSI) feedback.
- Finding new signal processing applications for the SUSVD and other tensor decompositions.

Bibliography

- [1] 3GPP. 3GPP Long Term Evolution (LTE). [Online]. Available: <http://www.3gpp.org/Highlights/LTE/LTE.htm>
- [2] 3GPP. 3GPP TR 25.876, Multiple Input Multiple Output (MIMO) antennae in UTRA. [Online]. Available: <http://www.3gpp.org/ftp/Specs/html-info/25876.htm>
- [3] 3GPP, “Spatial channel model for Multiple Input Multiple Output (MIMO) simulations,” Sept. 2003. [Online]. Available: <http://www.3gpp.org/ftp/Specs/html-info/25996.htm>
- [4] P. Almers, E. Bonek, A. Burr, N. Czink, M. Debbah, V. Degli-Esposti, H. Hofstetter, P. Kyösti, D. Laurenson, G. Matz, A. F. Molisch, C. Oestges, and H. Özcelik, “Survey of channel and radio propagation models for wireless MIMO systems,” *EURASIP Journal on Wireless Communications and Networking*, vol. 2007, 2007, article ID 19070.
- [5] P. Almers, K. Haneda, J. Koivunen, V.-M. Kolmonen, A. F. Molisch, A. Richter, J. Salmi, F. Tufvesson, and P. Vainikainen, “A dynamic multi-link MIMO measurement system for 5.3 GHz,” in *URSI General Assembly*, Chicago, USA, Aug. 7–16 2008.
- [6] M. Arulampalam, S. Maskell, N. Gordon, and T. Clapp, “A tutorial on particle filters for online nonlinear/non-Gaussian Bayesian tracking,” *IEEE Transactions on Signal Processing*, vol. 50, no. 2, pp. 174–188, Feb. 2002.
- [7] Y. Bar-Shalom, X. R. Li, and T. Kirubarajan, *Estimation with Applications to Tracking and Navigation*. John Wiley and Sons Ltd., 2001, 558 p.
- [8] D. Baum, J. Hansen, and J. Salo, “An interim channel model for beyond-3G systems: extending the 3GPP spatial channel model (SCM),” in *The 61st IEEE Vehicular Technology Conference (VTC 2005-spring)*, vol. 5, May–Jun. 2005, pp. 3132–3136.

- [9] G. Bienvenu and L. Kopp, "Adaptivity to background noise spatial coherence for high resolution passive methods," in *IEEE International Conference on Acoustics, Speech, and Signal Processing (ICASSP 1980)*, vol. 5, Denver, CO, Apr. 1980, pp. 307–310.
- [10] J. Blanz and P. Jung, "A flexibly configurable spatial model for mobile radio channels," *IEEE Transactions on Communications*, vol. 46, no. 3, pp. 367–371, Mar. 1998.
- [11] R. Bro and H. A. L. Kiers, "A new efficient method for determining the number of components in PARAFAC models," *Journal of Chemometrics*, vol. 17, no. 5, pp. 274–286, 2003.
- [12] R. G. Brown and P. Y. Hwang, *Introduction to Random Signals and Applied Kalman Filtering*, 3rd ed. New York, NY: John Wiley and Sons Inc., 1997, 484 p.
- [13] A. Burr, "Capacity bounds and estimates for the finite scatterers MIMO wireless channel," *IEEE Journal on Selected Areas in Communications*, vol. 21, no. 5, pp. 812–818, Jun. 2003.
- [14] J. Capon, "High-resolution frequency-wavenumber spectrum analysis," *Proc. IEEE*, vol. 57, no. 8, pp. 1408–2418, Aug. 1969.
- [15] J. D. Carroll and J. J. Chang, "Analysis of individual differences in multidimensional scaling via an N-way generalization of 'Eckart-Young' decomposition," *Psychometrika*, vol. 35, pp. 283–319, 1970.
- [16] J. D. Carroll, S. Pruzansky, and J. Kruskal, "Candelinec: A general approach to multidimensional analysis of many-way arrays with linear constraints on parameters," *Psychometrika*, vol. 45, no. 1, pp. 3–24, Mar. 1980.
- [17] P. Comon and J. ten Berge, "Generic and typical ranks of three-way arrays," in *IEEE International Conference on Acoustics, Speech and Signal Processing (ICASSP 2008)*, Las Vegas, NV, Apr. 2008, pp. 3313–3316.
- [18] G. Corazza, V. Degli-Esposti, M. Frullone, and G. Riva, "A characterization of indoor space and frequency diversity by ray-tracing modeling," *IEEE Journal on Selected Areas in Communications*, vol. 14, no. 3, pp. 411–419, Apr. 1996.
- [19] L. M. Correia, Ed., *Mobile Broadband Multimedia Networks*, 1st ed. Academic Press, May 2006, 608 p.
- [20] N. Costa, "Wideband MIMO channel models: Theory and practice," Ph. D. dissertation, ETD Collection for McMaster University, Canada, Jan. 2007, paper AAINR36025.

- [21] H. Cramér, *Mathematical Methods of Statistics*. Princeton, NJ: Princeton Univ. Press, 1946, 575 p.
- [22] N. Czink, “The random-cluster model,” Ph. D. dissertation, Vienna University of Technology, Institute of Communications and Radio-Frequency Engineering, Vienna, Austria, 2007. [Online]. Available: http://www.tuwien.ac.at/tu_vienna/research/publication_database/
- [23] N. Czink and C. Oestges, “The COST 273 MIMO channel model: Three kinds of clusters,” in *IEEE 10th International Symposium on Spread Spectrum Techniques and Applications (ISSSTA 2008)*, Aug. 2008, pp. 282–286.
- [24] A. de Almeida, G. Favier, and J. Mota, “A constrained factor decomposition with application to MIMO antenna systems,” *IEEE Transactions on Signal Processing*, vol. 56, no. 6, pp. 2429–2442, Jun. 2008.
- [25] A. L. F. de Almeida, G. Favier, J. C. M. Mota, and R. L. de Lacerda, “Estimation of frequency-selective block-fading MIMO channels using PARAFAC modeling and alternating least squares,” in *The 40th Asilomar Conference on Signals, Systems and Computers*, Pacific Grove, CA, Oct.–Nov. 2006, pp. 1630–1634.
- [26] L. De Lathauwer, “Decompositions of a higher-order tensor in block terms — Part II: Definitions and uniqueness,” *SIAM J. Matrix Anal. Appl.*, vol. 30, no. 3, pp. 1033–1066, 2008. [Online]. Available: http://publi-etis.ensea.fr/2008/De_08f
- [27] L. De Lathauwer, B. De Moor, and J. Vandewalle, “Computation of the canonical decomposition by means of a simultaneous generalized Schur decomposition,” *SIAM J. Matrix Anal. Appl.*, vol. 26, no. 2, pp. 295–327, 2004. [Online]. Available: <http://publi-etis.ensea.fr/2004/DDV04>
- [28] L. De Lathauwer, “A link between the canonical decomposition in multilinear algebra and simultaneous matrix diagonalization,” *SIAM J. Matrix Anal. Appl.*, vol. 28, no. 3, pp. 642–666, 2006.
- [29] L. De Lathauwer, B. De Moor, and J. Vandewalle, “A multilinear singular value decomposition,” *SIAM J. Matrix Anal. Appl.*, vol. 21, no. 4, pp. 1253–1278, 2000.
- [30] L. De Lathauwer, B. De Moor, and J. Vandewalle, “On the best rank-1 and rank- (r_1, r_2, \dots, r_n) approximation of higher-order tensors,” *SIAM Journal on Matrix Analysis and Applications*, vol. 21, no. 4, pp. 1324–1342, 2000. [Online]. Available: <http://link.aip.org/link/?SML/21/1324/1>

- [31] M. Debbah and R. Müller, “MIMO channel modeling and the principle of maximum entropy,” *IEEE Transactions on Information Theory*, vol. 51, no. 5, pp. 1667–1690, May 2005.
- [32] V. Degli-Esposti, D. Guiducci, A. de’ Marsi, P. Azzi, and F. Fuschini, “An advanced field prediction model including diffuse scattering,” *IEEE Transactions on Antennas and Propagation*, vol. 52, no. 7, pp. 1717–1728, Jul. 2004.
- [33] G. Del Galdo, “Geometry-based channel modeling for multi-user MIMO systems and applications,” Ph.D. dissertation, Ilmenau University of Technology, Ilmenau, Germany, 2007, ISBN: 978-3-938843-27-7. [Online]. Available: <http://www.delgaldo.com>
- [34] W. F. Denham and S. Pines, “Sequential estimation when measurement function nonlinearity is comparable to measurement error,” *AIAA Journal*, vol. 4, no. 6, pp. 1071–1076, 1966.
- [35] A. Doucet and A. Johansen, “A tutorial on particle filtering and smoothing: fifteen years later,” Department of Statistics, University of British Columbia, Technical report D1.1.2, 2008. [Online]. Available: <http://www.cs.ubc.ca/~arnaud/>
- [36] Elektrobit Ltd, “Propsound,” 2008. [Online]. Available: <http://www.propsim.com/>
- [37] N. K. M. Faber, R. Bro, and P. K. Hopke, “Recent developments in CANDECOMP/PARAFAC algorithms: a critical review,” *Chemometrics and Intelligent Laboratory Systems*, vol. 65, no. 1, pp. 119–137, Jan. 2003.
- [38] J. A. Fessler and A. O. Hero, “Space alternating generalized expectation maximization algorithm,” *IEEE Transactions on Signal Processing*, vol. 42, pp. 2664–2677, Oct. 1994.
- [39] B. H. Fleury, M. Tschudin, R. Heddergott, D. Dahlhaus, and K. I. Pedersen, “Channel parameter estimation in mobile radio environments using the SAGE algorithm,” *IEEE Journal on Selected Areas in Communications*, vol. 17, no. 3, pp. 434–450, Mar. 1999.
- [40] B. Fleury, P. Jourdan, and A. Stucki, “High-resolution channel parameter estimation for MIMO applications using the SAGE algorithm,” in *International Zürich Seminar on Broadband Communications, Access, Transmission, Networking*, Feb. 19–21 2002, pp. 30–1–30–9.
- [41] G. J. Foschini and M. J. Gans, “On the limits of wireless communications in a fading environment when using multiple antennas,” *Wireless Personal Communications*, vol. 6, no. 3, pp. 311–335, Mar. 1998.

- [42] F. Fuschini, H. El-Sallabi, V. Degli-Esposti, L. Vuokko, D. Guiducci, and P. Vainikainen, "Analysis of multipath propagation in urban environment through multidimensional measurements and advanced ray tracing simulation," *IEEE Transactions on Antennas and Propagation*, vol. 56, no. 3, pp. 848–857, Mar. 2008.
- [43] A. B. Gershman and N. D. Sidiropoulos, Eds., *Space-Time Processing for MIMO Communications*. Chichester, England: John Wiley and Sons, Ltd, 2005, 369 p.
- [44] G. H. Golub and C. F. van Loan, *Matrix Computations*, 3rd ed. The Johns Hopkins University Press, 1996, 728 p.
- [45] N. Gordon, D. Salmond, and A. Smith, "Novel approach to nonlinear/non-Gaussian Bayesian state estimation," *IEE Proceedings F*, vol. 140, no. 2, pp. 107–113, Apr. 1993.
- [46] M. S. Grewal and A. P. Andrews, *Kalman Filtering, Theory and Practice Using MATLAB*, 2nd ed. Wiley Interscience, 2001, 416 p.
- [47] F. Gustafsson, *Adaptive Filtering and Change Detection*. Chichester, England: John Wiley and Sons, Ltd., 2000, 500 p.
- [48] M. Haardt and J. Nosssek, "Simultaneous Schur decomposition of several nonsymmetric matrices to achieve automatic pairing in multidimensional harmonic retrieval problems," *IEEE Transactions on Signal Processing*, vol. 46, no. 1, pp. 161–169, Jan. 1998.
- [49] M. Haardt, F. Roemer, and G. Del Galdo, "Higher-order SVD-based subspace estimation to improve the parameter estimation accuracy in multidimensional harmonic retrieval problems," *IEEE Transactions on Signal Processing*, vol. 56, no. 7, pp. 3198–3213, Jul. 2008.
- [50] M. Haardt, M. Zoltowski, C. Mathews, and J. Nosssek, "2D unitary ESPRIT for efficient 2D parameter estimation," in *International Conference on Acoustics, Speech, and Signal Processing (ICASSP 1995)*, vol. 3, Detroit, MI, May 1995, pp. 2096–2099.
- [51] D. Hampicke, M. Landmann, C. Schneider, G. Sommerkorn, T. Thomä, T. Fügen, J. Maurer, and W. Wiesbeck, "MIMO capacities for different antenna array structures based on double directional wide-band channel measurements," in *The 56th IEEE Vehicular Technology Conference (VTC 2002-fall)*, vol. 1, Vancouver, Canada, Sept. 2002, pp. 180–184.
- [52] J. E. Hansen, *Spherical Near-Field Antenna Measurements*. London, UK: Peter Peregrinus Ltd., 1988, 387 p.

- [53] R. F. Harrington, *Field Computation by Moment Methods*. New York, NY: the Macmillan Co., 1968, 229 p.
- [54] R. A. Harshman, “Foundations of the PARAFAC procedure: Models and conditions for an ‘explanatory’ multi-modal factor analysis,” *UCLA working papers in phonetics*, vol. 16, 1970.
- [55] L. Hentilä, P. Kyösti, M. Käske, M. Narandzić, and M. Alatossava, “MATLAB implementation of the WINNER Phase II Channel Model ver1.1,” Dec. 2007. [Online]. Available: http://www.ist-winner.org/phase_2_model.html
- [56] IEEE. IEEE 802.11 Wireless Local Area Networks (WLAN). [Online]. Available: <http://www.ieee802.org/11/>
- [57] IEEE. IEEE 802.16 Wireless Metropolitan Area Networks (WMAN). [Online]. Available: <http://www.ieee802.org/16/>
- [58] International Telecommunication Union, Radiocommunication Sector (ITU-R). IMT-Advanced. [Online]. Available: <http://www.itu.int/ITU-R/>
- [59] A. Jaffer, “Maximum likelihood direction finding of stochastic sources: a separable solution,” in *International Conference on Acoustics, Speech, and Signal Processing (ICASSP 1988)*, vol. 5, New York, NY, Apr. 1988, pp. 2893–2896.
- [60] S. J. Julier and J. K. Uhlmann, “A new extension of the Kalman filter to nonlinear systems,” in *The 11th Int. Symp. on Aerospace/Defence Sensing, Simulation and Controls (AeroSense 1997)*, Orlando, FL, Apr. 1997.
- [61] S. J. Julier and J. K. Uhlmann, “Unscented filtering and nonlinear estimation,” *Proc. IEEE*, vol. 92, no. 3, pp. 401–422, Mar. 2004.
- [62] T. Kaiser, A. Bourdoux, H. Boche, J. R. Fonollosa, J. B. Andersen, and W. Utschick, Eds., *Smart Antennas — State of the Art*. New York, NY: Hindawi Publishing Corporation, 2005, 876 p.
- [63] K. Kalliola, “Experimental analysis of multidimensional radio channels,” Ph.D. dissertation, Helsinki University of Technology, Feb. 2002, Radio laboratory publication series S251. [Online]. Available: <http://lib.hut.fi/Diss/2002/isbn951225705X/>
- [64] K. Kalliola, H. Laitinen, L. Vaskelainen, and P. Vainikainen, “Real-time 3-D spatial-temporal dual-polarized measurement of wideband radio channel at mobile station,” *IEEE Transactions on Instrumentation and Measurement*, vol. 49, no. 2, pp. 439–448, Apr. 2000.

- [65] R. E. Kalman, "A new approach to linear filtering and prediction problems," *Transactions of the ASME—Journal of Basic Engineering*, vol. 82, no. Series D, pp. 35–45, 1960.
- [66] S. M. Kay, *Fundamentals of Statistical Signal Processing: Detection Theory*. Prentice-Hall International, 1998, vol. 2, 672 p.
- [67] H. A. Kiers and A. der Kinderen, "A fast method for choosing the numbers of components in Tucker3 analysis," *British Journal of Mathematical & Statistical Psychology*, vol. 56, no. 1, pp. 119–125, 2003.
- [68] J. Kivinen, T. Korhonen, P. Aikio, R. Gruber, P. Vainikainen, and S.-G. Häggman, "Wideband radio channel measurement system at 2 GHz," *IEEE Transactions on Instrumentation and Measurement*, vol. 48, no. 1, pp. 39–44, Feb. 1999.
- [69] E. Kofidis and P. A. Regalia, "On the best rank-1 approximation of higher-order supersymmetric tensors," *SIAM J. Matrix Anal. Appl.*, vol. 23, pp. 863–884, 2002.
- [70] J. Koivunen, P. Almers, V.-M. Kolmonen, J. Salmi, A. Richter, F. Tufvesson, P. Suvikunnas, A. Molisch, and P. Vainikainen, "Dynamic multi-link indoor MIMO measurements at 5.3 GHz," in *The 2nd European Conference on Antennas and Propagation (EuCAP 2007)*, Edinburgh, UK, Nov. 2007, pp. 1–6.
- [71] T. G. Kolda and B. W. Bader, "Tensor decompositions and applications," *SIAM Review*, vol. 51, no. 3, Sept. 2009, to appear.
- [72] V.-M. Kolmonen, "Kolmiulotteinen 5 GHz:n MIMO-kanavaluotaimen antennijärjestelmä," Master's thesis, Helsinki University of Technology, Radio laboratory, Espoo, Finland, Feb. 2004.
- [73] V.-M. Kolmonen, P. Almers, J. Salmi, J. Koivunen, K. Haneda, A. Richter, F. Tufvesson, A. F. Molisch, and P. Vainikainen, "A dynamic dual-link wideband MIMO measurement system for 5.3 GHz," *IEEE Transactions on Instrumentation and Measurement*, 2009, accepted.
- [74] V.-M. Kolmonen, J. Kivinen, L. Vuokko, and P. Vainikainen, "5.3-GHz MIMO radio channel sounder," *IEEE Transactions on Instrumentation and Measurement*, vol. 55, no. 4, pp. 1263–1269, Aug. 2006.
- [75] R. Kouyoumjian and P. Pathak, "A uniform geometrical theory of diffraction for an edge in a perfectly conducting surface," *Proceedings of the IEEE*, vol. 62, no. 11, pp. 1448–1461, Nov. 1974.

- [76] H. Krim and J. G. Proakis, "Smoothed eigenspace-based parameter estimation," *Automatica, Special Issue on Statistical Signal Processing and Control*, vol. 30, no. 1, pp. 27–38, Jan. 1994.
- [77] H. Krim and M. Viberg, "Two decades of array signal processing research: The parametric approach," *IEEE Signal Processing Magazine*, vol. 13, no. 4, pp. 67–94, Jul. 1996.
- [78] P. Kroonenberg and J. De Leeuw, "Principal component analysis of three-mode data by means of alternating least squares algorithms," *Psychometrika*, vol. 45, no. 1, pp. 69–97, Mar. 1980.
- [79] J. B. Kruskal, "Three-way arrays: rank uniqueness of trilinear decompositions, with application to arithmetic complexity and statistics," *Linear Algebra Appl.*, vol. 18, pp. 95–138, 1977.
- [80] T. Kurner, D. Cichon, and W. Wiesbeck, "Concepts and results for 3D digital terrain-based wave propagation models: an overview," *IEEE Journal on Selected Areas in Communications*, vol. 11, no. 7, pp. 1002–1012, Sept. 1993.
- [81] P. Kyösti, J. Meinilä, L. Hentilä, X. Zhao, T. Jämsä, C. Schneider, M. Narandzić, M. Milojević, A. Hong, J. Ylitalo, V.-M. Holappa, M. Alatossava, R. Bultitude, Y. de Jong, and T. Rautiainen, "WINNER II channel models," IST-WINNER, Deliverable D1.1.2, 2007. [Online]. Available: <http://www.ist-winner.org/WINNER2-Deliverables/D1.1.2v1.1.pdf>
- [82] M. Landmann, A. Richter, and R. Thomä, "DOA resolution limits in MIMO channel sounding," in *International Symposium on Antennas and Propagation and USNC/URSI National Radio Science Meeting*, Monterey, CA, Jun. 2004, pp. 1708–1711.
- [83] M. Landmann, "Limitations of experimental channel characterization," Ph. D. dissertation, Technischen Universität Ilmenau, Ilmenau, Germany, Mar. 2008. [Online]. Available: <http://www.db-thueringen.de>
- [84] M. Landmann, M. Käske, R. Thomä, J. Takada, and I. Ida, "Measurement based parametric channel modelling considering estimated diffuse scattering and specular components," in *The International Symposium on Antennas and Propagation (ISAP 2007)*, Niigata, Japan, Aug. 2007, pp. 153–156.
- [85] N. Leo and M. Gunnarsson, "Design och implementation av array-antennor för MIMO-mätningar," Master's thesis, Lunds Tekniska Högskola, Institutionen för Elektrovvetenskap, Lund, Sweden, Jun. 2005.

- [86] K. Levenberg, "A method for the solution of certain problems in least squares," *Quart. Appl. Math.* 2, pp. 164–168, 1944.
- [87] K. V. Mardia, *Statistics of Directional Data*. Academic Press, London, UK, 1972, 357 p.
- [88] D. Marquardt, "An algorithm for least-squares estimation of nonlinear parameters," *SIAM J. Appl. Math.*, vol. 11, pp. 431–441, 1963.
- [89] Mathworks. Matlab. [Online]. Available: <http://www.mathworks.com>
- [90] MEDAV GmbH, "RUSK channel sounder." [Online]. Available: <http://www.channelsounder.de/>
- [91] A. Molisch, H. Asplund, R. Heddergott, M. Steinbauer, and T. Zwick, "The COST259 directional channel model — Part I: Overview and methodology," *IEEE Transactions on Wireless Communications*, vol. 5, no. 12, pp. 3421–3433, Dec. 2006.
- [92] A. F. Molisch, "A generic model for MIMO wireless propagation channels in macro- and microcells," *IEEE Transactions on Signal Processing*, vol. 52, no. 1, pp. 61–71, Jan. 2004.
- [93] A. F. Molisch, *Wireless Communications*. Chichester, UK: John Wiley and Sons, 2005, 668 p.
- [94] O. Nørklit and J. Andersen, "Diffuse channel model and experimental results for array antennas in mobile environments," *IEEE Transactions on Antennas and Propagation*, vol. 46, no. 6, pp. 834–840, Jun. 1998.
- [95] C. Oestges, V. Erceg, and A. Paulraj, "A physical scattering model for MIMO macrocellular broadband wireless channels," *IEEE Journal on Selected Areas in Communications*, vol. 21, no. 5, pp. 721–729, Jun. 2003.
- [96] C. Oestges and B. Clerckx, *MIMO Wireless Communications: From Real-world Propagation to Space-time Code Design*. Oxford, UK: Elsevier Science & Technology, 2007, 480 p.
- [97] B. Ottersten, M. Viberg, and T. Kailath, "Analysis of subspace fitting and ML techniques for parameter estimation from sensor array data," *IEEE Transactions on Signal Processing*, vol. 40, no. 3, pp. 590–600, Mar. 1992.
- [98] A. Paulraj, R. Nabar, and D. Gore, *Introduction to space-time wireless communications*. New York, NY: Cambridge University Press, 2003, 277 p.

- [99] A. Paulraj, R. Roy, and T. Kailath, "Estimation of signal parameters via rotational invariance techniques — ESPRIT," in *The 19th Asilomar Conference on Circuits, Systems and Computers*, Pacific Grove, CA, Nov. 1985, pp. 83–89.
- [100] M. Pesavento, C. F. Mecklenbräuker, and J. F. Böhme, "Multidimensional rank reduction estimator for parametric MIMO channel models," *EURASIP J. Appl. Signal Process.*, vol. 2004, no. 1, pp. 1354–1363, 2004.
- [101] P. Petrus, J. Reed, and T. Rappaport, "Geometrical-based statistical macrocell channel model for mobile environments," *IEEE Transactions on Communications*, vol. 50, no. 3, pp. 495–502, Mar. 2002.
- [102] S. Pillai and B. Kwon, "Forward/backward spatial smoothing techniques for coherent signal identification," *IEEE Transactions on Acoustics, Speech and Signal Processing*, vol. 37, no. 1, pp. 8–15, Jan. 1989.
- [103] J. Poutanen, K. Haneda, J. Salmi, V.-M. Kolmonen, A. Richter, P. Almers, and P. Vainikainen, "Development of measurement-based ray tracer for multi-link double directional propagation parameters," in *The 3rd European Conference on Antennas and Propagation (EuCAP 2009)*, Berlin, Germany, Mar. 23–27 2009, pp. 2622–2626.
- [104] S. Ranvier, J. Kivinen, and P. Vainikainen, "Millimeter-wave MIMO radio channel sounder," *IEEE Transactions on Instrumentation and Measurement*, vol. 56, no. 3, pp. 1018–1024, Jun. 2007.
- [105] C. Ribeiro, "Propagation parameter estimation in MIMO systems," Ph. D. dissertation, Helsinki University of Technology, Dept. of Signal Processing and Acoustics, Espoo, Finland, Apr. 2008. [Online]. Available: <http://lib.tkk.fi/Diss/2008/isbn9789512293032/>
- [106] C. Ribeiro, E. Ollila, and V. Koivunen, "Stochastic maximum-likelihood method for MIMO propagation parameter estimation," *IEEE Transactions on Signal Processing*, vol. 55, no. 1, pp. 46–55, Jan. 2007.
- [107] C. Ribeiro, A. Richter, and V. Koivunen, "Joint angular- and delay-domain MIMO propagation parameter estimation using approximate ML method," *IEEE Transactions on Signal Processing*, vol. 55, no. 10, pp. 4775–4790, Oct. 2007.
- [108] A. Richter, "Estimation of radio channel parameters: Models and algorithms," Ph. D. dissertation, Technischen Universität Ilmenau, Germany, May 2005, ISBN 3-938843-02-0. [Online]. Available: www.db-thueringen.de

- [109] A. Richter, M. Landmann, and R. Thomä, “RIMAX - a flexible algorithm for channel parameter estimation from channel sounding measurements,” *COST273 9th Management Committee Meeting*, Athens, Greece, TD(04)045, Jan. 26–28, 2004.
- [110] A. Richter, M. Landmann, and R. Thomä, “Maximum likelihood channel parameter estimation from multidimensional channel sounding measurements,” in *The 57th IEEE Vehicular Technology Conference (VTC 2003-spring)*, vol. 2, Apr. 2003, pp. 1056–1060.
- [111] A. Richter, J. Salmi, and V. Koivunen, “An algorithm for estimation and tracking of distributed diffuse scattering in mobile radio channels,” in *IEEE International Workshop on Signal Processing Advances in Wireless Communications*, Cannes, France, Jul. 2–5 2006, pp. 1–5.
- [112] A. Richter, J. Salmi, and V. Koivunen, “Signal processing perspectives to radio channel modelling,” in *Proceedings of the 2nd European Conference on Antennas and Propagation (EuCAP 2007)*, Edinburgh, UK, Nov. 11–16 2007, pp. 1–6.
- [113] A. Richter and R. Thomä, “Parametric modeling and estimation of distributed diffuse scattering components of radio channels,” *COST273 8th Management Committee Meeting*, Prague, Czech Rep., TD(03)198, Sept. 24–26, 2003.
- [114] A. Richter, J. Salmi, and V. Koivunen, “On distributed scattering in radio channels and its contribution to MIMO channel capacity,” in *The 1st European Conference on Antennas and Propagation (EuCAP 2006)*, Nice, France, Nov. 2006, pp. 1–7.
- [115] A. Richter, J. Salmi, and V. Koivunen, “ML estimation of covariance matrix for tensor valued signals in noise,” in *IEEE International Conference on Acoustics, Speech, and Signal Processing (ICASSP 2008)*, Las Vegas, USA, Mar. 31–Apr. 4 2008, pp. 2349–2352.
- [116] A. Richter, J. Salmi, and V. Koivunen, “Tensor decomposition of MIMO channel sounding measurements and its applications,” in *URSI General Assembly*, Chicago, USA, Aug. 7–16 2008.
- [117] A. Richter and R. Thomä, “Parametric modelling and estimation of distributed diffuse scattering components of radio channels,” *COST273 8th Management Committee Meeting*, Prague, Czech Republic, TD(03)198, Sept. 24–26, 2003.
- [118] J. Rissanen, “Modeling by shortest data description,” *Automatica*, vol. 14, pp. 465–471, 1978.

- [119] R. Roy and T. Kailath, “ESPRIT — estimation of signal parameters via rotational invariance techniques,” *IEEE Transactions on Acoustics, Speech and Signal Processing*, vol. 37, no. 7, pp. 984–995, Jul. 1989.
- [120] A. Saleh and R. Valenzuela, “A statistical model for indoor multipath propagation,” *IEEE Journal on Selected Areas in Communications*, vol. 5, no. 2, pp. 128–137, Feb. 1987.
- [121] J. Salmi, A. Richter, and V. Koivunen, “Tracking of double directional radio propagation path parameters with EKF,” *COST2100 4th Management Committee Meeting*, Wroclaw, Poland, TD(08)471, Feb. 6–8, 2008.
- [122] J. Salmi, A. Richter, and V. Koivunen, “MIMO propagation parameter tracking using EKF,” in *IEEE Nonlinear Statistical Signal Processing Workshop (NSSPW 2006)*, Cambridge, UK, Sept. 13–15 2006, pp. 69–72.
- [123] J. Salmi, A. Richter, and V. Koivunen, “Angular doppler characterization in indoor channels,” in *The 3rd European Conference on Antennas and Propagation (EuCAP 2009)*, Berlin, Germany, Mar. 23–27 2009, pp. 3839–3843.
- [124] J. Salo, G. Del Galdo, J. Salmi, P. Kyösti, L. Hentil, M. Milojevic, D. Laselva, P. Zetterberg, and C. Schneider, “MATLAB implementation of the WINNER Phase I Channel Model ver1.5,” Dec. 2005. [Online]. Available: http://www.ist-winner.org/phase_model.html
- [125] J. Salo, G. Del Galdo, J. Salmi, P. Kyösti, M. Milojevic, D. Laselva, and C. Schneider, “MATLAB implementation of the 3GPP Spatial Channel Model (3GPP TR 25.996),” Jan. 2005, [Online]. Available: http://radio.tkk.fi/en/research/rf_applications_in_mobile_communication/radio_channel/scm.html.
- [126] S. R. Saunders, *Antennas and Propagation for Wireless Communication Systems*. Chichester, England: John Wiley and Sons Inc., 1999, 426 p.
- [127] A. Sayeed, “Deconstructing multiantenna fading channels,” *IEEE Transactions on Signal Processing*, vol. 50, no. 10, pp. 2563–2579, Oct. 2002.
- [128] L. Scharf, *Statistical Signal Processing, Detection Estimation and Time Series Analysis*. Reading, MA: Addison-Wesley, 1990, 524 p.

- [129] R. Schmidt, "Multiple emitter location and signal parameter estimation," *IEEE Transactions on Antennas and Propagation*, vol. 34, no. 3, pp. 276–280, Mar. 1986.
- [130] R. O. Schmidt, "A signal subspace approach to multiple emitter location and spectral estimation," Ph. D. Thesis, Stanford University, Dept. of Electrical Engineering, CA, USA, 1981.
- [131] D.-S. Shiu, G. Foschini, M. Gans, and J. Kahn, "Fading correlation and its effect on the capacity of multielement antenna systems," *IEEE Transactions on Communications*, vol. 48, no. 3, pp. 502–513, Mar. 2000.
- [132] N. Sidiropoulos, R. Bro, and G. Giannakis, "Parallel factor analysis in sensor array processing," *IEEE Transactions on Signal Processing*, vol. 48, no. 8, pp. 2377–2388, Aug. 2000.
- [133] A. Smilde, R. Bro, and P. Geladi, *Multisway Analysis with Applications in the Chemical Sciences*. Chichester, England: John Wiley and Sons, Ltd, 2004, 381 p.
- [134] H. W. Sorenson, "Least-squares estimation: from Gauss to Kalman," *IEEE Spectrum*, vol. 7, pp. 63–68, Jul. 1970.
- [135] Q. H. Spencer, B. D. Jeffs, M. A. Jensen, and A. L. Swindlehurst, "Modeling the statistical time and angle of arrival characteristics of an indoor multipath channel," *IEEE Journal on Selected Areas in Communications*, vol. 18, no. 3, pp. 347–360, Mar. 2000.
- [136] M. Steinbauer, A. Molisch, and E. Bonek, "The double-directional radio channel," *IEEE Antennas and Propagation Magazine*, vol. 43, no. 4, pp. 51–63, Aug. 2001.
- [137] M. Steinbauer, "The radio propagation channel — a non-directional, directional, and double-directional point-of-view," Ph. D. dissertation, Vienna University of Technology, Institute of Communications and Radio-Frequency Engineering, Vienna, Austria, 2001. [Online]. Available: http://www.nt.tuwien.ac.at/mobile/theses_finished
- [138] P. Stoica and Y. Selen, "Model-order selection: a review of information criterion rules," *IEEE Signal Processing Magazine*, vol. 21, no. 4, pp. 36–47, July 2004.
- [139] P. Stoica and R. Moses, *Spectral Analysis of Signals*. Upper Saddle River, NJ: Pearson Education, Inc., 2005, 452 p.

- [140] P. Suvikunnas, J. Salo, L. Vuokko, J. Kivinen, K. Sulonen, and P. Vainikainen, "Comparison of MIMO antenna configurations: Methods and experimental results," *IEEE Transactions on Vehicular Technology*, vol. 57, no. 2, pp. 1021–1031, Mar. 2008.
- [141] E. Telatar, "Capacity of multi-antenna Gaussian channels," *European Transactions on Telecommunications*, vol. 10, no. 6, pp. 585–596, Nov. 1999.
- [142] R. Thomä, D. Hampdicke, A. Richter, and G. Sommerkorn, "MIMO vector channel sounder measurement for smart antenna system evaluation," *European Transactions on Telecommunications*, vol. 12, no. 5, pp. 427–438, Sept.-Oct. 2001.
- [143] R. Thomä, D. Hampicke, M. Landmann, A. Richter, and G. Sommerkorn, "Measurement-based parametric channel modelling (MBPCM)," in *International Conference on Electromagnetics in Advanced Applications (ICEAA 2003)*, Torino, Italy, Sept. 8-13 2003.
- [144] R. Thomä, D. Hampicke, A. Richter, G. Sommerkorn, A. Schneider, U. Trautwein, and W. Wirnitzer, "Identification of time-variant directional mobile radio channels," *IEEE Transactions on Instrumentation and Measurement*, vol. 49, no. 2, pp. 357–364, Apr 2000.
- [145] R. Thomä, M. Landmann, G. Sommerkorn, and A. Richter, "Multidimensional high-resolution channel sounding in mobile radio," in *Proc. of the 21st IEEE Instrumentation and Measurement Technology Conference (IMTC 2004)*, vol. 1, Como, Italy, May 2004, pp. 257–262.
- [146] U. Trautwein, M. Landmann, G. Sommerkorn, and R. Thomä, "System-oriented measurement and analysis of MIMO channels," *COST273 12th Management Committee Meeting*, Bologna, Italy, TD(05)063, Jan. 19–21, 2005.
- [147] U. Trautwein, C. Schneider, and R. Thomä, "Measurement-based performance evaluation of advanced MIMO transceiver designs," *EURASIP Journal on Applied Signal Processing*, vol. 2005, no. 1, pp. 1712–1724, 2005.
- [148] M. Tschudin, C. Brunner, T. Kurpjuhn, M. Haardt, and J. Nossek, "Comparison between unitary ESPRIT and SAGE for 3-D channel sounding," in *The 49th IEEE Vehicular Technology Conference (VTC 1999-spring)*, vol. 2, Houston, TX, May. 1999, pp. 1324–1329.
- [149] D. Tse and P. Viswanath, *Fundamentals of Wireless Communications*. Cambridge University Press, 2005, 564 p.

- [150] L. R. Tucker, "Some mathematical notes on three-mode factor analysis," *Psychometrika*, vol. 36, pp. 279–311, 1966.
- [151] P. Vainikainen, M. Mustonen, M. Kyrö, T. Laitinen, C. Icheln, J. Villanen, and P. Suvikunnas, "Recent development of MIMO antennas and their evaluation for small mobile terminals," in *The 17th International Conference on Microwaves, Radar and Wireless Communications (MIKON 2008)*, Wroclaw, Poland, May 2008, pp. 1–10.
- [152] B. Van Veen and K. Buckley, "Beamforming: A versatile approach to spatial filtering," *IEEE ASSP Magazine*, vol. 5, pp. 4–24, Apr. 1988.
- [153] M. Vanderveen, B. Ng, C. Papadias, and A. Paulraj, "Joint angle and delay estimation (JADE) for signals in multipath environments," in *The 30th Asilomar Conference on Signals, Systems and Computers*, vol. 2, Pacific Grove, CA, Nov. 1996, pp. 1250–1254.
- [154] M. Vanderveen, C. Papadias, and A. Paulraj, "Joint angle and delay estimation (JADE) for multipath signals arriving at an antenna array," *IEEE Communications Letters*, vol. 1, no. 1, pp. 12–14, Jan. 1997.
- [155] J. Villanen, P. Suvikunnas, C. Icheln, J. Ollikainen, and P. Vainikainen, "Performance analysis and design aspects of mobile-terminal multiantenna configurations," *IEEE Transactions on Vehicular Technology*, vol. 57, no. 3, pp. 1664–1674, May 2008.
- [156] J. Wallace and M. Jensen, "Modeling the indoor MIMO wireless channel," *IEEE Transactions on Antennas and Propagation*, vol. 50, no. 5, pp. 591–599, May 2002.
- [157] S. Wang, A. Abdi, J. Salo, H. El-Sallabi, J. Wallace, P. Vainikainen, and M. Jensen, "Time-varying MIMO channels: Parametric statistical modeling and experimental results," *IEEE Transactions on Vehicular Technology*, vol. 56, no. 4, pp. 1949–1963, Jul. 2007.
- [158] W. Weichselberger, "Spatial structure of multiple antenna radio channels," Ph. D. dissertation, Vienna University of Technology, Institute of Communications and Radio-Frequency Engineering, Vienna, Austria, Dec. 2003. [Online]. Available: http://www.nt.tuwien.ac.at/mobile/theses_finished
- [159] K. Yee, "Numerical solution of initial boundary value problems involving Maxwell's equations in isotropic media," *IEEE Transactions on Antennas and Propagation*, vol. 14, no. 3, pp. 302–307, May 1966.
- [160] X. Yin, "High-resolution parameter estimation for MIMO channel sounding," Ph. D. dissertation, Department of Electronic Systems, Aalborg University, Aalborg, Denmark, 2006.

- [161] X. Yin, G. Steinbock, G. Kirkelund, T. Pedersen, P. Blattnig, A. Jaquier, and B. Fleury, "Tracking of time-variant radio propagation paths using particle filtering," in *IEEE International Conference on Communications (ICC 2008)*, Beijing, China, May 2008, pp. 920–924.
- [162] X. Yin, G. Steinböck, G. E. Kirkelund, T. Pedersen, P. Blattnig, A. Jaquier, and B. H. Fleury, "Tracking of the time-variant parameters of radio propagation paths using a particle filter," *COST2100 3rd Management Committee Meeting*, Duisburg, Germany, TD(07)380, Sept. 10–12, 2007.
- [163] K. Yu and B. Ottersten, "Models for MIMO propagation channels: a review," *Wiley Journal on Wireless Communications and Mobile Computing*, vol. 2, no. 7, pp. 653–666, 2002.
- [164] T. Zwick, C. Fischer, D. Didascalou, and W. Wiesbeck, "A stochastic spatial channel model based on wave-propagation modeling," *IEEE Journal on Selected Areas in Communications*, vol. 18, no. 1, pp. 6–15, Jan. 2000.